

Evolution of *caudal* translational repression in higher insects

Dissertation submitted in partial fulfilment of the requirements for the degree of
“Doctor rerum naturalium”
of the Georg-August-University Göttingen

by

Claudia Jasmin Rödel

Bremerhaven,
Germany

Göttingen, 2010

First Referee: Prof. Dr. Ernst Wimmer (Department of Developmental Biology,
Georg-August-University Göttingen, Germany)

Second Referee: Prof. Dr. Gregor Bucher (Department of Developmental Biology,
Georg-August-University Göttingen, Germany)

Date of submission: 07. December 2010

The experimental part of this thesis was performed at the

Department of Developmental Biology
Institute of Molecular Biology and Biotechnology (IMBB)
Foundation for Research and Technology - Hellas (FoRTH)
Heraklion, Crete, Greece

under the supervision of Dr. Michalis Averof.

Herewith I declare that I prepared the Dissertation
“Evolution of *caudal* translational repression in higher insects”
on my own and with no other source and aids than quoted.

_____ Göttingen, 07. December 2010
Claudia Rödel

Index

Index	I
List of Figures	V
List of Tables	VI
Abbreviations	VII
1 Abstract	1
2 Introduction	2
2.1 AP axis determination and polarity during insect development	2
2.1.1 AP axis determination in <i>Drosophila melanogaster</i>	3
2.1.2 AP axis determination in other insects	6
2.2 The anterior patterning factor Bicoid	10
2.2.1 Evolution of Bicoid.....	10
2.2.2 Function of Bicoid.....	11
2.2.3 The Bicoid isoforms.....	12
2.3 Mechanism of <i>cad</i> translational regulation in <i>Drosophila</i>	14
2.4 miRNA function during early <i>Drosophila</i> development	16
2.5 Rationale	17
3 Results and Discussion	19
3.1 Mapping of BCD-binding RNA-elements <i>in vitro</i>	19
3.1.1 Establishment of RNA-binding assay using recombinant BCD homeodomain protein	20
3.1.2 Analysis of recombinant BCD homeodomain binding to RNA.....	22
3.1.3 Characterization of the BCD binding element BRE_257-319 in the <i>Drosophila cad</i> 3'UTR.....	26
3.1.4 Identification of a <i>Haematopota cad</i> 3'UTR element that is bound by the BCD homeodomain	31
3.1.5 Conclusions.....	34
3.2 Mapping Bicoid RNA-binding elements <i>in vivo</i>	36

3.2.1 The making of a fluorescent protein reporter assay in early <i>Drosophila</i> embryogenesis.....	36
3.2.1.1 Strategy 1: Translational reporter assay using a single ϕ C31-integrase recombination site	39
3.2.1.2 Strategy 2: Translational reporter assay using the ϕ C31-integrase mediated cassette exchange (RMCE).....	40
3.2.1.3 Strategy 2b: A translational reporter assay using RMCE in conjunction with BCD protein expressed using the UAS/GAL4 induction system.....	43
3.2.1.4 Strategy 3: Translational reporter assay using a d2EGFP-CAD fusion	46
3.2.1.5 Conclusions.....	49
3.2.2 Identification of <i>cad</i> 3'UTR homologues that are translationally regulated by BCD.....	50
3.2.2.1 The BRE_257-319 fragment of the <i>cad</i> 3'UTR is mediating translational repression in the presence of BCD	50
3.2.2.2 The <i>Haematopota cad</i> 3'UTR mediates translational repression in the presence of BCD.....	50
3.2.2.3 The <i>Tribolium cad</i> 3'UTR fails to mediate BCD-dependent translational repression of the dnGFP sensor	51
3.2.2.4 Conclusions.....	52
3.3 Testing the role of different Bicoid isoforms during <i>Drosophila</i> early embryogenesis.....	54
3.3.1 <i>hb</i> transcriptional activation and CAD translational repression by different BCD isoforms	54
3.3.2 Translational repression of sensor 38F-Dm3' by different BCD isoforms.....	58
3.3.3 Conclusions.....	59
3.4 Hints for alternative mechanisms of BCD-mediated translational repression.....	61
3.4.1 Mutations in the miR-308 target site abolish BCD-mediated translational repression	62
3.4.2 Translational repression of 38F-BRE_257-319 and 38F-H2 by BCD isoform F	64

3.4.3 Conclusions.....	65
4 General Discussion	67
4.1 Insights into translational control of <i>cad</i> in <i>Drosophila</i>	67
4.2 Alternative mechanisms of translational control of <i>cad</i> mRNA.....	71
4.2.1 Evidence for d4EHP- <i>independent cad</i> translational repression	71
4.2.2 The putative role of miR-308 in BCD-dependent <i>cad</i> translational repression	72
4.3 Implications for the evolution of <i>cad</i> translational regulation	74
4.4 Summary and future directions	78
5 Materials and Methods	80
5.1 Oligonucleotides	80
5.1.1 Oligonucleotides for cloning procedures	80
5.1.2 Oligonucleotides for template generation of <i>in vitro</i> synthesized RNA probes.....	81
5.1.3 Oligonucleotides for generation of ds DNA probe	81
5.2 In vitro Methods	82
5.2.1 Cloning procedures	82
5.2.1.1 Cloning of protein expression construct	82
5.2.1.2 Cloning of 3'UTRs used for EMSAs	82
5.2.2 RNA probes.....	84
5.2.2.1 Template generation	84
5.2.2.2 <i>In vitro</i> transcription and radioisotope-labeling of RNA probes.....	85
5.2.3 Radioisotope-labeling of dsDNA oligonucleotides.....	86
5.2.4 Protein purification.....	86
5.2.4.1 Purification of HisMBP-HD fusion protein.....	86
5.2.4.2 Purification of GST-HD fusion protein	87
5.2.4.3 Tev-protease digest of HD	87
5.2.5 Electrophoretic Mobility Shift Assays (EMSAs)	88
5.2.5.1 RNA EMSAs.....	88
5.2.5.2 DNA EMSAs.....	88
5.3 In vivo Methods	89
5.3.1 Cloning procedures of in vivo methods	89
5.3.1.1 Cloning of sensor constructs.....	89

5.3.1.2 Cloning UAS constructs	93
5.3.2 <i>Drosophila melanogaster</i> handling and husbandry	94
5.3.3 Transgenesis.....	94
5.3.3.1 ϕ C31 integrase mediated recombination system using a single <i>attP</i> landing site (strategy 1).....	95
5.3.3.2 Recombinase-mediated exchange cassette (RMCE) using ϕ C31 integrase (strategy 2)	95
5.3.3.3 P-element based transgenesis.....	95
5.3.4 <i>Drosophila</i> husbandry for expression of UAS-BCD isoforms during early embryogenesis	97
5.3.5 <i>Drosophila</i> husbandry for expression of UAS-BCD and sensor constructs during early embryogenesis.....	97
5.3.6 Immunohistochemistry	100
5.3.6.1 Antibody stainings	100
5.3.6.2 <i>In situ</i> hybridization	101
5.3.7 Microscopy and Imaging	102
6 Literature	104
APPENDIX	112
A1 EMSAs	112
A2 Alignment of <i>cad</i> 3'UTR homologues	116
A3 Myc-stainings	118
A4 Secondary structure predictions and RNAforester alignments	119
A5 Genomic region of <i>bcd</i>	127
A6 Measurements of <i>in vivo</i> translational reporter assay	130
Curriculum vitae	134
Acknowledgements	136

List of Figures

Fig. 2.1: AP axis patterning and segmentation gene cascade in <i>Drosophila melanogaster</i>	5
Fig. 2.2: Long-germband development vs. short-germ development and the evolution of <i>Hox3</i> -like genes in the lineage of <i>Tribolium</i> and <i>Drosophila</i>	9
Fig. 2.3: Schematic overview of putative evolution of <i>bcd</i> and <i>zen</i> in taxa of diptera. ...	11
Fig. 2.4: The protein domains of BCD isoform G.	12
Fig. 2.5: Schematic overview of the <i>bcd</i> transcripts produced by differential splicing of four major exons.	14
Fig. 2.6: Model of <i>cad</i> translational repression, proposed by Cho et al. (2005).	15
Fig. 3.1: <i>Drosophila cad</i> 3' UTR and RNA fragments previously described as Bicoid binding elements	20
Fig. 3.2: DNA- and RNA-binding assay of BCD homeodomain.	24
Fig. 3.3: Binding of BCD homeodomain to BRE_164-339.	25
Fig. 3.4: Sequence alignment of <i>cad</i> 3'UTRs from different <i>Drosophila</i> species.	28
Fig. 3.5: Binding of BCD homeodomain to BRE_257-319	29
Fig. 3.6: Specificity of BCD homeodomain binding to BRE_257-319.	30
Fig. 3.7: Comparison of secondary structures of Hp3' and BRE_257-319.	32
Fig. 3.8: Binding of the BCD homeodomain to <i>Haematopota</i> 3'UTR fragments H1, H2 and H3.	33
Fig. 3.9: Schematic overview of translational reporter assays.	38
Fig. 3.10: Translational repression assay.	45
Fig. 3.11: Translational repression of a reporter carrying a d2GFP-CAD fusion and the Dm3'.	48
Fig. 3.12: Translational repression assay on BRE_257-319, <i>Haematopota</i> and <i>Tribolium</i> 3'UTRs.	52
Fig. 3.13: <i>hb</i> expression in the presence of different BCD isoforms.	56
Fig. 3.14: <i>cad</i> translational repression in the presence of different BCD isoforms.	57
Fig. 3.15: Translational repression effect of different BCD isoforms on the 38F-Dm3' sensor.	59
Fig. 3.16: Predicted secondary structures of BRE_257-319 and H2.	62
Fig. 3.17: Translational reporter assay for repression of the mutated <i>cad</i> 3'UTR in sensor 38F-Dm3'mut by different BCD isoforms.	63
Fig. 3.18: Translational reporter assay for repression of BRE_257-319 and H2 by BCD isoforms G and F.	65
Fig. 4.1: Phylogeny of insect species (after Savard et al., 2006) discussed with features of <i>cad</i> translational repression mapped on.	77

List of Tables

Tab. 3.1: <i>Drosophila</i> sensor lines generated by ϕ C31-integrase mediated insertion into the pJBattPM44 locus on the second chromosome.....	40
Tab. 3.2: <i>Drosophila</i> sensor lines generated by ϕ C31-integrase-mediated RMCE.	42
Tab. 4.1: Presence of d4EHP-binding domain in different BCD isoforms and their ability to mediate translational repression of different sensors.....	73

Abbreviations

♀	female
♂	male
aa	amino acid
AP	Alkaline Phosphatase
as	antisense
ATP	adenosine triphosphate
BCIP	5-Bromo-4-chloro-3-indolyl phosphate
bp	base pair
cap	7-methylguanosine cap structure
cDNA	complementary DNA
DIG	Digoxigenin-11-2'-deoxyuridin-5'-triphosphate
Dm	Drosophila melanogaster
ds	double stranded
DTT	1,4-Dithiothreit
EDTA	Ethylediamintetraacetate
FA	formaldehyde
h	hours
HD	homeodomain
HEPES	4-(2-Hydroxyethyl)-1-piperazin
Hp	Haematopota pluvialis
kb	Kilobase
LB	Luria-Bertani (medium)
LEW	Lysis-Elution-Wash-buffer
min	minutes
miRNA	micro RNA
mRNA	messenger RNA
NBT	Nitro blue tetrazolium chloride
nt	nucleotide
OD	Optical density
ORF	open reading frame
PCR	Polymerase chain reaction
PEM	Pipes-EGTA-MgCl ₂ -buffer
rpm	rounds per minute
RT	Room temperature

sec	seconds
SSC	Standar Sline Citrate Buffer
TBE	Tris-Borate-EDAT-Electrophoressis buffer
Tc	Tribolium castaneum
tRNA	transfer RNA
UTR	untranslated region

Abbreviations of amino acids

A	Alanin
C	Cystein
D	Aspartate
E	Glutamate
F	Phenylalanin
G	Glycine
H	Histidine
I	Isoleucine
K	Lysine
L	Leucine
M	Methionine
N	Asparagine
P	Proline
Q	Glutamine
R	Arginine
S	Serine
T	Threonine
V	Valine
W	Tryptophane
Y	Tyrosine

Abbrevations of nucleotides

A	Adenine
C	Cytosine
G	Guanine
T	Thymine
U	Uridine

1 Abstract

caudal/Cdx genes are homeobox genes involved in posterior patterning of the embryo in a wide range of bilaterian species, including arthropods, nematodes and vertebrates. In the fruit fly *Drosophila melanogaster* the homeobox gene *bicoid* (*bcd*), an anterior patterning factor that orchestrates anterior patterning, prevents translation of the uniformly distributed *cad* mRNA. The mechanism through which BCD mediates this repression has been proposed as a new paradigm for translational control: BCD binds directly through its homeodomain to the *cad* 3' UTR and simultaneously interacts with the cap-binding protein d4EHP. Thus the *cad* mRNA remains translationally repressed.

The anterior patterning factor *bcd* is an evolutionary novelty present only in higher dipterans, therefore other insect species must follow different strategies to restrict *cad* expression to the posterior. In the beetle *Tribolium castaneum*, the homeodomain protein Tc'ZEN-2 and the KH-domain protein Tc'MEX-3 restrict *Tc'caudal* (*Tc'cad*) to the posterior part of the embryo. Nevertheless, when expressed in *Drosophila* embryos, BCD translationally represses *Tc'cad* mRNA. The region to which BCD binds has been speculated to be in the *Tc'cad* 3'UTR and raised the question whether BCD may recognize regulatory element(s) that are conserved between *Drosophila* and *Tribolium*.

By establishing an *in vivo* sensor for BCD-mediated translational repression I was able to identify small regions in the *cad* 3'UTR of *Drosophila* and the horsefly *Haematopota pluvialis* that mediate BCD-dependent translational repression. These elements show similarities in their predicted secondary structures, which could be the basis for a conserved BCD-binding element. Using electrophoretic mobility shift assays I could show direct binding of the BCD homeodomain to these 3'UTR regions. Surprisingly, the 3'UTR of the *Tc'cad* homologue does not seem to contain BCD-binding elements.

The BCD-binding region of the *Dm'cad* 3'UTR co-localizes with a target site of the microRNA miR-308 and mutations in this region abolish miRNA-binding and BCD-mediated translational repression. Furthermore, BCD isoforms that lack the d4EHP-binding domain are able to mediate translational repression of sensors carrying BCD-binding regions. Taken together, these findings suggest that alternative mechanism(s) for the translational repression of *cad* mRNA are likely to exist in *Drosophila* and may also be present in other insect species.

2 Introduction

2.1 AP axis determination and polarity during insect development

Evo-Devo field combines areas of developmental biology and evolution. The question of the evolutionary origin of the bilaterian body axes is addressed by investigating the earliest patterning events during development in different bilaterian species. Starting from a single cell, the zygote, the bilaterian body develops with an anterior-posterior (AP) axis, two similar sides (left and right) and an upper and lower surface. The developmental patterning programs that underlie the specification of the body axes have been modified within different bilaterian lineages (De Robertis, 2008).

In most arthropods, the body polarity information derives from cues provided by the mother in form of maternal determinants. Detailed studies in the fruit fly *Drosophila melanogaster* have given us insight into the developmental mechanisms that pattern the body axes. However, these mechanisms are suspected to have derived from the ancestral mode of axis patterning in arthropods. This derived state is most likely the result of adaptations during development, associated with the rapid embryogenesis. Through comparative analyses of the developmental mechanisms of AP patterning in other species, we are beginning to understand the processes that directed the evolution of body axis patterning in arthropods.

The expression of the homeobox gene *caudal* (*cad/Cdx*) is conserved among a wide range of species including nematodes and vertebrates. *cad/Cdx* genes are consistently expressed in association with posterior polarity and patterning of posterior structures. In *Drosophila*, *cad* (*Dm'cad*) functions as a posterior activator of segmentation genes and is essential for the development of posterior abdominal segments, the anal plates and the hindgut (Macdonald and Struhl, 1986; Mlodzik et al., 1985; Moreno and Morata, 1999; Schulz and Tautz, 1995). In the red flour beetle *Tribolium castaneum*, *Tc'cad* is involved in the patterning of posterior head, thoracic and abdominal segments. In *Tc'cad* RNAi embryos, only the pre-gnathal segments are present, which is in agreement with the *Tc'cad* expression pattern during early development and subsequent expression in the posterior region, the so-called growth zone (Copf et al., 2004). In crustaceans like *Artemia franciscana*, *Af'cad* is expressed in the posterior growth zone that gives rise to posterior segments of the developing larvae and is

essential for the development of posterior thoracic, genital and post-genital segments (Copf et al., 2003; Copf et al., 2004). In the nematode *Caenorhabditis elegans* the *cad/Cdx* homologue is called *pal-1* and is expressed in the posterior blastomere P1. Loss of *pal-1* function results in severe posterior patterning defects (Edgar et al., 2001; Hunter and Kenyon, 1996). In mice, the *caudal* homologues *Cdx1* and *Cdx2* are important in processes of embryonic axial elongation and anterior-posterior patterning (Chawengsaksophak et al., 2004; van den Akker et al., 2002). These observations in different species suggest that *cad/Cdx* genes had an ancestral role in patterning of posterior segments and body parts.

2.1.1 AP axis determination in *Drosophila melanogaster*

In insects, maternal mRNAs and proteins are deposited into the oocyte to provide positional information during early development. These maternal determinants, depending on their distribution within the embryo, provide differential positional information that will result in the determination of the anterior and posterior ends. Most of our knowledge on AP patterning comes from extensive studies in *Drosophila melanogaster*, where a gradient system of maternal determinants organizes the patterning of the AP axis in the syncytial blastoderm.

The axial specification occurs in oocyte through polarized microtubules of the cytoskeleton, which leads to the specific localisation of maternal transcripts of *bicoid* (*bcd*), *oskar* (*osk*), *nanos* (*nos*) and *gurken* (*grk*) (Steinhauer and Kalderon, 2006). *grk* is an EGF signalling ligand, essential for the establishment of the anteroposterior and dorsoventral axes (MacDougall et al., 2003), whereas anteriorly localized *bcd* and posteriorly localized *nos* and *osk* specify the AP axis (Becalska and Gavis, 2009).

The graded maternal gene expression stands on top of a gene activation hierarchy, inducing differential activation of segmentation genes along the AP axis of the *Drosophila* embryo. The protein products of these genes become asymmetrically distributed, creating the network of graded maternal determinants (St Johnston and Nüsslein-Volhard, 1992). The first level of segmentation genes are the gap genes, which become specifically activated by maternal genes (Fig. 2.1, A). Gap genes are the first zygotically expressed genes and specify the body of the embryo into broad domains. Combined activity of maternal and gap genes activate the pair-rule genes, which are expressed in distinct stripes. The expression of the pair-rule genes results in

expression on the segment polarity genes, establishing the final output of segments (Fig. 2.1, A). Finally, the homeotic genes provide segment identity and determine the functional and morphological fate of each segment (F. Gilbert and R. Singer, 2010; Peel et al., 2005).

Three maternal genetic systems specify the AP axis of the early *Drosophila* embryo. The terminal system ensures specification of the unsegmented, anterior and posterior most part of the embryo. This specification depends on *Torso* (*Tor*), a receptor-tyrosine-kinase that becomes activated at the poles of the embryo. At the posterior, *Tor* target genes *tailless* (*tll*) and *huckebein* (*hkb*) are activated by relief of repression. At the anterior, *Tor* and the anterior maternal determinant BCD function antagonistically and cooperatively to activate segmentation gene expression (Furriols and Casanova, 2003; Li, 2005). The anterior system ensures the localization of maternal *bcd* mRNA at the anterior pole of the oocyte; genes of the posterior system promote localization of *nos* mRNA at the posterior pole of the oocyte. In the embryo, translation from these localized mRNA sources form two opposing concentration gradients that provide the symmetry breaking information and subsequent activation of segmentation genes (St Johnston and Nüsslein-Volhard, 1992). In contrast, maternal mRNAs of *hunchback* (*hb*) and *caudal* (*cad*) are provided uniformly in the early embryo, while their protein products are specifically produced in the anterior (HB) and posterior (CAD) through translational repression (Cho et al., 2006). The translational repression of *cad* mRNA is dependent of BCD activity and results in the posterior-to-anterior gradient of the CAD protein (Dubnau and Struhl, 1996; Rivera-Pomar et al., 1996) (Fig. 2.1, B), whereas *hb* mRNA is translationally repressed through NOS and Pumilio proteins (Murata et al., 1995; Gamberi et al., 2002; Cho et al., 2006). CAD contains a homeodomain and is essential for the expression of posterior gap genes and morphogenesis of posterior structures. The maternal and zygotic contributions of *cad* are partially redundant and only embryos mutant for both maternal and zygotic *cad* expression show severe segmentation effects (Macdonald and Struhl, 1986; Mlodzik et al., 1985; Moreno and Morata, 1999; Schulz and Tautz, 1995).

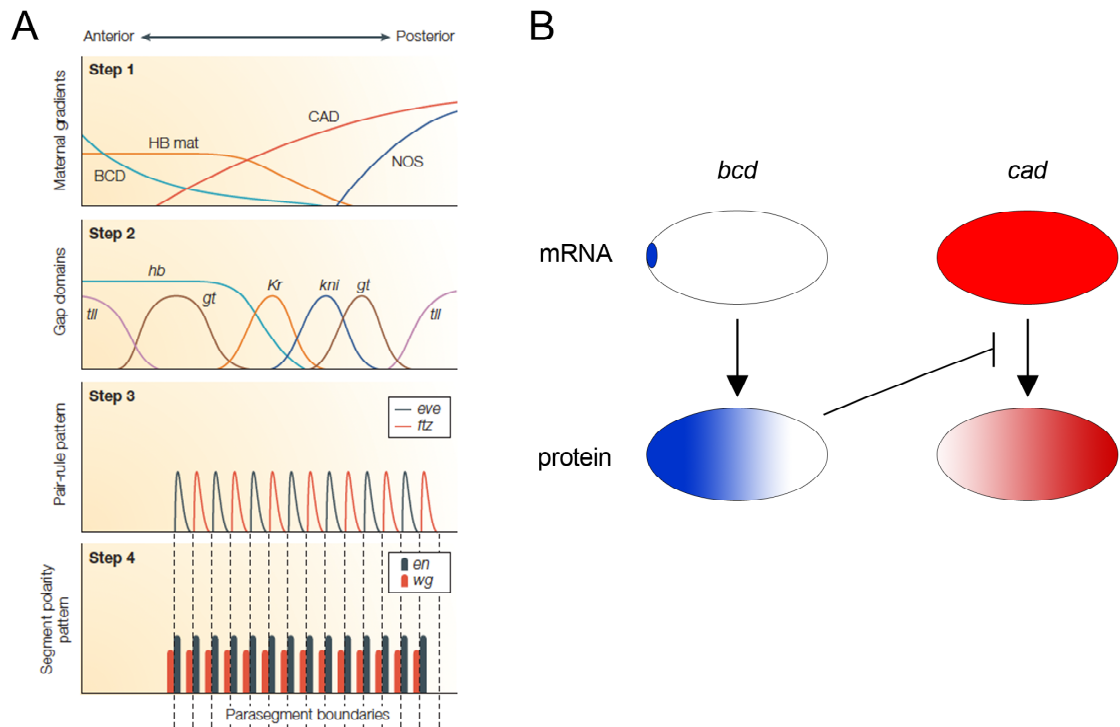


Fig. 2.1: AP axis patterning and segmentation gene cascade in *Drosophila melanogaster*. (A) Schematic overview of the gene cascade that leads to the formation of body segments along the AP axis. Step 1 includes the differential distribution of maternal genes along the AP axis. *bcd* and *nos* are localized as mRNAs at the anterior and posterior pole, respectively, whereas *cad* and *hb* mRNAs are distributed homogeneously. Upon egg laying the translation of protein products of *bcd* and *nos* results in the formation of two opposing concentration gradients. Besides being a transcription factor, BCD also represses the translation of CAD in the anterior, whereas NOS prevents translation of *hb* transcripts posteriorly. The coordinates created by the resulting concentration gradients along the AP axis results in the division of the embryo into smaller domains, which are marked by the expression of the gap genes. The gap genes *tailless (tll)*, *hb*, *giant (gt)*, *Krüppel (Kr)* and *knirps (kni)* specify broad domains along AP body axis, which are cross-regulated between them (step 2). Together with the maternal genes, the gap gene coordinates are transformed into the periodic expression of the pair-rule genes *hairy*, *runt* and *even-skipped (eve)* (step 3). The expression of these primary pair-rule genes, together with secondary pair-rule genes like *fushi-tarazu (ftz)* and *paired (prd)* are cross regulating to define the boundaries of the parasegments. The parasegments are distinguished into even and odd-numbered units, which are marked by the expression of different pair-rule genes. This expression pattern results in expression of the same segment polarity genes in every parasegment (step 4). The expression of *engrailed (en)* marks the anterior border of each parasegment and the neighbouring *wingless (wg)* expressing cells are posterior to every parasegment boundary. Segment boundaries are later marked by *en* at the posterior border of each segment. (B) Schematic overview of *bcd* as a translational repressor. *bcd* mRNA is localized at the anterior pole of the embryo and forms a protein gradient as embryogenesis begins, with highest concentrations at the anterior and lowest at the posterior. *cad* mRNA is distributed uniformly in the embryo, however due to translational repression by BCD, the CAD proteins form a gradient with highest concentration at the posterior. (A taken from Peel et al., 2005)

2.1.2 AP axis determination in other insects

A major evolutionary acquisition of *Drosophila* and some other holometabolous insect species is the patterning of all body segments during the syncytial blastoderm stage (Peel, 2008). This mode of development is often referred to as “long-germ development” and is thought to have evolved along with changes in extraembryonic tissue formation and underlying molecular networks of axial patterning systems. However many insects, like *Tribolium castaneum*, pattern only the anterior most segments during the early blastoderm stages and posterior segments are added sequentially after cellularization from a posterior patterning zone. In this mode of “short-germ development”, the embryo proper initially occupies only a small region at the posterior end of the egg and elongates as new segments appear sequentially (Fig. 2.2, A) (Schröder et al., 2008). In fact most arthropod species develop using this mode of sequential segmentation and it is therefore thought to represent the ancestral form of early development (Peel et al., 2005; Rosenberg et al., 2009).

The acquisition of *bcd* as a maternal anterior determinant is thought to have occurred in a small group within the diptera, specifically in the Cyclorrhapha (Stauber et al., 2002). Therefore, the anterior patterning network with *bcd* as the main anterior patterning factor during *Drosophila* development is a derived state and poses the question of how anterior-posterior patterning is realized in other insect species. Here I describe some examples of other insect species that pattern the AP axis independently of *bcd*.

In the wasp *Nasonia vitripennis*, the embryos pattern all segments at the same time during the blastoderm stage through maternal gradient systems. A *bcd* orthologue is not present in *Nasonia*. Anterior patterning is dependent on maternal expression of *otd1*, which is localized as mRNA at both poles of the embryo. Later on during development, gradients of OTD1 protein are established at both poles of the embryo (Lynch et al., 2006). In contrast to the anterior translational repression of *cad* as it is known in *Drosophila*, *Nasonia* has evolved a different strategy to restrict *Nv'cad* function to the posterior. Maternal *Nv'cad* mRNA itself is localized at the posterior pole of the egg resulting in a posterior-to-anterior gradient of *Nasonia* CAD protein. Whereas the role of *Drosophila cad* seems to be more restricted, in *Nasonia* lack of *cad* activity results in loss of most thoracic and abdominal segments, placing it on top of a cascade of early posterior patterning (Olesnicky et al., 2006).

It seems that divergent long-germ insects like *Nasonia* and *Drosophila* use similar long-range gradients to establish AP pattern, however the specific factors and regulatory mechanisms that establish these gradients are not widely conserved. In the fly *Episyrphus balteatus* (Syrphidae), which belongs to the Cyclorrhapha, the maternal regulation of *Episyrphus caudal* (*Eba'cad*) seems to depend on a combinatorial regulation by *Eba'BCD* and *Eba'TOR*, though it is not clear, whether *Eba'TOR* has a direct effect on *Eba'BCD* activity or whether *Eba'TOR* and *Eba'BCD* together could regulate an unknown repressor of *Eba'cad* translation (Lemke et al., 2010). Thus it is not entirely clear how *Eba'cad* translational regulation is mediated in *Episyrphus*.

During early *Tribolium* embryogenesis, the embryo develops from a syncytial blastoderm, where nuclei aggregate at the posteroventral side to form the embryo proper and anterior nuclei shape the extraembryonic tissues, namely the amnion and the serosa (Schröder et al., 2008). *Tribolium* does not possess a *bcd* homologue and anterior patterning seems to be dependent on the function of at least two maternal determinants, *Tribolium orthodenticle-1* (*Tc'otd1*) and *Tribolium hunchback* (*Tc'hb*). In the absence of *Tc'otd1* and *Tc'hb*, *Tribolium* embryos fail to develop head, thoracic and anterior abdominal segments, which is reminiscent of severe *bcd* mutants in *Drosophila* (Schröder, 2003).

Two other maternal genes carry out the repression of uniform maternal *Tc'cad* mRNA in *Tribolium* embryos. *Tribolium zen-2* (*Tc'zen-2*) and *Tribolium Mex-3* (*Tc'Mex-3*) are expressed in the serosa and anterior head region, respectively, and have been shown to restrict Tc'CAD protein from these anterior regions by RNAi analysis (Schoppmeier et al., 2009). In *C. elegans*, the KH-domain protein MEX-3 is required to restrict the *cad*-like homeodomain protein PAL-1 to the posterior blastomeres (Draper et al., 1996; Hunter and Kenyon, 1996). Anterior repression of *Tc'cad* mRNA by Tc'MEX-3 was therefore suggested to be an ancient patterning mechanism that was taken over by *bcd* in the lineage of higher dipterans (Schoppmeier et al., 2009).

Very little is known about the origins of polarity and the mechanisms that set up the localization and expression of maternal mRNAs in *Tribolium* embryos (Lynch et al., 2010; Peel and Averof, 2010). Because of the connection between the evolution of *caudal* regulation and the evolution of *bcd* and its function as a translational regulator, it is important to assess the role of *bcd*-related genes during insect embryogenesis. Both genes *Tc'zen-2* and *Drosophila bcd* stem from a *Hox3/zen-like* progenitor (Fig. 2.2, B). First evidence for a common underlying mechanism responsible for the regulation of *caudal* in *Tribolium* and *Drosophila* came from experiments performed by Wolff et al.

(1998), where *Tc'cad* transcripts expressed in *Drosophila* transgenic embryos were translationally repressed in a BCD-dependent manner. The *zen* genes in *Tribolium*, however, are not maternally expressed (Falciani et al., 1996; Dearden et al. 2000). Anterior repression of *Tc'cad* mRNA seems to depend therefore on zygotic activity of *Tc'zen-2*.

Tc'zen-2 has a sister gene, *Tc'zen-1*. Both genes arose through a gene duplication event from a *Hox3/zen*-like progenitor in the lineage of *Tribolium* (Fig. 2.2, B) and share overlapping expression patterns (Brown et al., 2002; Falciani et al., 1996). *Tc'zen-1* acts early in development and specifies the extraembryonic serosa. Lack of *Tc'zen-1* activity results in loss of serosa and an expanded posterior germband. The loss of the anteriormost cells can be compensated by the embryo, which then develops normally. *Tc'zen-2* has more severe effects, as it is also necessary for the fusion of the extraembryonic tissues amnion and serosa, which is required for dorsal closure. Embryos that fail to express *Tc'zen-2* close ventrally and take on an “inside-out” topology (van der Zee et al., 2005). The early role in anterior patterning of *Tc'zen-1* was interpreted as a favourable condition for the evolution of *bcd* (van der Zee et al., 2005). Furthermore it was proposed that the acquisition of an mRNA localization signal in the 3'UTR and the presence of a pre-existing anterior localization mechanism lead to the evolution of *bcd* (Bucher et al., 2005).

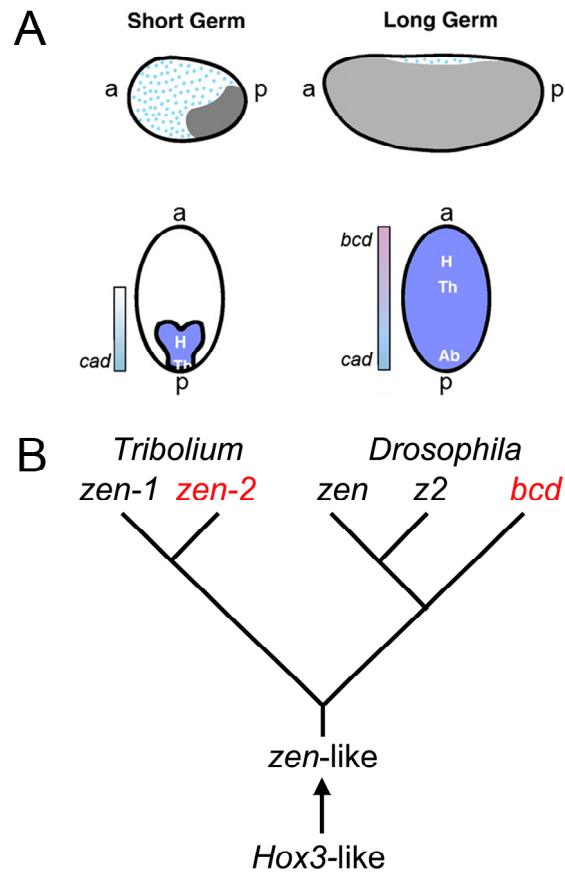


Fig. 2.2: Long-germband development vs. short-germ development and the evolution of *Hox3*-like genes in the lineage of *Tribolium* and *Drosophila*. (A) In the short-germband embryo, the embryo proper occupies a small region at the posterior part of the egg (grey), whereas the rest gives rise to extraembryonic tissue (blue dots). The body segments that are patterned in this blastoderm are the head segments (H) and thoracic segments (Th) (ventral view in blue); posterior segments will be added progressively from a posterior growth zone. In the long-germ embryo, most of the blastoderm will give rise to the embryo proper (grey) and the segments of the head (H), thorax (Th) and abdomen (Ab) are specified simultaneously (ventral view in blue). *Tribolium* forms a short germ, whereas *Drosophila* forms a long germ. (B) The common ancestor of *Tribolium* and *Drosophila* most likely owned one *Hox3*-like gene of the *zen*-type. In the lineage that lead to *Tribolium*, this *zen*-like progenitor duplicated giving rise to two *zen* homologues, *zen-1* and *zen-2*. In the lineage of *Drosophila*, a gene duplication resulted in appearance of the *zen*-type gene progenitor and the *bcd*-type gene progenitor. The *bcd* progenitor evolved into the *bcd* gene, the *zen*-type progenitor duplicated again and gave rise to the two *zen*-orthologues, *zen* and *z2*. (A modified after Rosenberg et al., 2009).

2.2 The anterior patterning factor Bicoid

2.2.1 Evolution of Bicoid

bcd and *zen* are sister genes belonging to the Hox-gene cluster and have evolved after a gene duplication from a *Hox3*-like ancestor (Falciani et al., 1996; Stauber et al., 1999). The gene duplication that gave rise to the progenitors of *bcd* and *zen* occurred in the diptera, as *bcd* orthologues have only been found in flies that belong to the Cyclorrhapha (Fig. 2.3) (Lemke et al., 2008; Stauber et al., 2000). Both genes have evolved much more rapidly than their neighbouring Hox genes (Falciani et al., 1996; Sommer and Tautz, 1991; Stauber et al., 1999) and have acquired different functions during early development. In the lineage leading to *Drosophila melanogaster* a second gene duplication gave rise to the two orthologues *zen* and *z2*. Both genes share identical expression patterns, however as deletion experiments showed, only *zen* can provide full *zen* gene function (Pultz et al., 1988; Rushlow et al., 1987a).

In *Drosophila*, *bcd* is required for the patterning of the head and thorax, while *zen* is involved in the specification of the extraembryonic tissue anlagen (amnioserosa). *bcd* is a maternal gene, expressed only in the nurse cells and deposited as mRNA into the oocyte, where it becomes localized anteriorly. *zen* is zygotically expressed in a broad region at the dorsal side of the embryo and retracts later into a narrow dorsal domain to specify the amnioserosa (Bate and Martínez Arias, 1993; Rushlow et al., 1987a; Rushlow et al., 1987b).

The maternal expression of *bcd* homologues is conserved among different cyclorrhaphan flies, whereas maternal expression of the *zen* progenitor was lost in the lineage of Cyclorrhapha. Stauber et al. (2001) have analysed the expression patterns of *Hox3*/*zen*-like orthologues from several non-cyclorrhaphan dipterans and found that the identified gene sequences are more similar to the *zen*-type gene. However they share expression patterns similar to both *bcd* and *zen* homologues (Stauber et al., 2002).

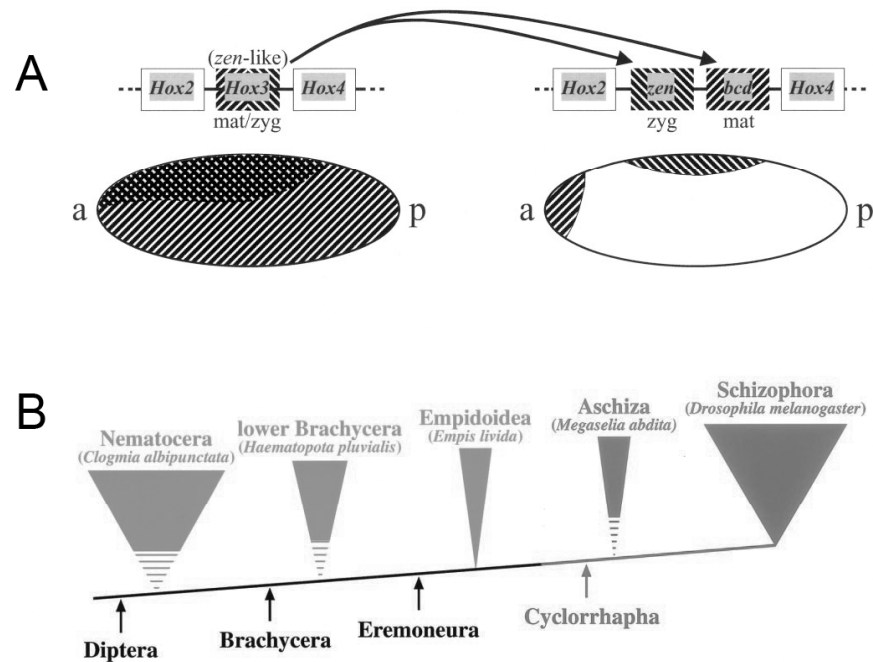


Fig. 2.3: Schematic overview of putative evolution of *bcd* and *zen* in taxa of diptera. (A) A gene duplication of a *Hox3/zen*-like gene with putative combined maternal and zygotic expression patterns gave rise to the sister genes *zen* and *bcd*. (B) This duplication occurred in the lineage of the cyclorrhaphan flies (indicated by arrow). The Nematocera (like *Clogmia albipunctata*), Brachycera (like *Haematopota pluvialis*) and Aschiza (like *Megaselia abdita*) are most likely paraphyletic groups, whereas the monophyly of the taxa Empidoidea (like *Empis livida*) and Schizophora (like *Drosophila melanogaster*) is well supported (Yeates and Wiegmann, 1999). (Taken from Sander and Schmidt-Ott, 2004; Stauber et al., 2002).

2.2.2 Function of Bicoid

The full-length Bicoid protein consists of 494 amino acids, including several functional domains that are indicated in Fig. 2.4. BCD is a special transcription factor because it has a dual function in DNA-binding where it acts as a transcription factor and in RNA-binding where it acts as a translational repressor (Dubnau and Struhl, 1996; Rivera-Pomar et al., 1996; Struhl et al., 1989). With its K50-homeodomain it binds to the DNA consensus sequence TAATCC (Driever and Nüsslein-Volhard, 1989). The residue with key role in target specificity is a lysine at position 50 in the third helix of the homeodomain. Position 54 is occupied by an arginine and this modification is unique to the homeodomain of BCD (Mcgregor, 2005). The arginine-rich motif in the homeodomain and specifically R54 is crucial for RNA-binding during translational repression of *cad* mRNA (Niessing et al., 2000). Two other domains of the BCD protein have been reported to be involved in translational repression. The d4EHP-binding

domain, through which BCD directly binds to the 5'-cap binding factor d4EHP (Cho et al., 2005). and the PEST domain (amino acids 170-203) (Niessing et al., 1999).

Fig. 2.4 shows additional regions of the BCD protein that have been identified and found to influence its activity as a transcriptional activator (Janody et al., 2001; Schaeffer et al., 1999; Zhao et al., 2002).

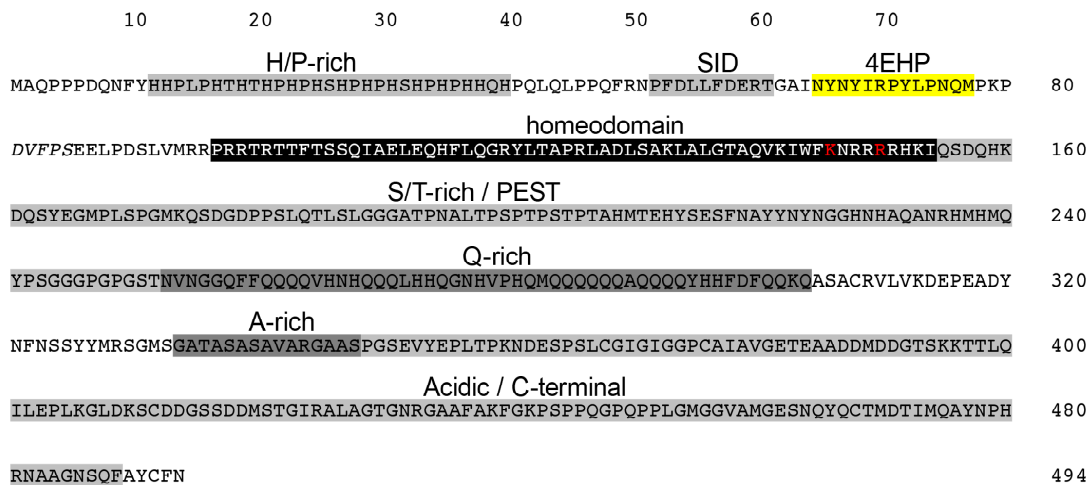


Fig. 2.4: The protein domains of BCD isoform G. The BCD protein is a polypeptide of 494 amino acid residues and the homeodomain is indicated in black and the lysine and arginine at position 50 and 54 highlighted in red. The self-inhibitory domain (SID) spanning at least aa 52-61 repressed BCD activity in S2 cells (Zhao et al., 2002). The 4EHP-domain (4EHP, indicated in yellow) and the PEST domain have been shown to be involved in translational regulation of *cad* mRNA (Cho et al., 2005; Niessing et al., 1999). In cell culture, the serine/threonine rich domain (S/T-rich, aa 152-252), the glutamine-rich domain (Q-rich, aa 253-300), and acidic C-terminal domain (Acidic/C-terminal aa 349-489) act as activation domains, whereas the alanine-rich domain (A-rich, aa 334-348) seems to be a repression domain. The function of the histidine/proline-rich domain (H/P-rich, aa 11-42) remains elusive. Furthermore, the S/T-rich domain and the C domain mediate the downregulation by Torso (Janody et al., 2001; Schaeffer et al., 1999).

2.2.3 The Bicoid isoforms

The *bcd* gene generates five mRNAs through alternative splicing of four major exons (termed exon 1-4, Fig. 2.5). Exon 1, present in all isoforms, encodes the 5'UTR and a histidine/proline-rich repeat (H/P-rich) at the N-terminus. Exon 2 encodes the self-inhibitory domain (SID) and the 4EHP-binding domain, exon 3 encodes the homeodomain, the serine/threonine-rich domain (S/T-rich), a glutamine-rich domain (Q-

rich) and an alanine-rich domain (A-rich). The acidic C-terminal domain (Acidic) is encoded in part by the exons 3 and 4. Exon 4 also contains the 3'UTR and is present in all isoforms. The presence of alternative splice acceptor sites on exons 2 and 3 results in isoforms containing slightly longer or shorter versions of exon 2 (2a or 2b) and exon 3 (3a or 3b), respectively (Fig. 2.5).

mRNA isoforms G and D code for the longest protein products. Whether the mRNA isoforms E and F result in their respective protein products is unclear because of an in frame stop codon in exon 2a (Fig. 2.5, indicated by arrows). A putative ORF could start from a start codon that lies further downstream in exon 2a (Fig. 2.5, indicated in red; Fig. A5.1). Isoform A, which has the shortest ORF of all isoforms consists only of exon 1 and 4.

Most studies refer to isoform G as the wt BCD protein, however, to date, the existence of *bcd* splicing variants has been largely ignored and it is unclear to what extent each isoform contributes to BCD function during embryogenesis. Interestingly, the putative protein isoforms E and F contain all domains crucial for transcriptional activation of target genes, but are lacking the 4EHP-binding domain implicated in the 5'-cap structure mediated translational repression of the *cad* mRNA (Cho et al., 2005) (Fig. 2.5). The *bcd* gene has five annotated transcripts, of which all isoform cDNAs have been recovered from ESTs of *Drosophila* embryonic libraries; only BCD isoform D and G are annotated as fully sequenced cDNA clones. There are indications from RNA sequencing expression profiling that at least the transcripts of isoform G, D, E and F are all present in the early embryo (Tweedie et al., 2009)(Fig. A5.2).

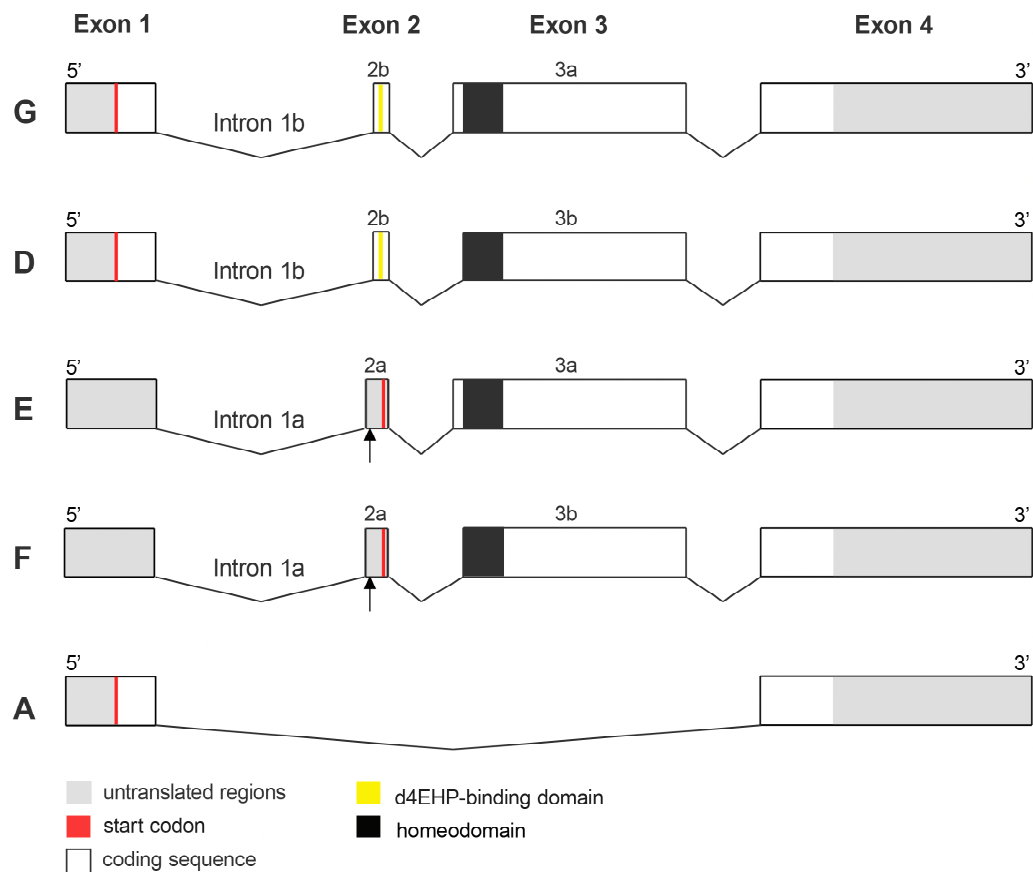
bcd isoforms

Fig. 2.5: Schematic overview of the *bcd* transcripts produced by differential splicing of four major exons. Exon 1 and 4 are present in all isoforms. Alternative splicing with two splice acceptors at the 5' end of exon 2 results in the presence of either exon 2a, which contains an in frame stop codon (arrows) and is thought to initiate translation on a downstream AUG. Exon 2b maintains the ORF from the upstream AUG in exon 1. Alternative splicing with two splice acceptors at the 5' end of exon 3 results in the presence of exon 3a or 3b, which differ in their capacity to encode a short peptide sequence (DVFPS). Untranslated regions are marked in grey, the coding sequences are marked in white. The 4EHP-binding domain is indicated in yellow, the homeodomain is indicated in black.

2.3 Mechanism of *cad* translational regulation in *Drosophila*

Maternal *cad* mRNA is distributed uniformly in the oocyte and early *Drosophila* embryo. The formation of the BCD AP gradient generates an opposing gradient of the CAD protein (Fig. 2.1, B). In this process, BCD directly binds to specific region(s) in the *cad* 3'UTR to mediate the translational repression of the *cad* transcripts. The BCD RNA-binding property stems from its K50/R54-homeodomain, which is capable of binding directly to BCD-binding element(s) (Chan and Struhl, 1997; Dubnau and Struhl, 1996;

Rivera-Pomar et al., 1996). The dual DNA and RNA-binding function of BCD depends on two amino acid residues (K50 and R54) in the third helix of the homeodomain that, in this combination, are unique to BCD (Niessing et al., 2000). The 3'UTR element to which BCD binds has been characterized biochemically and genetically and includes a 120 nt and a 323 nt fragment of the *cad* 3'UTR (Dubnau and Struhl, 1996; Rivera-Pomar et al., 1996) (see Fig. 3.1). When the 323 nt fragment is removed from the *cad* 3'UTR, CAD becomes ectopically expressed in the anterior part of the embryo (Dubnau and Struhl, 1996; Rivera-Pomar et al., 1996). A specific homeodomain/RNA recognition motif as not yet been identified.

For the translational repression of *cad* transcripts, BCD requires direct interaction with *Drosophila* 4E homolog protein (d4EHP) through its d4EHP-binding domain. d4EHP is a eIF4E-related protein, which binds directly to the 5'-cap structure of the mRNA, but has lost its ability to interact with eIF4G (Hernández et al., 2005). The simultaneous interaction of BCD with the 3'UTR and the cap-associated d4EHP renders the *cad* mRNA translationally inactive. The mechanism of d4EHP-dependent BCD-mediated translational repression of *cad* has been proposed as a new paradigm for translational control (Cho et al., 2005) (Fig. 2.6).

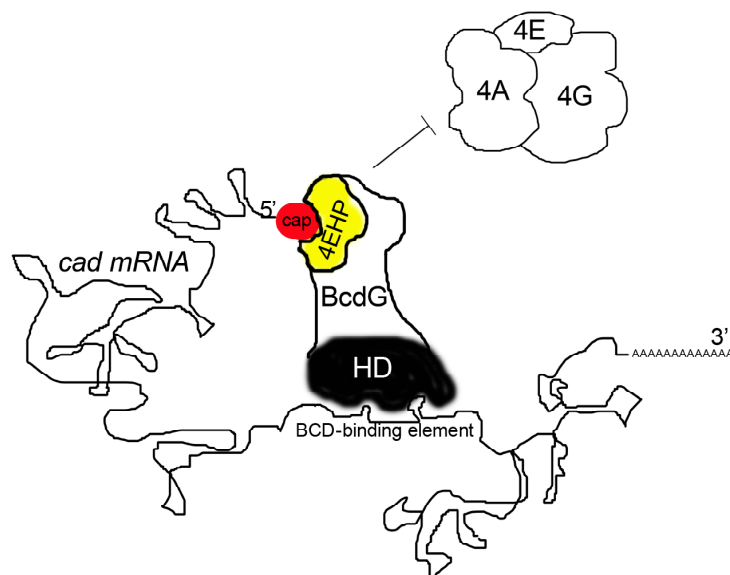


Fig. 2.6: Model of *cad* translational repression, proposed by Cho et al. (2005). BCD binds via its homeodomain (black) to the BCD-binding element(s) in the 3'UTR of the *cad* mRNA and at the same time interacts with 4EHP (yellow), which binds to the 5' cap structure (red). Hence, the translational initiation factors are prevented from binding to the *cad* mRNA and remains untranslated. (Modified after Cho et al., 2005).

2.4 miRNA function during early *Drosophila* development

During this PhD, the analysis of *cad* 3'UTR elements that mediate BCD-dependent translational repression lead me to investigate the putative role of microRNAs (miRNAs) in *cad* translational regulation. miRNAs are short (~22 nt) non-coding RNAs. They have gained increasing recognition in the post-transcriptional regulation of gene expression in animals and plants. In animals, miRNAs interfere with mRNA translational and/or stability through imperfect base pairing to the 3'UTR of their target mRNAs. Target-site recognition requires complementarity of the miRNA 5'-region, which is called the seed sequence, with sequences in the target mRNA. Incorporated in the RNAi induced silencing complex (RISC), miRNAs guide the RISCs to their targets in a sequence specific manner and mediate translational control (Ameres et al., 2007; Jackson and Standart, 2007; van den Berg et al., 2008). The target mRNAs become translationally repressed or subjected to degradation by RISC, depending on the degree of sequences complementarity of the miRNA to the mRNA (Bartel, 2004; Carrington and Ambros, 2003). The core proteins of RISC belong to the protein family of Argonaute (Ago) proteins. In *Drosophila*, the Ago proteins Ago1 and Ago2 associate with different types of small RNAs (miRNAs and siRNAs) which dictates their functions. Ago1-RISC mediates translational repression of the target mRNA by de-polyadenylation of the poly(A)-tail, whereas Ago2-RISC blocks the functions of the cap-structure (Iwasaki et al., 2009). Translational repression by Ago1 and Ago2 are therefore mechanistically different. However, it seems that translational repression by RISC is put into effect through various mechanism acting on different steps of translational initiation (Chendrimada et al., 2007; Humphreys et al., 2005; Kiriakidou et al., 2007; Mathonnet et al., 2007; Pillai et al., 2005; Thermann and Hentze, 2007).

For a number of miRNAs in *Drosophila*, the expression profiles have been identified and their role in development has been analysed during early development (Aravin et al., 2003; Leaman et al., 2005). Injections of 2'O-methyl oligoribonucleotides with complementary to miRNAs into early *Drosophila* embryos demonstrated the involvement of miRNAs in processes like cellularization, segmentation, dorsal closure and apoptosis. (Leaman et al., 2005).

The *cad* 3'UTR harbours two putative miRNA target sites that have been predicted computationally; the target sequence of miR-308 is located in region nt 299-316 and the miR-305 target sequence in region nt 534-545 in the *cad* 3'UTR. (Betel et al., 2008; Brennecke et al., 2005; Lai et al., 2003; Stark et al., 2005). Both miR-308 and miR-305

have been cloned from embryonic tissues, however neither of these two miRNAs has been detected by Northern blotting analysis. For miR-308, 4 independent clones have been isolated from a cDNA library of 0-2h of embryogenesis and 1 clone from a cDNA library of 2-4h of embryogenesis. For miR-305 there has been only 1 clone isolated from a cDNA library of 0-2h embryogenesis (Aravin et al., 2003). A function during development has been reported for miR-308 in control of apoptosis during embryogenesis. Embryos that are depleted of miR-308 activity show a mild increase in apoptosis during mid-embryogenesis (Aravin et al., 2003; Leaman et al., 2005).

2.5 Rationale

In the investigation of the anterior patterning factor(s) in *Tribolium*, Wolff et al. (1998) conducted a crucial experiment, in which they expressed the *Tribolium cad* homologue in *Drosophila* embryos. Surprisingly, the *Tribolium* transcripts were translationally regulated in a BCD-dependent manner. *Tribolium* itself though does not possess a *bcd* homologue. It was inferred that the *Tc'cad* 3'UTR sequence most likely contained a conserved binding element that could be recognized by BCD.

Eventually, more than ten years later, the translational regulators of the *Tc'cad* mRNA have been identified as *Tc'zen-2* and *Tc'Mex-3* (Schoppmeier et al., 2009). The putative binding elements in the *Tc'cad* 3'UTR to which *Tc'ZEN-2* and *Tc'MEX-3* bind have not been identified yet. *Tc'MEX-3* is a KH-domain protein and might require different sequences for RNA-binding than BCD. *Tc'ZEN-2*, however, is phylogenetically related to BCD.

Experiments with a *cad* homologue from the dipteran *Megaselia abdita* have shown that *Drosophila* BCD does not translationally regulate the *Mab'cad* 3'UTR, although a *Megaselia bcd* homologue is present in this species. Interestingly, *Mab'cad* mRNA is not maternally expressed as its homologues in *Drosophila* or *Tribolium* (Stauber et al., 2008).

These findings have posed some questions. Can BCD bind to a wide range of *cad* 3'UTR homologues and what are the requirements for BCD-recognition? What does the binding element of the *Tc'cad* 3'UTR, to which BCD can bind consist of and can we find any similarities to the BCD-binding element(s) in *Drosophila*?

The characterization of the *cad* 3'UTR homologues that are recognized by BCD and the detailed analysis of the BCD-binding element in *Drosophila* can help to gain further insight into when and how *cad* translational repression arose during evolution.

The aim of this study was to establish an *in vitro* assay using bacterially expressed BCD homeodomain and electrophoretic mobility shift assays for the detailed mapping of BCD-binding elements in the 3'UTR of different *cad* homologues. In a parallel approach, I aimed to establish an *in vivo* reporter assay, to test these BCD-binding elements in their capability to mediate BCD-dependent translational repression in living embryos.

3 Results and Discussion

3.1 Mapping of BCD-binding RNA-elements *in vitro*

Several studies have shown *in vitro* evidence for direct binding of the BCD homeodomain to distinct elements within the 3' UTR of *cad*. These elements range from nt 67 - 186 (BBR, Rivera-Pomar et al., 1996), nt 210 - 318 and nt 319 - 433 (termed BRE fragments B and C, Dubnau and Struhl, 1996) of the *cad* 3'UTR (Fig. 3.1). The initial experiments from Dubnau and Struhl could not be reproduced (Dubnau and Struhl, 1997), however it was possible to confirm sequence-specific binding of BCD to a 3'UTR fragment containing nt 210 - 253 using different conditions (Chan and Struhl, 1997).

BCD also seems to recognize mRNA sequences from the *Tribolium cad* homologue in transgenic *Drosophila* (Wolff et al., 1998), although in *Tribolium* the early regulation of maternal transcripts is taken over by other factors, such as *Tc'mex-3* and *Tc'zen-2* (Schoppmeier et al., 2009). The element that provides the BCD-dependent signal in the *Tribolium cad* mRNA has not been identified yet, but it is likely to be situated in the 3'UTR.

The horsefly *Haematopota pluvialis*, a dipteran and like *Drosophila* belonging to the group of the brachycera, does not possess a BCD homologue (Stauber et al., 2002). Nonetheless, maternal transcripts of the *Haematopota cad* (*Hp'cad*) homologue have been found in the nurse cells and oocyte (Stauber et al., 2008), suggesting the need for a mechanism that prevents maternal *Hp'cad* transcripts from being expressed in the anterior.

Taken together, these observations suggest that BCD may recognize the mRNAs of a range of *cad* homologues via element(s) that have been conserved in the course of evolution and mediate translational repression of the transcript. In order to identify these conserved elements, I conducted electromobility shift-assays (EMSA) using bacterially expressed BCD homeodomain (HD) and tested the binding of the homeodomain to different *in vitro* transcribed RNA fragments.

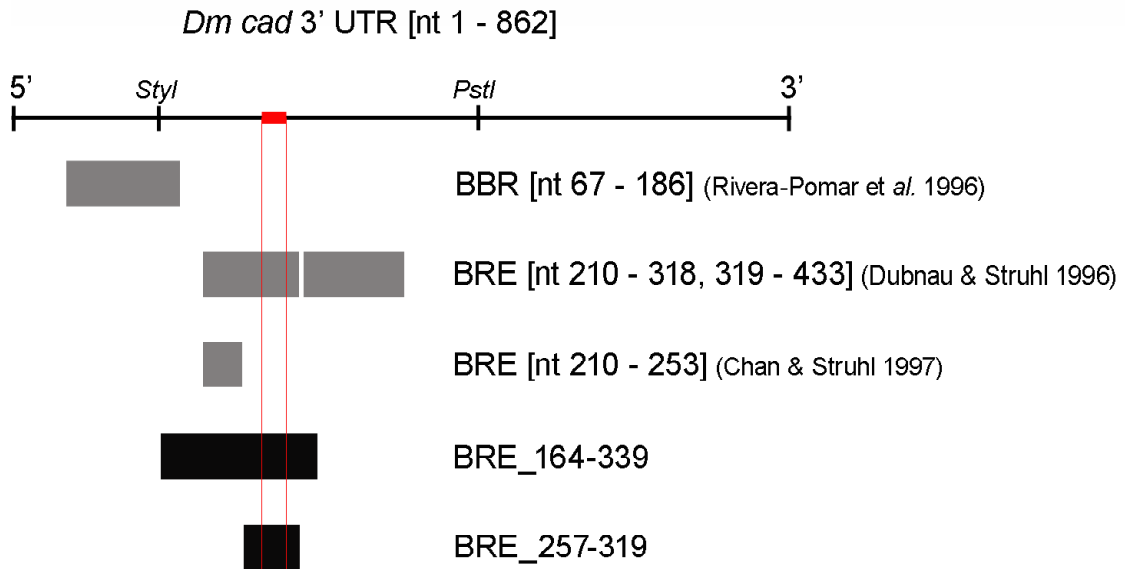


Fig. 3.1: *Drosophila cad* 3' UTR and RNA fragments previously described as Bicoid binding elements are indicated as grey shaded boxes. RNA fragments used in this study are indicated as black shaded boxes. The predicted miR-308 binding site in the *cad* 3'UTR is indicated with a red box. Numbering starts with the first nt after the stop codon.

3.1.1 Establishment of RNA-binding assay using recombinant BCD homeodomain protein

For the establishment of an RNA-binding assay with the BCD homeodomain I drew information for *in vitro* binding conditions from previously published work. The direct and specific interaction of the BCD homeodomain with the fragments BRE_210-318, BRE_319-433 of the *cad* 3'UTR were initially shown by *in vitro* binding of the BCD homeodomain from bacterial cell lysates to radiolabeled RNA probes and PAGE-analysis (Dubnau and Struhl, 1996). However the competition experiments done in this study were not reproducible. By using different binding conditions, competition experiments with bacterially expressed, purified BCD homeodomain and an RNA probe containing nt 210-253 of the *cad* 3'UTR were successful and confirmed the RNA sequence-specificity of the BCD homeodomain (Chan and Struhl, 1997). The binding conditions used by Chan and Struhl (1997) were used here as a first reference point.

Rivera-Pomar et al. (1996), using crosslinked RNA from full-length *cad* mRNA and derivatives to nuclear proteins from *Drosophila* embryos, demonstrated BCD-dependent binding of a 120 nt *cad* 3'UTR fragment, which was assigned as position 1350-1470 with the first nucleotide of the start codon as position 1 of the *cad* mRNA.

This region most likely corresponds to nt 66-185 of the *cad* 3'UTR (NCBI accession number AY069565), here termed BBR_66-185. However, there have been no attempts to show sequence-specificity of BCD homeodomain binding on this fragment by competition experiments. In subsequent binding experiments with bacterially expressed and purified BCD homeodomain, Rivera et al. (1996) used a 110 nt fragment, which was referred to as the BBR. With this fragment, the RNA-binding vs. DNA-binding capacity of mutagenised BCD homeodomain derivatives were tested (Niessing et al., 2000). An analysis of the sequence-specificity of the BCD homeodomain during RNA-binding was not performed.

Despite several attempts, I was not able to reproduce RNA-binding of bacterially expressed and purified BCD homeodomain using the same conditions as described by Chan and Struhl (1997) or Niessing et al. (2000). I found that the presence of 2,5 µg/µl heparin during the RNA binding reaction was inhibiting complex formation with the bacterially expressed BCD homeodomain (Fig. A1.1, C). I therefore decided to omit heparin from the RNA binding reactions. Furthermore, Chan and Struhl (1997) used 0.1 µg/µl yeast tRNA, whereas Niessing et al. (2000) used 5 µg/µl *E.coli* tRNAs. I found that the presence of 5 µg/µl of yeast tRNA inhibits complex formation with the fusion protein HisMBP-HD and a RNA probe spanning nt 164-512 of the *cad* 3'UTR determined that a concentration of 0.25µg/µl yeast tRNAs blocks unspecific binding properties of HisMBP-HD while allowing complex formation with the RNA probe (Fig. A1.1, A,B). After liberation of the homeodomain from HisMBP, the affinity to the RNA-target increased, so that 0.5µg/µl of yeast tRNAs were used during the binding reaction.

Because translational repression and transcriptional activation mediated by BCD both depend on the homeodomain, I further tested the functionality of the recombinant protein by binding to a dsDNA target site containing the consensus sequence 5'-CTAATCC-3' (Fig. 3.2, lanes 1-4). The binding of the BCD homeodomain to dsDNA was performed under the conditions determined to be best for RNA binding. DNA-binding of the BCD homeodomain is specific, which was also revealed by competition experiments (Fig. A1.2 and Fig. A1.3). This indicates that the bacterially expressed BCD homeodomain is functional.

3.1.2 Analysis of recombinant BCD homeodomain binding to RNA

For RNA binding I chose a 175 nt fragment spanning nt 164-339 of the *cad* 3'UTR (BRE_164-339, see Fig. 3.1), which contains the BRE_210-318 fragment (Dubnau and Struhl, 1996) and subsequently verified fragment BRE_210-253 (Chan and Struhl, 1997). The homeodomain was purified as a MBP-HD or GST-HD fusion protein. For the binding reaction, 5-40 pmole of the homeodomain were incubated with 300 fmole radiolabeled BRE_164-339 probe and run on a non-denaturing polyacrylamide gel (Fig. 3.2, lanes 5-7). Parallel binding reactions were performed using 300 fmole of an unrelated RNA fragment of similar size (*Adh3'* 184 nt) (Fig. 3.2 lane 8-10) and 2 pmole of the target dsDNA (Fig. 3.2, lanes 1-4).

The BRE_164-339 runs in two major bands (I. and II.), which is probably due to different structural conformations of the RNA molecule (Fig. 3.2, lane 5). With 40 pmole BCD homeodomain complexes are formed with BRE_164-339 bands I. and II., indicated by a higher running band in the gel (Fig. 3.2, lane 7), whereas the unrelated RNA fragment *Adh3'* does not shift at similar homeodomain concentrations. The binding affinity for the dsDNA seems to be higher, as the DNA shift occurs already with 2.5 pmole of BCD homeodomain.

To test whether the observed binding to BRE_164-339 is specific, I performed competition experiments using 40 pmole of homeodomain and 300 fmole of radiolabeled BRE_164-339 in the presence of different amounts of unlabeled (cold) specific (BRE_164-339) and unspecific (*Adh3'*) RNA (Fig. 3.3, lane 6-13, respectively). The HD:BRE_164-339 complexes (with both RNA species I. and II.) are strongly inhibited by a 20-fold excess of cold BRE_164-339 and completely absent at the presence of a 100-fold excess (Fig. 3.3, lane 6 and 7). At a 20-fold or 5-fold excess of cold BRE_164-339, the HD:BRE_164-339 complex is competed only slightly more efficiently than at similar amounts of cold *Adh3'* (Fig. 3.3, compare lane 7 to lane 11 and lane 8 to lane 12). In comparison, the homeodomain binds with high affinity to the dsDNA target, which was observed in DNA-binding and competition experiments (Fig. A1.2 and Fig. A1.3).

It is still unknown how binding to the RNA target occurs and what the minimal RNA binding motif exactly consists of. Using electrophoretic mobility shift assays I aimed to map the exact region(s) of the BCD binding element in the *Dm'cad* and in 3'UTRs of other *cad* homologues. I established *in vitro* binding conditions under which binding of recombinant BCD homeodomain to its RNA-binding target can occur. I found that

under native conditions RNA-binding of the bacterially expressed BCD homeodomain to the BRE_164-339 fragment occurs with a very low binding affinity. The low binding affinity to the BRE_164-339 fragment was not expected, since this fragment contains previously identified BCD binding elements (see Fig. 3.1), which were reported to be bound with high specificity by the BCD homeodomain (Chan and Struhl, 1997). Nonetheless, the here described recombinant BCD homeodomain is functional, which I could demonstrate in DNA-binding and -competition experiments.

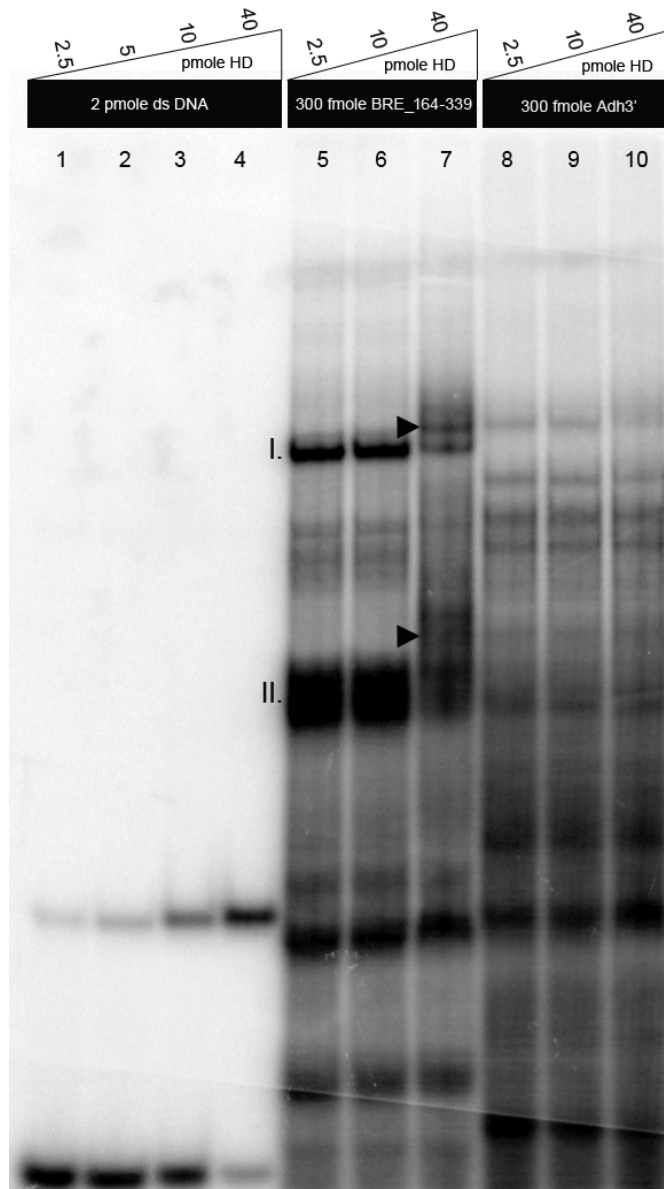


Fig. 3.2: DNA- and RNA-binding assay of BCD homeodomain. Lanes 1-4 show binding to 2 pmole of dsDNA target site at increasing homeodomain concentrations. With 300 fmole of BRE_164-339 probe (lane 5-7), the RNA is shifted at a homeodomain concentration of 40 pmole (lane 7). The RNA molecule of BRE_164-339 exists in two conformations (I. and II.) which are bound by the homeodomain (lane 7, arrowheads). In contrast, with 300 fmole of Adh3' the homeodomain does not seem to form a complex that migrates at shifted positions in the gel (lane 8-10).

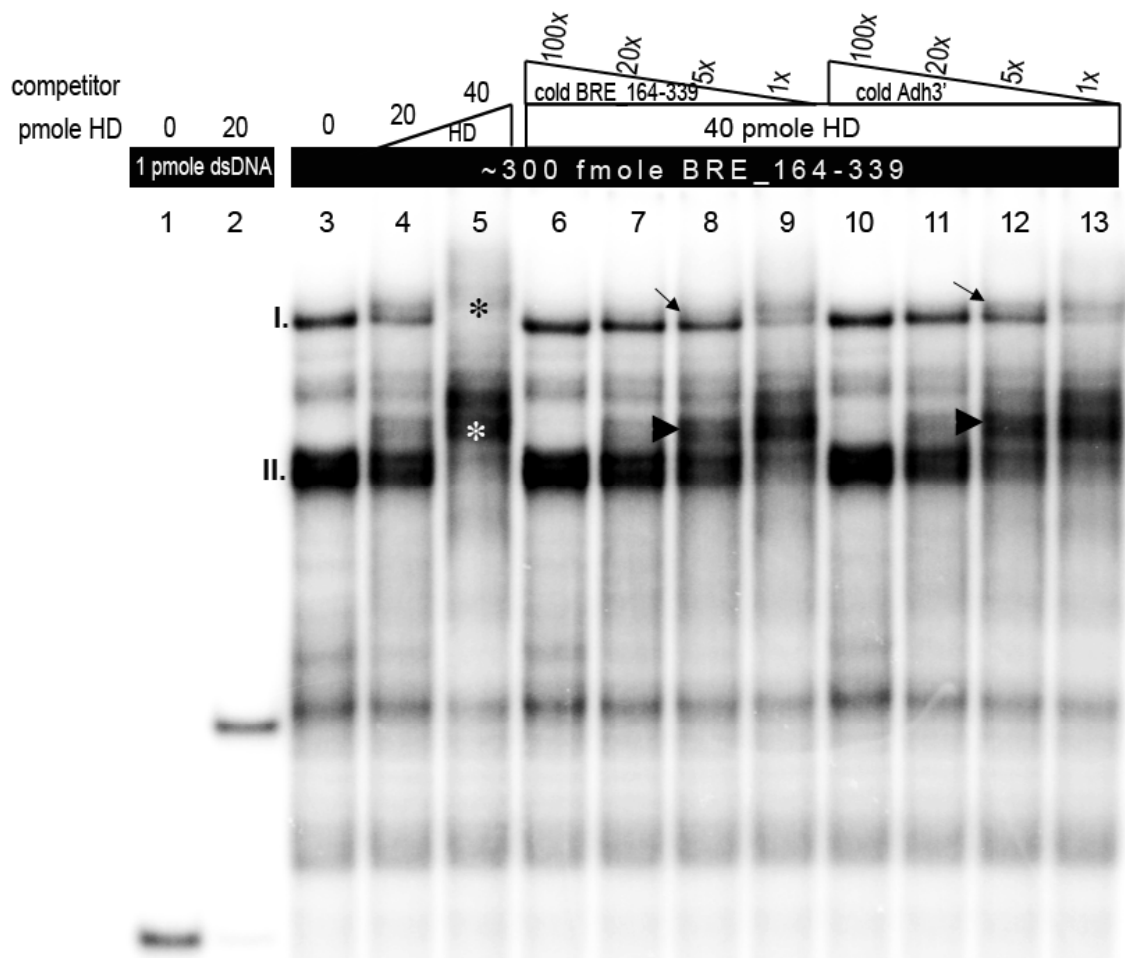


Fig. 3.3: Binding of BCD homeodomain to BRE_164-339. Both complexes of the homeodomain with BRE_164-339 I. and II. (indicated with asterisks in lane 5) are inhibited in the presence of 100-fold excess of cold BRE_164-339 or Adh3' (lanes 6 and 10). At 5-fold excess of cold competitor, complex HD: BRE_164-339 II is less severely inhibited by cold Adh3' (lane 12, arrowhead) than by the specific competitor (lane 8, arrowhead). Also the higher running complex of HD: BRE_164-339 I seems to be less severely inhibited by cold Adh3' (compare lane 8 with lane 12, arrows). Lanes 1-2 show DNA binding as a control for proper functionality of the homeodomain.

3.1.3 Characterization of the BCD binding element BRE₂₅₇₋₃₁₉ in the *Drosophila cad* 3'UTR

So far there have been three different Bicoid binding elements described in the *cad* 3'UTR (Chan and Struhl, 1997; Dubnau and Struhl, 1996; Rivera-Pomar et al., 1996) (see Fig. 3.1). Alignments of *cad* 3'UTRs from different *Drosophila* species do not show extensive sequence similarities among each other, apart from a highly conserved region of 38 nucleotides (Fig. 3.4, nt 271-308 in the *cad* 3'UTR, region indicated with asterisks, for the full alignment see Fig. A2.1), which is lying within the BRE₂₁₀₋₃₁₈ (Dubnau and Struhl, 1996), but outside of the BRE₂₁₀₋₂₅₃ fragment studied by Chan and Struhl (1997). Although translational repression of the maternal *cad* mRNA most likely depends on BCD in all *Drosophila* species, the overall level of sequence conservation of the previously described fragments BBR₆₆₋₁₈₅ and BRE₂₁₀₋₂₅₃ seems to be very low (Fig. 3.4).

In order to investigate whether the BCD homeodomain is able to bind to the BRE₂₅₇₋₃₁₉ fragment, I performed band-shift experiments (Fig. 3.5). At the same time I investigated the binding specificity of the bacterially produced homeodomain to RNA fragments with different structural qualities. The shSV40 fragment (79 nt from the SV40 3'UTR) is predicted to form several secondary structures (not shown). The CU58mer fragment, a CU polymer consisting of 76 nt with a random sequence of C and U, can not form a secondary structure and remains linear in structure predictions (not shown). The shSV40 and the CU58mer fragments were used to test for binding of the BCD homeodomain to randomly structured vs. unstructured RNA molecules. Since the shSV40 fragment is not a natural target of BCD, the structure of this fragment is referred to as random.

For RNA binding, 2.5 - 20 pmole homeodomain were incubated with 20 fmole BRE₂₅₇₋₃₁₉, 24 fmole shSV40 and 22 fmole CU58mer and the HD:RNA complexes separated in a native polyacrylamide gel (Fig. 3.5, lanes 1-15). A visible complex of the homeodomain and the BRE₂₅₇₋₃₁₉ fragment occurs at a concentration of 5 pmole of BCD homeodomain, whereas at similar concentrations the unrelated RNA fragments CU58mer and shSV40 are not bound by the homeodomain. In the EMSAs with the BRE₁₆₄₋₃₃₉ fragment, 40 pmole of BCD homeodomain were needed to produce a shift in mobility. With the BRE₂₅₇₋₃₁₉ fragment much less protein is required to produce shift in mobility. This shows that the shorter BRE₂₅₇₋₃₁₉ fragment is bound by the homeodomain with significantly higher affinity as the larger BRE₁₆₄₋₃₃₉

fragment and therefore smaller amounts of probes were allowed in the binding reactions (20 fmole BRE_257-319 vs 300 fmole BRE_164-339).

I observed slower migrating complexes at increasing homeodomain concentrations in the gel, which were also noticeable in band-shift experiments with the BRE_164-339 fragment, (Fig. 3.5, lane 9 and 10, Fig. 3.6, lane 3). These super-shifts could be interpreted as RNA:HD complexes with either multiple homeodomain molecules bound to the RNA or with multiple homeodomain molecules associated in protein-protein-RNA interactions. Experiments at more stringent binding conditions (elevated KCl concentrations) showed that the super-shifts become inhibited with increasing salt concentrations (Fig. A1.4).

The BCD homeodomain also binds to CU58mer and shSV40 at high concentrations (with 20 pmole homeodomain, Fig. 3.5, lanes 5 and 15), suggesting that the bacterially expressed homeodomain has a general RNA-binding affinity (“stickiness”), which is independent of the RNA sequence or structure. Hence, the super-shift complexes observed with the *cad* 3’UTR fragments appearing at high homeodomain concentrations (40 pmole homeodomain with the BRE_164-339 fragment and 20 pmole homeodomain with the BRE_257-319 fragment) might reflect saturation of all specific binding sites and subsequent “sticky” binding to unspecific sites in the RNA fragment.

In order to test the specificity of the RNA-binding below homeodomain concentrations that lead to the non-specific binding just mentioned I performed competition experiments with low concentrations of BCD homeodomain (Fig. 3.6, lanes 4-15). 5 pmole of homeodomain were incubated with 20 fmole of BRE_257-319 and competed with cold BRE_257-319 (lanes 4-7), shSV40 (lanes 8-11) and CU58mer RNA (lanes 12-15). I find that the formation of the BRE_257-319:HD complex is inhibited about 2 times more effectively by cold BRE_257-319 than by cold shSV40 (compare lane 5 and 9) and does not seem to be severely inhibited by the cold CU58mer RNA (lanes 12-15). These results suggest that the homeodomain can bind directly and specifically to the BRE_257-319 fragment *in vitro*, but again, only with a relatively low binding affinity. Interestingly, the cold RNA competitor shSV40 is able to disrupt binding while the unstructured RNA molecule CU58mer is not. The ability to form secondary structures may therefore be necessary for competing BRE_257-319 binding.

```

32
Dmel -----AC AGUAACAACU ACAUGGAGCC CCAUCAUCCG CUGCUGGGUG
Dpse GCGCUCGACA GCAAUGUGCU AUAGCAACAA UAUCAUCC.. .AC....GU. .U.....U.A U.....CGA. .A..AUCCGC
Dwil -----CU AUAACAACAC CAACAACA.U ..C.G...A ..ACA.C.A .A.C..GAAC .AU.A.CA.A
Dvir -----GA AUAGCUAUGA AAGCAGC--- -.GGGG.GGC .GCG..G.AG G..G.GGGG. .G..A.CUAU
Dmoj -----GC AUGGCUACCA GA--AUG--- -.G.G..G.. .UC.AAU.GA G..G..G.UA .A..AACAGU
Consensus ..... auagc.ac.a .a.ca.c.a. ag.agc.gcu ..auggagca .c...ag..g .ag.agc...

74
Dmel GUAGCGAGCG GGUGGAGUA GGAGCGUAG GAGCGUAGG AGGAGGAGGC GGACAACCGU GCGAUGUGUC CUUCAGUGCU
Dpse UA.UG.G.GU .....U.GU ..U.UGAGC. .GC.G.G... ..AU.....U ..UG----- ..... .A.....
Dwil A.G..A.CA. CA.CUAUA.G .A.CAA.GGC AGCAACA.UC .UCUUUG..U ----- UCA G.GUU.CU..
Dvir .G----- CUA..C..CG U.UCCACGU. AUCUG.CC.- U.....UUU... ----- .UAA GCA.UU..UA
Dmoj UGGAGACCA. CUA..C.ACG U.UUC.AGU. AGCUG.CUU- ..CUUCUA.U ----- .A.A GAAA....GG
Consensus .....g c.gug.ag.g ggu....g.g agc.gg.ag. ag.uu.g.u ..... .u.a.a guacagugcu

154
Dmel CCGCGUCUCG CCUUGGACUU GGCUUAACCC UUA-GGUCGC GCAGUCAGAC UGUUUUCGACC GAACCGAAAA GUUAAUAGGC
Dpse U.U.....U. .AG....U.. ..... .C...U.. A...U.... .GUGA. CCCAA..U.. UGGGCG.AUG
Dwil .A.AACA.GU ...A.UGA.. U.GCCGUGGA ..UG.C.UAG AGUUGGGACA GUACC.AUU. CC.AAC.GUC AGACUGUCAG
Dvir UUG.UCGG.C AGGG..GGG. U.UGGGUGAG .GUGU..G.G AG..GGGAUG GUGGG..GGG UC.AAC.GUU AGACUGUUUG
Dmoj .GU.GCAAGC AG..A....G CUUC..CAG. .GAUAAA.A .A..GAGA.G G.G.GG..GG UGGAGU.GG- -----
Consensus c..g.c.u.. c.uugga.uu .g.ua....c .u.ggu.g. a.agg.gaa. gg.u.cg..c .caaa..g.. .g...g...g

232
Dmel AGCCGGACGA AUGGAGGACU UGGCGGCCGU UGCACCUGGA AUAUUGCACG UUGUUA-UU UUUGUGAUUG UAUAUCCUG
Dpse U.AAU.GGAG .A..UA.UG. G.CGCAG..A ..-U... ..-... ..-... ..-... ..-... ..-...
Dwil G.A.U.U.AC CAUA..AUUA GA.GCAA.AG C.UCAU.U. ....C... ..-... ..-... ..-... ..-... ..-...
Dvir U.-----AG CC...U.CG. AU..C.U... C.AC.U.U. ....-... ..-... ..-... ..-... ..-...
Dmoj -----AG GC..C..CG- -----C.U.U. ....-... ..-... ..-... ..-... ..-...
Consensus .g...g.cag ..ggagg.gu ..g.c..cg. .g.ccu.u. ....-... ..-... ..-... ..-... ..-...

312
Dmel GUUUCGAC GCGCCAGAGU CCUCACAGCU AAACAAGU-- -----
Dpse ..G.UAUA.. ..UG.CCCAC G.....CGC .C....AAAC CCCUCCAAAA GCUCUCCAAU UUGAUGUAAA UUUGAUAAA
Dwil .CGCUA.A- -----A UG.UG.CA.G .CC...AAUA AAAAAAGUAGA GGAGUAGAAG AGGUUUUCUG UCUAAGCCAU
Dvir .CG.UCGUGG CACG.CUCC. GGCU----- GGC..C.CCC ACAGCGGCAC A-----
Dmoj .CG.UC.ACG CACG.CUCCA .GC.UUCAAC GGC..C.CCC ACAGCCAGGC AGCAGCAAGA GAAAUUUUAU UUAUUUUAAA
Consensus .cguu.aaa. ...gcc.c.. .guc.c.... a.c..ag..c aca.c.... .....a... ..u.u... u.....a.

```

Fig. 3.4: Sequence alignment of *cad* 3'UTRs from different *Drosophila* species. The BBR₆₆₋₁₈₅ (indicated with bold, blue letters) and the BRE₂₁₀₋₂₅₃ (indicated with green, bold letter) of the *D. melanogaster cad* 3'UTR do not show extensive sequence similarities to the other *Drosophila* species. The BRE₂₅₇₋₃₁₉ fragment (indicated as yellow box) contains a 38 nt sequence region, which is present in all species (conserved nt are indicated with a point). Interestingly, this box overlaps with a predicted target site of miR-308 (underlined) in *Drosophila* (Brennecke et al., 2005; Stark et al., 2005). Identical nucleotide to the Dmel sequence are indicated by a dot. Numbering refers to the Dmel sequence, with 1 being the first nucleotide after the stop codon of the ORF. The full alignment can be seen in Fig. A2.1. Alignments were performed with Multalin program version 5.4.1. (Multiple sequence alignment with hierarchical clustering, CORPET, 1988, Nucl. Acids Res., 16 (22), 10881-10890) Dmel = *D. melanogaster*, Dpse = *D. pseudoobscura*, Dwil = *D. willistoni*, Dvir = *D. virilis*, Dmoj = *D. mojavensis*.

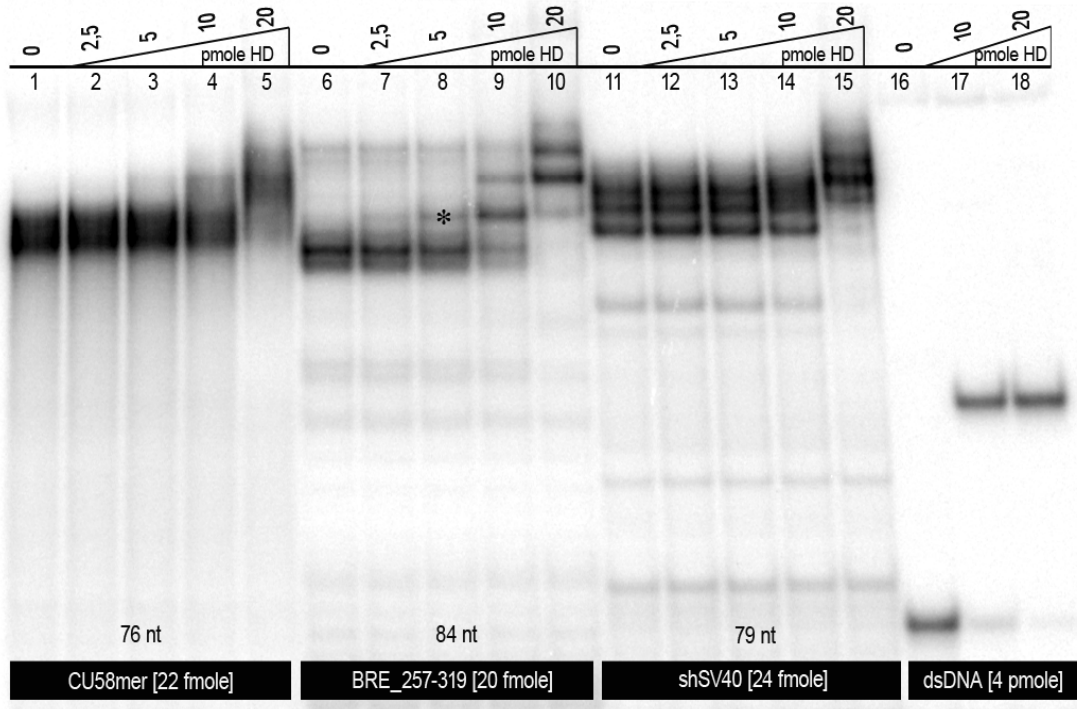


Fig. 3.5: Binding of BCD homeodomain to BRE_257-319 (lanes 5-10), to CU58mer RNA (lanes 1-5) and to shSV40 (lanes 11-15). The homeodomain binds to BRE_257-319 at a concentration of 5 pmole (lane 8, asterisk), but not to the unrelated RNA fragments (compare to lane 8 to 3 and 13). Lanes 16-17 show DNA binding as a control for functionality of the homeodomain.

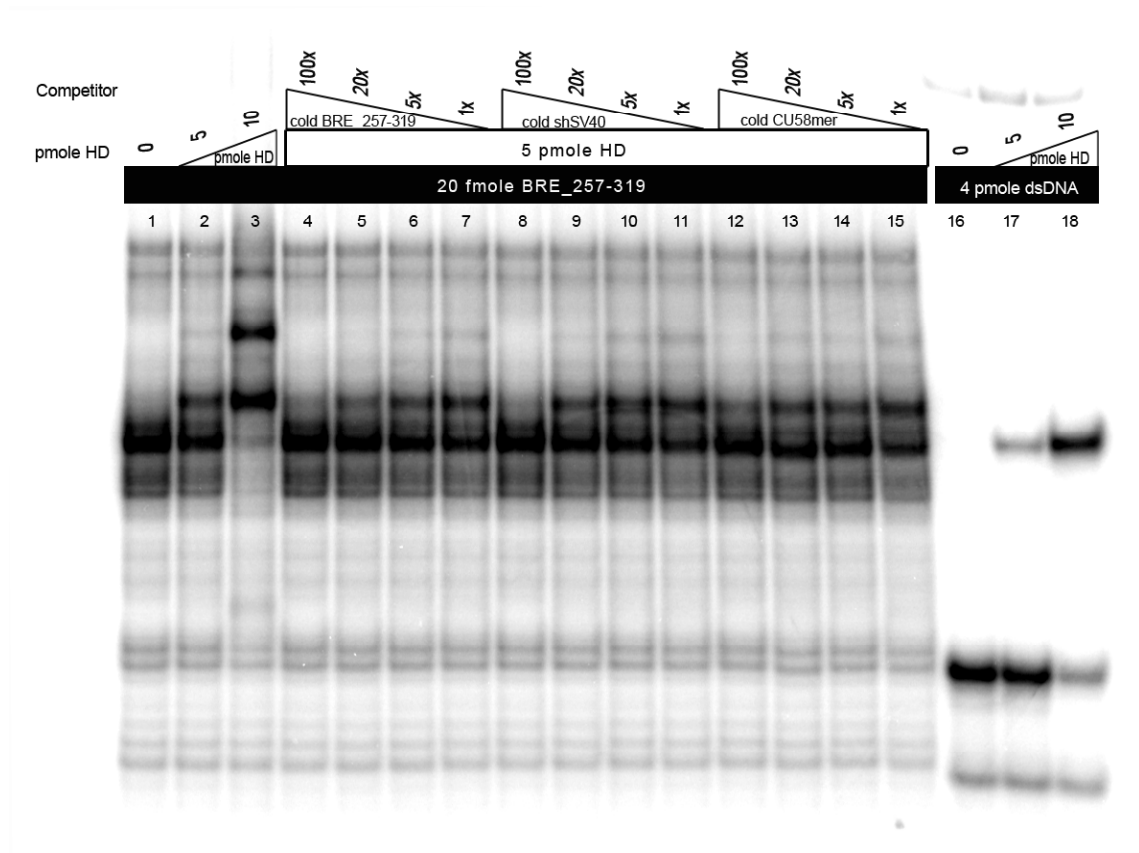


Fig. 3.6: Specificity of BCD homeodomain binding to BRE_257-319. The BRE_257-319 is shifted at a homeodomain concentration of 5 pmole (lane 2). Lanes 4-15 show competition of the BRE_257-319:HD complex with cold BRE_257-319, shSV40 and CU58mer. Binding of BRE_257-319 is competed slightly more efficiently by cold BRE_257-319 than cold shSV40 (compare lanes 5 and 9). The CU58mer RNA does not severely inhibit the formation of the BRE_257-319:HD complex (lanes 12-15). Lanes 16-18 show DNA binding, as a control for functionality of the homeodomain.

3.1.4 Identification of a *Haematopota cad* 3'UTR element that is bound by the BCD homeodomain

An interesting candidate in the study of BCD binding elements is the *cad* 3' UTR homologue from the dipteran *Haematopota*. This fly expresses maternal *cad* (*Hp'cad*) whose transcripts are present in nurse cells and in the oocyte (Stauber et al., 2008), however a BCD homologue does not exist in *Haematopota* (Stauber et al., 2002) and sequence alignments of the *Drosophila* and *Haematopota cad* 3'UTRs do not show any obvious sequence similarities. The 3'UTR of *Hp'cad* (*Hp3'*) consists of only 139 nt and is predicted to fold into a structure containing three stem-loops (H1 spanning nt 1 - 52, H2 spanning nt 52 - 89 and H3 spanning nt 88 - 126 of the *Hp'cad* 3'UTR) predicted by the *mfold* RNA folding prediction program (Mathews et al., 1999; Zuker, 2003) (Fig.3.7, A). Fig. 3.7 B shows the predicted secondary structures of the three stem-loop structures of the *Hp'cad* 3'UTR individually. Of which only H2 is likely to exist, due to the low free energy value ΔG ($\Delta G = 26.99$). Note that for fragments H1 and H3 each two secondary structures were predicted with ΔG values > -10 , indicating that these structures might not exist individually, however they might be present in the full-length RNA molecule of the *Hp'cad* 3'UTR (Fig. A4.1). The BRE_257-319 fragment forms a stem-loop structure with $\Delta G = -16.60$ (Fig. 3.7, C).

Interestingly, pairwise alignments of these distinct RNA structures using the RNAforester program (<http://bibiserv.techfak.uni-bielefeld.de/rnaforester>, (Höchsmann et al., 2003; Höchsmann et al., 2004)) revealed highest structure similarity between BRE_257-319 and H2, with structural similarity in the stem region (Fig. 3.7, D, marked in blue in the BRE_257-319 structure and in green in the H2 structure, Fig. A4.2).

In order to test whether the BCD homeodomain can bind to the *Hp'cad* 3'UTR, I performed band-shift experiments, using three different fragments (termed H1, H2 and H3). 30 pmole of each *Hp'cad* 3'UTR fragment were incubated with 2.5 - 7.5 pmole homeodomain (Fig. 3.8, lanes 9-20) and compared to binding of 30 pmole of BRE_257-319 (Fig. 3.8, lanes 1-4). I observed that the BCD homeodomain can shift the H2 fragment (Fig. 3.8 lanes 15 and 16), but not H1, H3 or shSV40 (Fig. 3.8, shSV40 lanes 5 - 8, H1 lanes 9 -12 and H3 lanes 17 -20). The observed shift of H3 in Fig. 3.8 could not be reproduced in an independent experiment.

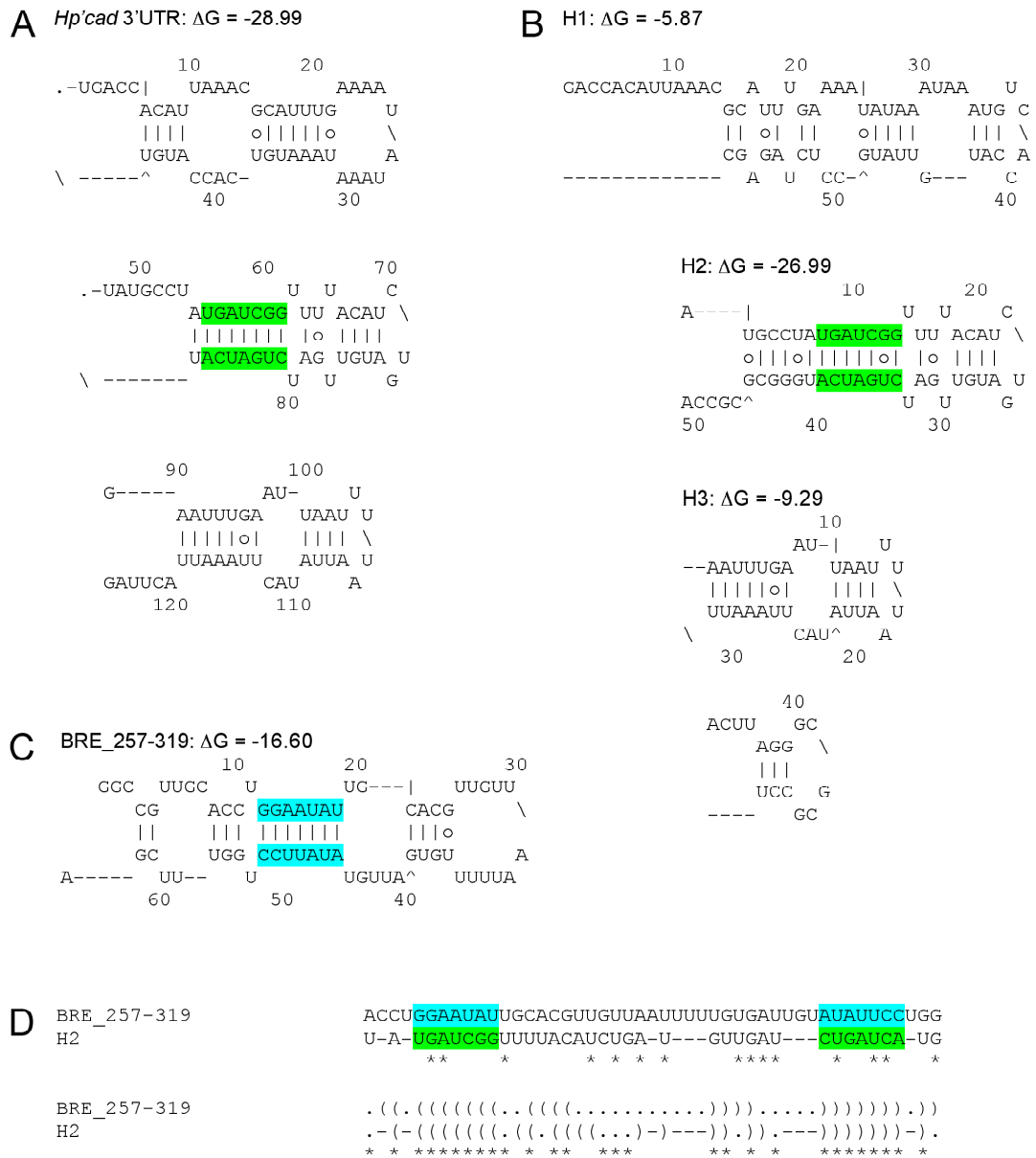


Fig. 3.7: Comparisons of secondary structures of the *Hp'cad* 3'UTR and BRE_257-319. (A) Secondary structures prediction of the *Hp'cad* 3'UTR and **(B)** the individual *Hp'cad* 3'UTR fragments H1, H2 and H3, numbers in parentheses indicate ΔG at 25°C. Note that H2 and BRE_257-319 show the highest ΔG values. **(C)** Secondary structure prediction of BRE_257-319 fragment. Secondary structure predictions were performed using the mfold program (version 2.3). **(D)** Secondary structure alignment of BRE_257-319 and H2 using the RNAforester program. The sequences of the stem-structures are indicated in blue (BRE_257-319) and green (H2). All RNAforester alignments can be seen in APPENDIX 4.

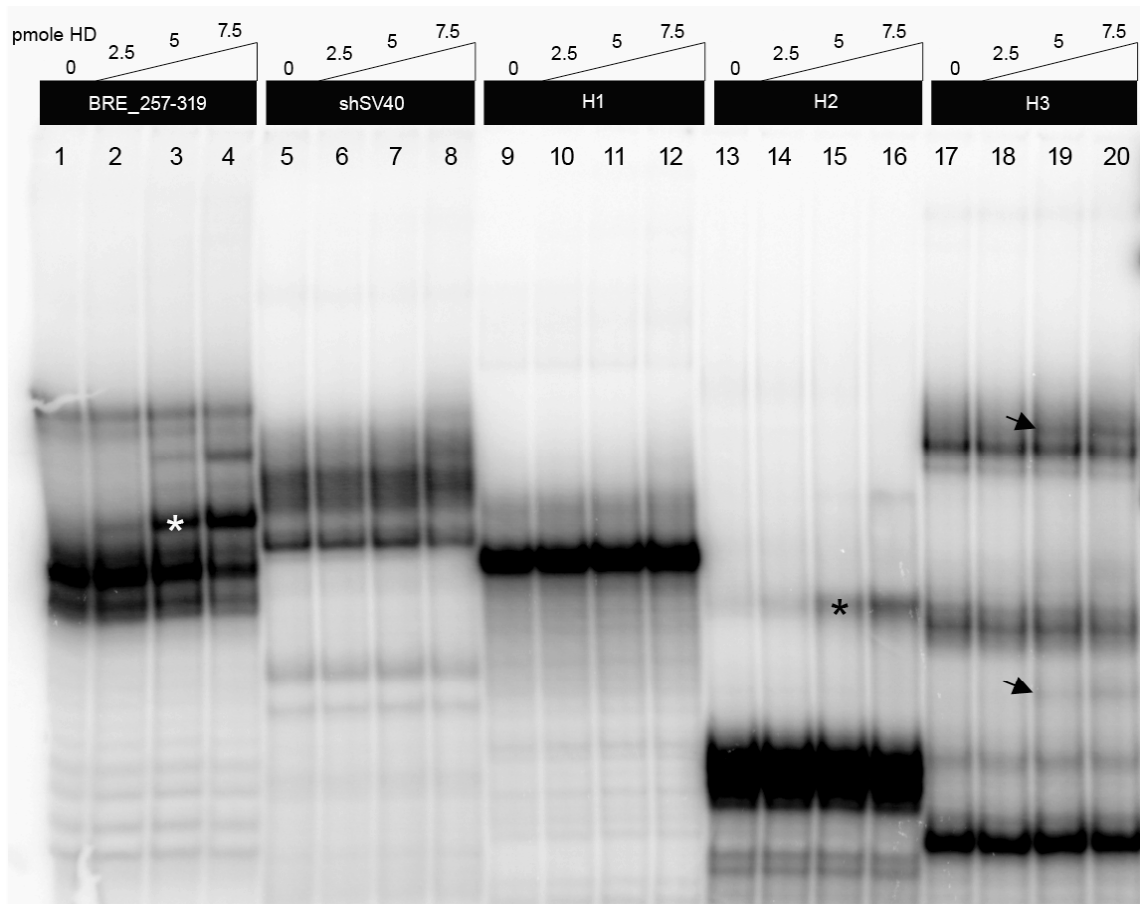


Fig. 3.8: Binding of the BCD homeodomain to *Haematopota* 3'UTR fragments H1, H2 and H3. Mobility shifts can be observed of the BRE_257-319 fragment (lane 3 and 4, white asterisk) and to a lesser extent of the H2 fragment (lane 15 and 16, black asterisk) at a homeodomain concentration of 5 nM, but not of shSV40 or H1 and H2 fragments. Shifted bands in lane 19 and 20 (arrows) could not be reproduced in an independent experiment.

3.1.5 Conclusions

The bacterially expressed BCD homeodomain can bind to fragments of the *cad* 3'UTR (BRE_164-339 and BRE_257-319). However, competition experiments revealed that the binding occurs with low affinity, since these fragments are not more than 2-fold efficient as competitors than unrelated RNA fragments. The bacterially expressed BCD homeodomain used by Chan and Struhl (1997) was used in the presence of 1µg/µl yeast tRNA and 2.5 µg/µl heparin. Both molecules are used as reagents to block unspecific binding of the RNA/DNA-binding BCD homeodomain. In comparison, the BCD homeodomain discussed here shows a much lower tolerance for these reagents during the RNA-binding reaction. This could be the result of different protein purification methods used here and by Chan and Struhl (1997). I have used two different methods for the purification of the BCD homeodomain, which are dependent on the fusion peptide (His-tag and GST-tag purification). For both protein preparations methods I obtained similar results for the BCD homeodomain RNA-target affinity. The DNA/RNA-binding domain of the BCD homeodomain from both preparation methods seems to be intact, because DNA-binding and competition experiments revealed high DNA-binding specificity of these BCD homeodomains.

The unspecific RNA probe (Adh3') can not be directly bound by the BCD homeodomain, however its presence in a 5-100 fold excess to the specific probe inhibits the formation of the HD: BRE_164-339 complex extensively, albeit slightly less efficient than the specific competitor (BRE_164-339). This small difference in competition efficiency is most likely due to a somewhat higher binding specificity to the BRE_164-339 fragment than to the unrelated probe Adh3'. Nevertheless, there seems to be a discrepancy between the ability of the Adh3' probe to bind to the homeodomain and the ability to act as a competitor.

An explanation for this could be that Adh3' and the BRE_164-339 can interact with each other through imperfect or partial hybridizations, which interfere with BCD homeodomain binding. I noticed in an earlier EMSA experiment that higher running bands occur according to the addition of cold specific or unspecific competitor. These putative RNA-RNA-complexes were distinguishable according to their different sizes (not shown). In that particular EMSA and unlike in the here described method, the cold competitor was added to the labelled RNA probes prior to the addition of the protein. Hence, RNA-RNA-interactions between the labelled and unlabelled RNA molecules were given an advantage to occur and to form imperfect hybridized RNA-complexes. In

combination with a low RNA-binding affinity of the BCD homeodomain, these RNA-RNA-hybrids may cause great interference to the formation of HD: BRE₁₆₄₋₃₃₉ complexes. In binding reactions, where the labelled BRE₁₆₄₋₃₃₉ probe was first added to the homeodomain and the competitors after homeodomain binding has occurred, the above mentioned RNA-RNA-interactions may be less likely to interfere. Generally, during the binding reaction the formation of equilibrium of the free RNA molecules, free protein and complexes of RNA and protein is depending of the RNA-binding affinity of the protein and the amount of specific RNA-binding sites in the RNA molecule. This process however is not static and protein and RNA constantly associate and disassociate. Therefore, besides the competitive binding of the cold RNA to the homeodomain, there may also have been competition by RNA-hybridizations between the competitor and the BRE₁₆₄₋₃₃₉. At the same time, the homeodomain may not be able to compete with these RNA-RNA-complexes, as the RNA molecules may have a stronger affinity towards each other than the BCD homeodomain to its targets in BRE₁₆₄₋₃₃₉. With smaller RNA probes, this effect should become smaller as the probability of cross-hybridizations becomes smaller. With the BRE₂₅₇₋₃₁₉ fragment I could achieve a slight improvement of BCD homeodomain RNA-affinity in the competition experiments (see below).

These putative RNA-RNA-interaction artefacts are not likely to occur *in vivo*, unless there is a role of RNA-RNA interactions of 3'UTR targets involved in RNA-binding of BCD. For example, dimerization of the *bcd* 3'UTR is essential for the *bcd* mRNA localization process during oogenesis and early embryogenesis. The *bcd* 3'UTR associates to form loop-loop interactions through intermolecular base-pairing, however the process of anterior localization requires additional factors that act within other regions of the *bcd* 3'UTR. The STAU target recognition is not dependent of the loop-loop interaction. (Ferrandon et al., 1997; Snee et al., 2005; Wagner et al., 2004; Wagner et al., 2001).

With the BRE₂₅₇₋₃₁₉ fragment, the affinity to the RNA-target becomes slightly increased, as much smaller amounts of BCD homeodomain are necessary to shift the BRE₂₅₇₋₃₁₉ probe. Furthermore, competition experiments with shSV40 and CU58mer as competitors showed that the BCD homeodomain is more affected by competitors that are structured such as shSV40, then by unstructured RNA such the CU polymer. This could be an indication for the general preference of the BCD homeodomain to interact with structured RNA molecules. Further indication for this can be taken from the binding experiments with the *Hp'cad* 3'UTR fragments H1, H2 and

H3. From the three fragments only H2 is predicted to form a stable secondary structure, indicated by the ΔG value of -26.99. In contrast, H1 and H2 have $\Delta G > -10$, which indicate that these fragments may exist as linear RNA molecules. Consequently, the BCD homeodomain can bind only to the H2 fragment and not to H1 or H3.

Binding of the homeodomain to the full *Tribolium cad* 3'UTR or to a shorter fragment termed Tc_245-307 (spanning nt 245-307) did not yield reproducible results (data not shown). The Tc_245-307 fragment was chosen as it showed a high degree of sequence similarity in sequence alignments with the BRE_257-319. This may be an indirect indication that the conserved BCD-binding element in the 3'UTR *cad* homologues may not depend on the primary sequence.

Taken together, the BCD homeodomain described here shows a low RNA-binding affinity, with a preference to bind to structured RNA molecules. Restrictions from the *in vitro* technique of competition experiments and EMSA may omit target specificity of the BCD homeodomain. It is possible that BCD binding to RNA targets behave more specific when tested *in vivo*. Analysis *in vivo* might provide better binding conditions and possibly presence of putative factors that are absent during the *in vitro* binding reaction. These factors could be additional domains of the BCD homeodomain or additional *trans*-acting factors, all of which may increase binding specificity.

To corroborate and further extent the results observed in the band-shift assays, the RNA fragments discussed here (except CU58mer and Adh3') have been analysed using the *in vivo* translational reporter assay discussed in chapter 3.2.

3.2 Mapping Bicoid RNA-binding elements *in vivo*

3.2.1 The making of a fluorescent protein reporter assay in early *Drosophila* embryogenesis

To define translational control elements in the 3'UTR of *cad* homologues *in vivo*, I aimed to establish a translational reporter assay using the ϕ C31-integrase-mediated recombination system. The ϕ C31-integrase promotes site-specific integration of transgenes into a specific genomic locus. A major advantage of this system is

avoidance of position effect due to different transgene insertion sites (Groth et al., 2003; Thorpe, 1998), allowing direct comparisons of transgene expression from different transgenic lines. By designing this translational reporter assay with a fluorescent marker gene containing a nuclear localisation signal, I aimed to observe *in vivo* the appearance of *de novo* translated protein from maternally provided reporter transcripts during early embryogenesis. I anticipated that if the fluorescent marker gene is followed by 3'UTR sequences with BCD-responsive elements (e.g. the *cad* 3'UTR) the translation of the marker protein along the anteroposterior axis would become inhibited in a BCD-dependent manner. In this reporter assay, the *cad* 3' UTR serves as a positive control for anterior repression by BCD, whereas the SV40 3'UTR (SV40) serves as a negative control, as it contains no known BCD-binding elements. Thereafter, the translational reporter assay could be used to determine whether 3'UTRs from *cad* homologues are regulated in a BCD-dependent manner.

Here I describe three strategies that I followed consecutively in the pursuit of a functional translational reporter assay. Translational reporter assays designed after strategy 1 and 2 did not sense anterior BCD-dependent translational repression of the reporter and therefore did not accomplish my initial requirements for a functional reporter assay (Fig. 3.9, A and B, see 3.2.1.1 and 3.2.1.2). However, by supplementing the reporter of strategy 2 with UAS/GAL4 induced expression of BCD protein (strategy 2b) I was able to establish a reporter assay that faithfully reported BCD-dependent translational repression of reporter transcripts carrying the *cad* 3'UTR (see 3.2.1.3 and 3.2.2). Strategy 2b was then used to analyse *cad* 3'UTRs of other insect species and additional experiments were carried out to investigate why the reporter in strategy 2 could not be translationally repressed by the endogenous BCD protein (see 3.2.1.4). Based on this investigation, I succeeded in the last months of my PhD in establishing a reporter that showed translational repression by anterior BCD in the embryos (strategy 3, see 3.2.1.4).

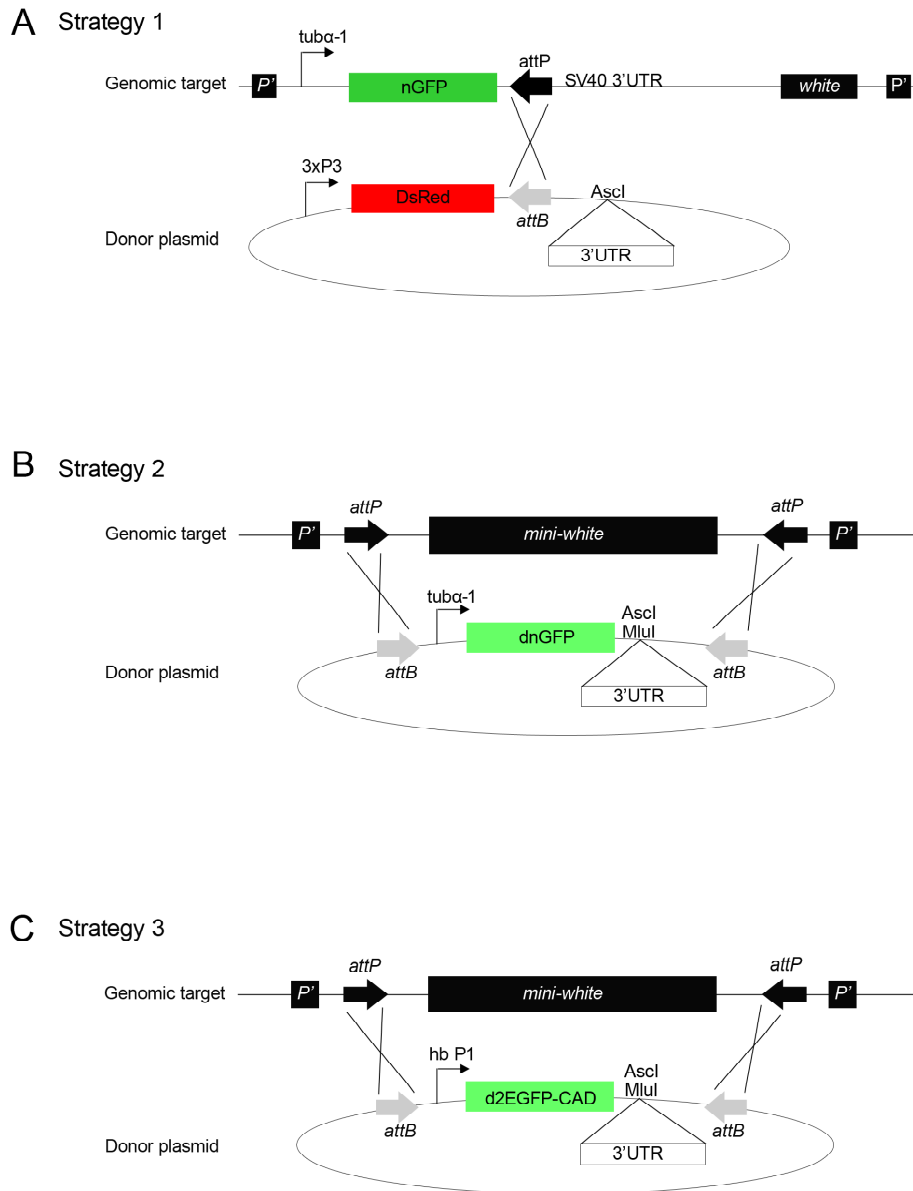


Fig. 3.9: Schematic overview of translational reporter assays. (A) Strategy 1: the genomic target sequence contains the tubulin α -1 promoter ($tub\alpha$ -1), an EGFP fusion with six Myc-tag repeats (6xMyc) and a nuclear localisation signal (NLS) (EGFP-6xMyc-NLS termed nGFP), the *attP* recombination site and the SV40 3'UTR. The donor plasmid contains the 3xP3-DsRed marker followed by *attB* and an *Ascl* site for cloning of 3'UTRs of interest. Upon an integration event the SV40 3'UTR will be replaced by the 3'UTR of interest. (B) Strategy 2: the genomic target consists of two inverted *attP* sites flanking the *mini-white* gene, which serves as a negative marker after the integration event has occurred. The donor plasmid provides the reporter construct comprising of the $tub\alpha$ -1 promoter, d2EGFP-6xMyc-NLS (termed dnGFP) and an *Ascl* or *Mlul* site for cloning of 3'UTRs of interest. d2EGFP is a EGFP variant with shorter half life time. Upon an integration event, the *mini-white* gene will be replaced by the reporter construct. Donor plasmid sequences will not be integrated. (C) Strategy 3: the genomic target is the same as in strategy 2a, however the donor plasmid contains a modified reporter construct comprising of the maternal *hb* P1 promoter (*hb* P1), a d2EGFP fusion with the *Drosophila caudal* protein (d2EGFP-CAD) and *Ascl* or *Mlul* sites for cloning of 3'UTR sequences of interest.

3.2.1.1 Strategy 1: Translational reporter assay using a single ϕ C31-integrase recombination site

The initial strategy was to establish *P*-element mediated transgenic lines, carrying the tubulin α -1 promoter (*tub α -1*) followed by an EGFP fusion with six Myc-tag repeats (6xMyc) and a nuclear localisation signal termed nGFP, an *attP* recombination site and the SV40 3'UTR. The donor plasmid contained the 3xP3-DsRed marker, an *attB* recognition site and a cloning site for inserting diverse 3'UTRs (Fig. 3.9, A). I established several independent transgenic lines containing the construct with the *attP* target site. I chose one transgenic line with an insertion on the second chromosome that was expressing uniform and moderate levels of nGFP in the syncytial embryo (termed pJBattPM44, Tab. 3.1). After integration of the donor plasmid into the *attP* target site of pJBattPM44, nGFP was no longer followed by the SV40 3'UTR, but by other 3'UTRs of interest. Table 3.1 summarizes the transgenic lines and the resulting genotypes that were generated using this approach. The introduction of 3'UTR carrying element(s) that are recognized by BCD (e.g. *Drosophila cad* 3'UTR) was expected to result in the formation of an anterior-to-posterior gradient of nGFP due to anterior translational repression. However, after integration of the donor plasmid pHAE-3xP3-DsRed-*attB*-Dm3'-SV40 with the *cad* 3'UTR the anticipated anterior repression did not occur. Instead, the nGFP levels were reduced homogenously in the embryo and at all subsequent developmental stages (larvae, adults). The same was observed upon integration of donor plasmids carrying other 3'UTRs like the SV40 3'UTR or no 3'UTR at all (see Tab. 3.1), indicating that the integration of plasmid sequences, or the creation of an *attL* between nGFP and the 3'UTR of interest after the integration event, resulted in a general downregulation of nGFP levels. The reasons for this general nGFP downregulation remain unclear. Nevertheless, it was clear that this reporter assay is not suitable for the *in vivo* analysis of BCD-interacting 3'UTR elements.

Tab. 3.1: *Drosophila* sensor lines generated by ϕ C31-integrase mediated insertion into the pJBattPM44 locus on the second chromosome.

Donor plasmid	Genotype after integration event	Anterior repression
pHAE-3xP3-DsRed- <i>attB</i> -Dm3'-SV40	yw; P[w+, tub α -1-nGFP- <i>attL</i> -Dm3'_plasmid-sequence_3xP3-DsRed- <i>attR</i> -SV40]/CyO	no
pHAE-3xP3-DsRed- <i>attB</i> -Hp3'-SV40	yw; P[w+, tub α -1-nGFP- <i>attL</i> -Hp3'_plasmid-sequence_3xP3-DsRed- <i>attR</i> -SV40]/CyO	no
pHAE-3xP3-DsRed- <i>attB</i> -Tc3'-SV40	yw; P[w+, tub α -1-nGFP- <i>attL</i> -Tc3'_plasmid-sequence_3xP3-DsRed- <i>attR</i> -SV40]/CyO	no
pHAE-3xP3-DsRed- <i>attB</i> -SV40	yw; P[w+, tub α -1-nGFP- <i>attL</i> -SV40_plasmid-sequence_3xP3-DsRed- <i>attR</i> -SV40]/CyO	no
pHAE-3xP3-DsRed- <i>attB</i> (no inserted 3'UTR)	yw; P[w+, tub α -1-nGFP- <i>attL</i> _plasmid-sequence_3xP3-DsRed- <i>attR</i> -SV40]/CyO	no

3.2.1.2 Strategy 2: Translational reporter assay using the ϕ C31-integrase mediated cassette exchange (RMCE)

In order to avoid the integration of plasmid sequences, I decided to use the ϕ C31-integrase mediated cassette exchange (RMCE) system (Bateman, 2006). In this system a target cassette, which is inserted in the genome containing the *mini-white* gene flanked by two *attP* sites in inverted orientation, becomes exchanged with a donor cassette delivered by a plasmid carrying inverted *attB* sites flanking the desired construct. The advantage of this system is the exclusive integration of construct sequences into the target sites (Fig. 3.9, B). The recombination products *attL* will be flanking the construct sequence and absent in the transgenic transcripts and their 3'UTRs.

Several *Drosophila* lines transgenic for the RMCE target cassette are available; I chose line 38F1 (from here on called 38F), which is located on the second chromosome (Bateman, 2006). The donor plasmid used to deliver the sensor construct (Fig. 3.9, B), contained the tub α -1 promoter (T), a destabilized version of EGFP (d2EGFP, BD Biosciences Clontech) fused to 6xMyc and the NLS (termed dnGFP) and an *Ascl* site for cloning of 3'UTRs. Table 3.2 summarizes the transgenic lines created by ϕ C31-integrase-mediated RMCE events using this reporter construct carrying different 3'UTR

sequences. Unexpectedly, embryos with the sensor construct carrying the *cad* 3'UTR showed no repression of dnGFP translation at the anterior pole (Fig. 3.10, A line 38F-Dm3', embryos on top row).

Seeking to explain why the embryos of the 38F-Dm3' sensor line were not showing the anticipated dnGFP gradient, I noticed that in ovaries of the females of these flies dnGFP protein is already present in nurse cell and oocyte nuclei (not shown). Maternally expressed mRNAs of embryonic patterning genes like *caudal* are supposed to be translationally inactive during oogenesis. The signals that mediate this are likely to reside in the 3'UTR of these messages (Tadros and Lipshitz, 2005). Unexpectedly, the 38F-Dm3' sensor does not seem to contain a signal(s) for translational repression during oogenesis and therefore the reporter protein is prematurely translated. This has some severe implications for the sensitivity of the reporter assay. In particular, if dnGFP protein is produced during oogenesis and dumped into the oocyte, then it will most likely perdure until embryogenesis begins and perhaps for an even longer period. Although the turnover rate of d2EGFP is only 2h (in mammalian cell culture, BD Biosciences Clontech), the addition of the nuclear localisation signal could have significantly increased protein stability (G. Struhl, pers. comm.). In addition, the maturation time required for fluorescence of d2EGFP could limit the amount of visible, newly-produced EGFP in the embryo. Maternally produced fluorescent protein could thus mask the BCD-dependent gradient to such an extent that differences in fluorescence along the AP-axis are not detectable in the embryo.

Alternatively, the 38F-Dm3' sensor could be lacking signals that normally protect maternal *cad* transcripts from mRNA degradation. Insufficient amounts of maternal sensor transcripts in the embryo might make it more difficult to detect the effects of BCD repression. These questions will be addressed in section 3.2.1.4.

Tab. 3.2: *Drosophila* sensor lines generated by ϕ C31-integrase-mediated RMCE. Integration of donor plasmids was performed into RMCE target cassette 38F1 on the second chromosome.

Name of donor plasmid	Name of integrant line	Genotype after integration event	Anterior repression
piB-TdnGFP-Dm3'	38F-Dm3'	yw; P[attR- tub α -1-dnGFP-Dm3'-attR]	no
piB-TdnGFP-Dm3'mut	38F-Dm3'mut	yw; P[attR- tub α -1-dnGFP-Dm3'mut-attR]	no
piB-TdnGFP-Hp3'	38F-Hp3'	yw; P[attR- tub α -1-dnGFP-Hp3'-attR]	no
piB-TdnGFP-Tc3'	38F-Tc3'	yw; P[attR- tub α -1-dnGFP-Tc3'-attR]	no
piB-TdnGFP-SV40	38F-SV40	yw; P[attR- tub α -1-dnGFP-SV40-attR]	no
piB-TdnGFP-BRE_257	38F-BRE_257-319	yw; P[attR- tub α -1-EGFP-6xMyc-NLS-BRE_257-SV40-attR]	no
piB-TdnGFP-H1	38F-H1	yw; P[attR- tub α -1-EGFP-6xMyc-NLS-H1-SV40-attR]	no
piB-TdnGFP-H2	38F-H2	yw; P[attR- tub α -1-EGFP-6xMyc-NLS-H2-SV40-attR]	no
piB-TdnGFP-H3	38F-H3	yw; P[attR- tub α -1-EGFP-6xMyc-NLS-H3-SV40-attR]	no
piB-HdnGFP-Dm3'	38F-HDN-Dm3'	yw; P[attR- hbP1-dnGFP-Dm3'-attR]	no
piB-HdnGFP-SV40	38F-HDN-SV40	yw; P[attR- hbP1-dnGFP-SV40-attR]	no
piB-HGFPCAD-Dm3'	38F-HGFPCAD-Dm3'	yw; P[attR- hbP1-d2EGFP-CAD-Dm3'-attR]	yes

3.2.1.3 Strategy 2b: A translational reporter assay using RMCE in conjunction with BCD protein expressed using the UAS/GAL4 induction system

Because of prematurely translated EGFP protein in the nurse cells and the oocyte of 38F-Dm3' females, I assumed that perdurance of prematurely produced EGFP protein during oogenesis omits the detection of BCD-mediated repression of the reporter in the embryo. I therefore addressed the question whether the reporter of 38F-Dm3' is susceptible to BCD translational repression at the time when the reporter transcripts are being made, during oogenesis.

I employed the UAS/GAL4 induction system to ectopically express BCD protein during oogenesis and tested for the translational repression of the dnGFP reporter that carries the *Dm'cad* 3'UTR (38F-Dm3'). The ORF of BCD isoform G was fused at its C-terminus to 6xMyc repeats and inserted in the pUASp2 vector (Rørth, 1998) without *bcd* UTR sequences. Transgenic flies with the UAS-BCDG responder crossed to flies carrying the nos-GAL4:VP16 (Rørth, 1998) driver gave rise to female progeny that express BCD protein during oogenesis and deposit transgenic BCD protein and mRNA that is not subjected to anterior localisation, into the oocytes (two transgenic lines tested, UAS-BCDG^{F4M6} and UAS-BCDG^{F8M1}). The nuclear-localized transgenically expressed protein was detected by α -Myc stainings (APPENDIX 3, Fig. A3.1). The function of transgenic BCD as a transcriptional activator was tested by *in situ* hybridizations for the natural BCD target gene *hunchback*. Its activity as a translational repressor was tested by CAD antibody staining in embryos. Both ectopic activation of *hb* and downregulation of CAD protein were observed (see 3.2.3.1, Fig. 3.13, D-F and Fig. 3.14, A and B).

Next, flies carrying both the sensor 38F-Dm3' and the UAS-BCDG were crossed to the nos-GAL4:VP16 line. dnGFP fluorescence intensities were measured in blastoderm stage embryos (nuclear division cycle 11) derived from females expressing the sensor 38F-Dm3', nos-GAL4:VP16 and either of the two UAS lines (maternal genotypes: UAS-BCDG^{F4M6}/+;38F-Dm3'/+;nos-GAL4:VP16/+ and UAS-BCDG^{F8M1}/+;38F-Dm3'/+;nos-GAL4:VP16/+). For simplicity the embryos will be referred to with their mothers' genotype. The average dnGFP intensity of the sensor was compared in the absence (n = 22) and in the presence of the UAS responder (n = 30 for UAS-BCDG^{F4M6} and n = 23 for UAS-BCDG^{F8M1}). Fig. 3.10 B shows that in the presence of UAS-BCDG the dnGFP intensities are reduced to about 40% (40 % \pm 1.4 with UAS-BCDG^{F4M6}, $p = 1.86 \times 10^{-10}$ and 41.8 % \pm 1.7 with UAS-BCDG^{F8M1}, $p = 2.5 \times 10^{-10}$) of the dnGFP levels in flies carrying the sensor alone, indicating that the sensor expression is repressed by BCD. In contrast, dnGFP levels in embryos of the SV40 3'UTR sensor

line (38F-SV40/+;nos-GAL4:VP16/+) did not change in the presence of ectopically expressed BCD (UAS-BCDG^{F4M6}/+;38F-SV40/+;nos-GAL4:VP16/+, $p = 0.24$, Fig. 3.10 C).

In summary, the translational reporter assay from strategy 2a is not suitable for the detection of endogenous BCD-mediated repression. However, in combination with UAS/GAL4-induced ectopic expression of BCD protein, the 38F-Dm3' reporter expression reliably shows BCD-mediated repression of the *cad* 3'UTR. Thus, this reporter in conjunction with the UAS/GAL4 system, was applied for the analysis of BCD-dependent repression of *cad* 3'UTR homologues from different insect species (section 3.2.2 and Tab. 3.2).

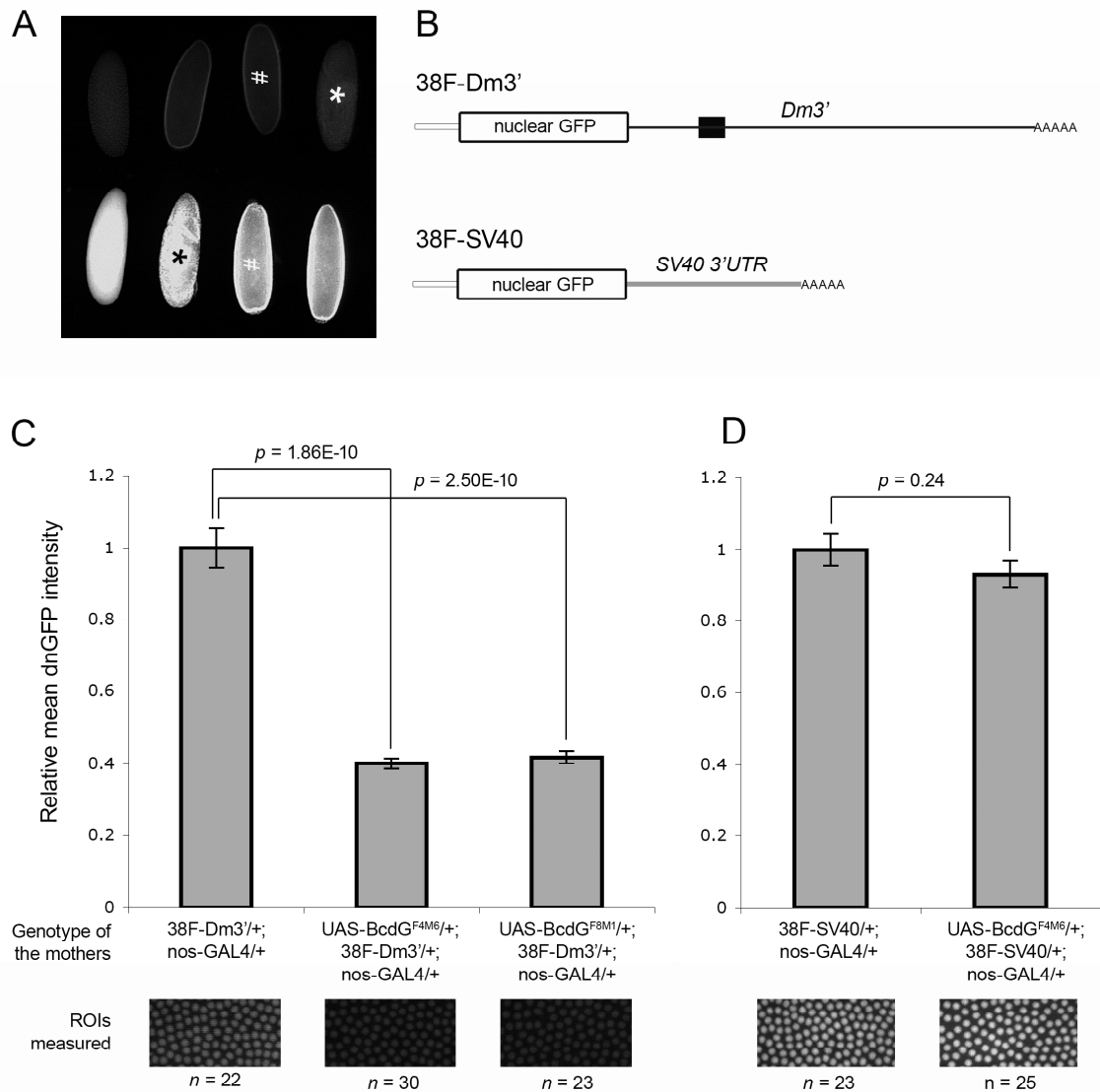


Fig. 3.10: Translational repression assay. (A) Comparison of dnGFP levels in transgenic *Drosophila* embryos of 38F-Dm3' (upper row) and 38F-SV40 (lower row). Note that not all embryos are at similar embryonic stages (similar stages are indicated by asterisks and dash sign), however overall dnGFP intensities are consistently lower in 38F-Dm3' embryos than in 38F-SV40 embryos. (B) Schematic overview of the reporter transcripts. The black box of the 38F-Dm3' transcript indicates the location of the BRE_257-319 fragment. (C) Relative dnGFP intensities measured in embryos of the 38F-Dm3' line in the absence (intensity level arbitrarily set to 1) and presence of two independent lines expressing UAS-BCDG (UAS-BCDG^{F4M6} and UAS-BCDG^{F8M1}). Both UAS-BCDG lines induce a reduction of relative dnGFP levels by about 60%. (D) The presence of UAS-BCDG^{F4M6} does not have an effect on the dnGFP intensity of 38F-SV40 line embryos. Bars represent relative mean values \pm SE; statistical significance was analysed using Student's t-test (p). GFP intensity values were taken from regions of interest (ROI) of identical size from the surface of blastoderm embryos at nuclear division cycle 11.

3.2.1.4 Strategy 3: Translational reporter assay using a d2EGFP-CAD fusion

I conducted further investigations of *cad* 3'UTR homologues using the translational reporter assay developed in strategy 2b, using ectopically expressed BCD protein and the *Drosophila cad* 3'UTR as a positive control (see 3.2.1.3, 3.2.2). In the endeavour to corroborate this strategy and to be able to correctly interpret results generated with this translational reporter assay, I performed a set of control experiments. Furthermore, by investigating possible reasons for the premature presence of EGFP protein during oogenesis of the reporter from strategy 2, I aimed to generate a translational reporter that mediates translational repression via endogenous BCD.

Mlodzik et al. (1990) investigated the effect of heat-shock induced ectopic expression of *cad* and reported that anterior repression of *cad* translation was lost due to an mRNA overload in these embryos (Mlodzik et al., 1990). To test whether an overload of sensor transcripts might omit the detection of BCD-dependent repression I utilized the *hb* maternal promoter, which is promoting expression at lower levels than the *tub α -1*. I created a reporter construct containing the maternal *hb* P1 promoter (H) (Wimmer et al., 2000), dnGFP and the *cad* 3'UTR (piB-H-dnGFP-Dm3'). The RMCE donor cassette with the reporter construct was inserted into the 38F line, creating sensor line 38F-HDN-Dm3' (Tab. 3.2). In females of 38F-HDN-Dm3', I detected dnGFP protein in the nurse cells and the oocyte (not shown) and, although the overall dnGFP levels were much lower compared to the previous reporter (38F-Dm3'), there was no anterior repression detectable in the embryos (data not shown). Therefore, a sensor mRNA overloading effect is unlikely to have been the primary cause for lack of detectable anterior repression. Furthermore, the notion that premature degradation of the sensor mRNA could be preventing the formation of a protein gradient in the embryo could be ruled out as *in situ* hybridizations using an antisense probe of the reporter gene (d2EGFP) showed that sensor transcripts are present in the early embryo of 38F-HDN-Dm3' (data not shown).

Next, I addressed whether maternally inherited dnGFP protein together with long-lasting GFP protein perdurance might be concealing the BCD-mediated repression of sensor transcripts in the embryo. Revising the literature, I noticed that in previous studies, the *cad* translational reporter assays utilized the reporter genes *cad-lacZ*, the *ftz* coding region or the *Megaselia cad* coding region for the detection of BCD-mediated repression (Dubnau and Struhl, 1996; Stauber et al., 2008). These reporters presumably had important properties, such as high protein turnover, which secures fast

removal of maternal protein, or elements that prevent premature translation during oogenesis and that lack from my previous GFP reporters.

To address this question, I created a reporter construct containing the *hb* maternal promoter (P1) and d2EGFP fused to the *cad* coding region, followed by the *cad* 3'UTR (Fig. 3.9, C). Due to the *cad* coding region, the d2EGFP-CAD fusion protein should localize to the nucleus, which facilitates the imaging of protein gradients in the syncytial blastoderm. Furthermore, I expected a high turnover rate similar to that of endogenous CAD protein, promoting fast removal of any maternally produced protein in the embryo. Dissected ovaries of flies containing the d2GFP-CAD sensor construct with the *cad* 3'UTR (38F-HGFPCAD-Dm3', schematic overview of the sensor transcript in Fig. 3.11, A) showed no GFP fluorescence (not shown), indicating the absence of translation of the sensor in the nurse cells and the oocyte, or a very fast degradation of translated protein. In the embryos, fluorescence of that reporter could be detected in an anterior-to-posterior gradient (Fig. 3.11, B), also detected by immunohistochemical stainings using α -GFP antibody (Fig. 3.11, C). The mRNA of this reporter is distributed homogeneously in the embryo, indicating that the protein gradient is generated through post-transcriptional regulation (Fig. 3.11, D).

Thus, the 38F-HGFPCAD-Dm3' reporter line faithfully reproduces the natural CAD gradient during early embryogenesis. These results indicate that the CAD ORF adds crucial properties to the fluorescent reporter, which were lacking in reporters 38F-Dm3' or 38F-HDN-Dm3' and which allow the formation of a translational repression gradient of the reporter protein in the 38F-HGFPCAD-Dm3' line. The reason why I could not detect a gradient in embryos of strategy 2 is most likely due to the perdurance of maternal dnGFP protein in the embryo or a lack of signal(s), residing in the CAD coding sequences that prevent translation of the sensor in the ovary.

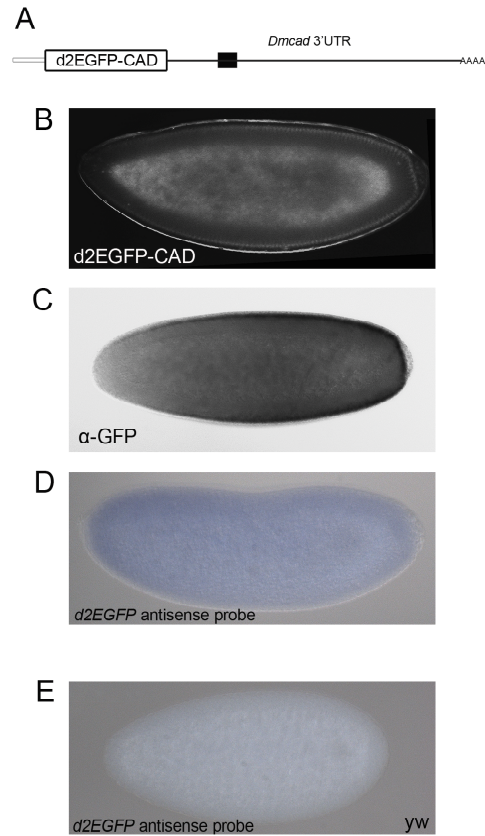


Fig. 3.11: Translational repression of a reporter carrying a d2GFP-CAD fusion and the Dm3'. (A) Schematic overview of the transgenic transcript. The ORF of the d2EGFP-CAD fusion protein is followed by the *cad* 3'UTR (Dm3'); the location of the BRE_257-319 fragment is indicated by a black box. (B) d2EGFP-CAD fluorescence in the blastoderm embryo of line 38F-HGFPCAD-Dm3'^{M52}. The autofluorescence of the yolk is initially almost as strong as the d2EGFP-CAD fluorescence, however, it photobleaches very rapidly, whereas the fluorescence of the d2EGFP-CAD remains stable; these pictures were taken after 10-15 sec of photobleaching. Note the nuclear localization of the protein and the anterior lack of fluorescence as compared to the posterior end of the embryo. (C) α-GFP immunohistochemical detection of the GFP-CAD reporter protein showing the asymmetric distribution of the reporter gene, with highest concentration at the posterior. (D) *In situ* hybridization using an antisense probe for d2EGFP-CAD mRNA. In contrast to the protein, the sensor transcripts are distributed homogenously throughout the embryo. (E) yw embryos are not stained using this probe. All embryos are oriented with anterior to the left and dorsal up.

3.2.1.5 Conclusions

The *Drosophila* maternal genes have neatly orchestrated expression patterns and their proper spatiotemporal expression is of vital importance. Maternal gene expression is very dynamic, as BCD rapidly builds up an anterior-to-posterior protein gradient, necessary for activation of anterior gap genes and repression of translation of ubiquitously distributed *cad* mRNA. In fact, the establishment of the BCD gradient occurs so fast that current models trying to explain the formation of the gradient differ in their interpretations of how the gradient forms (Gregor et al., 2007a; Gregor et al., 2007b; Spirov et al., 2009). In concert with other maternal factors such as *hunchback*, *nanos* and *torso*, *bcd* activity provides key positional information for the patterning of segments along the AP-axis.

The time window of BCD activity ranges from 30 min to 2 h of development in which repression of *cad* mRNA occurs. Thus, for the establishment of a translational reporter assay that would detect BCD activity during early *Drosophila* embryogenesis, specific properties of the reporter protein were required. With the translational reporter assay (as in strategy 2), in which reporter mRNA and protein become deposited in the embryo, factors such as maturation time and lifetime of the reporter protein are of crucial importance for the detection of an emerging protein gradient in the embryo. In the reporter line 38F-Dm3' the detection of anterior BCD-dependent repression in the embryos is masked due to perdurance of maternal dnGFP protein, which is distributed ubiquitously in the embryo (strategy 2). By fusing the CAD coding sequence to d2EGFP, I changed the reporter protein properties such that the reporter with the *cad* 3'UTR became translationally repressed by endogenous BCD in the anterior of the embryo.

The *cad* 3'UTR faithfully reproduces BCD-dependent translational repression in the 38F-Dm3' line when the transcripts are exposed to ectopically expressed BCD protein during oogenesis (strategy 2b) or when the perdurance of the maternal reporter protein could be eliminated (strategy 3).

3.2.2 Identification of *cad* 3'UTR homologues that are translationally regulated by BCD

3.2.2.1 The BRE_257-319 fragment of the *cad* 3'UTR is mediating translational repression in the presence of BCD

The BCD homeodomain shows weak binding affinity for the BRE_257-319 fragment in band shift experiments (see 3.1.2). I wanted to further this result, by investigating *in vivo* whether the translation of a sensor transcript bearing the BRE_257-319 fragment is regulated by BCD (Fig. 3.12 A). Fig. 3.12 B shows that dnGFP levels of embryos derived from females expressing the sensor and BCD isoform G (*yw,UAS-BCDG^{F4M6}/+;38F-BRE_257-319/+;nos-GAL4:VP16*) are reduced (60.5 % \pm 2.4, $p = 1.56 \times 10^{-12}$) compared to embryos whose mothers lack the UAS responder. This suggests that the sensor transcript bearing BRE_257-319 fragment is indeed recognized by BCD and can mediate translational repression. In contrast, the sensor 38F-SV40 is not affected in the presence of BCD. It has to be noted that the only difference between transcripts of 38F-BRE_257-319 and 38F-SV40 is the presence of the BRE_257-319 fragment upstream of the SV40 3'UTR in 38F-BRE_257-319 (Fig. 3.12 A). Interestingly, the dnGFP intensity is reduced in 38F-BRE_257-319 embryos to 59.2 % \pm 1.7 ($p = 3.49 \times 10^{-9}$) as compared to the levels in 38F-SV40 (Fig. 3.12 B). This result provides evidence for the existence of a BCD-independent *cis*-regulatory element(s) in the BRE_257-319 fragment and is concurring with the downregulation of dnGFP fluorescence observed in the sensor carrying the full Dm3' (38F-Dm3', see Fig. 3.10, A).

3.2.2.2 The *Haematopota cad* 3'UTR mediates translational repression in the presence of BCD

Sensor lines carrying the full *Hp'cad* 3'UTR (Hp3') or one of the three fragments H1, H2 or H3 of the *Hp'cad* 3'UTR followed by the SV40 3'UTR (see Tab. 3.2, Fig. 3.12 A) were crossed to the UAS-BCDG^{F4M6} and the nos-GAL4:VP16 line. Fig. 3.12 C shows the relative dnGFP intensities of the sensors measured in the absence (white bars) and presence (grey bars) of UAS-BCDG^{F4M6} in embryos. The full *Hp'cad* 3'UTR mediates translational repression with sensor 38F-Hp3' and in the presence of BCD isoform G

(UAS-BCDG^{F4M6}/+;38F-Hp3'/+;nos-GAL4) with dnGFP intensity of 80.8 % ± 2.4 as compared to the dnGFP levels of the sensor alone ($p = 2.97 \times 10^{-16}$). In the EMSAs, I could show that only *Hp'cad* 3'UTR fragment H2 was bound by the BCD homeodomain (see 3.1.3).

In order to investigate which region of the *Hp3'cad* 3'UTR mediates BCD-dependent repression in the reporter assay, I tested the three fragments H1, H2 and H3 individually. Only the sensor with fragment H2 mediates a significant reduction in dnGFP levels to 87 % ± 2.9 in the presence of UAS-BCDG^{F4M6} (maternal genotype: UAS-BCDG^{F4M6}/+;38F-H2/+;nos-GAL4/+) as compared to the sensors in the absence of the UAS responder ($p = 0.001$). These results confirm that BCD isoform G can influence reporter activity via the *Hp3'* fragment H2 *in vivo*.

3.2.2.3 The *Tribolium cad* 3'UTR fails to mediate BCD-dependent translational repression of the dnGFP sensor

Wolff et al. (1998) showed that *Tribolium cad* cDNA, expressed in transgenic *Drosophila* embryos can be translationally repressed in a BCD-dependent manner. They concluded that the *Tc'cad* mRNA carries an element that is recognized by BCD. Because the BCD-binding element of the *Drosophila cad* mRNA is situated in the 3'UTR, it seemed likely that the element recognized by BCD in the *Tc'cad* mRNA might also be situated in its 3'UTR.

Sensor lines carrying the full *Tc'cad* 3'UTR (38F-Tc3', Tab. 3.2) were crossed to a line carrying UAS-BCDG^{F4M6} and nos-GAL4:VP16, and the dnGFP intensities were measured in embryos (maternal genotype: UAS-BCDG^{F4M6}/+;38F-Tc3'/+nos-GAL4VP:16) (Fig. 3.12, C). The dnGFP intensities of sensor 38F-Tc3' showed no statistically significant difference in the presence or absence of BCD isoform G. This result indicates that the translational repression of the *Tc'cad* transcript observed previously (Wolff et al., 1998) is not mediated by its 3'UTR.

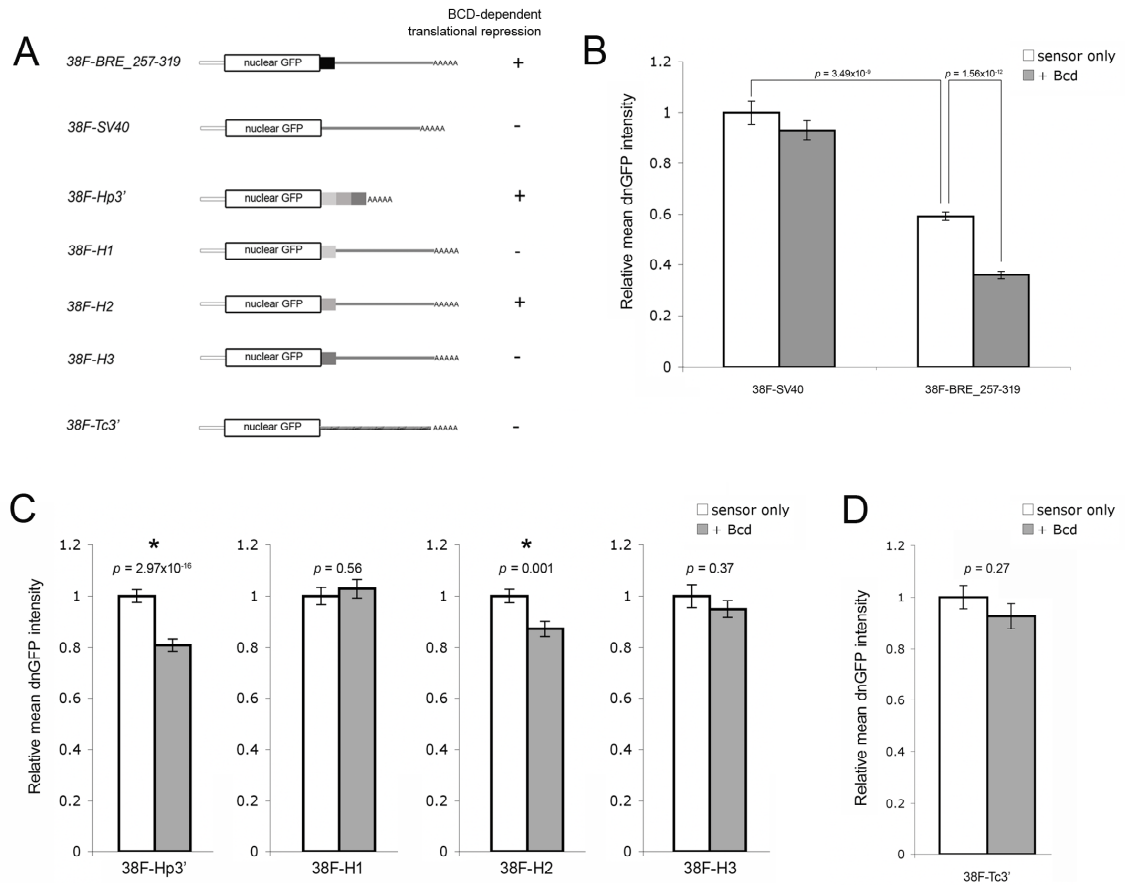


Fig. 3.12: Translational repression assay on BRE_257-319, *Haematopota* and *Tribolium* 3'UTRs. (A) Schematic overview of the reporter transcripts: 38F-BRE_257-319 transcript carries the BRE_257-319 fragment (black box) upstream of the SV40 3'UTR; 38F-SV40 carries the SV40 3'UTR; 38F-Hp3' carries the full Hp3'; 38F-H1, 38F-H2 and 38F-H3 carry the H1, H2 and H3 fragments upstream of the SV40 3'UTR; 38F-Tc3' carries the full Tc3'. (B) Average dnGFP intensities in the absence (white bars) or presence (grey bars) of UAS-BCDG^{F4M6} in sensor lines 38F-SV40 and 38F-BRE_257-319. The relative fluorescence levels in 38F-BRE_257-319 are about 40% lower than in 38F-SV40 ($p = 3.49 \times 10^{-9}$). In the presence of UAS-BCDG^{F4M6} the relative dnGFP levels of 38F-BRE_257-319 become reduced by about 40% ($p = 1.50 \times 10^{-12}$) as compared to the sensor alone. (C) Average dnGFP intensities are reduced in the presence of UAS-BCDG^{F4M6} in sensors 38F-Hp3' and 38F-H2 ($p = 2.97 \times 10^{-16}$ and $p = 0.001$, respectively). dnGFP levels in sensors 38F-H1 or 38F-H3 are unchanged in the presence or absence of UAS-BCDG^{F4M6}. (D) The dnGFP levels of sensor line 38F-Tc3' do not change in the presence of UAS-BCDG^{F4M6}. Bars represent relative mean values \pm SE; statistical significance was analysed using Student's t-test (p). GFP intensity values were taken from regions of interest (ROI) of identically size from the surface of blastoderm embryos at nuclear division cycle 11 ($n=20-30$). All carry nos-GAL:VP16.

3.2.2.4 Conclusions

Sensor 38F-Dm3' is reduced to $40\% \pm 1.4$ dnGFP fluorescence in the presence of BCD isoform G as compared to the sensor alone. The sensor 38F-BRE_257-319 however is

reduced to only $60\% \pm 2.4$ dnGFP fluorescence levels, demonstrating that the full-length *cad* 3'UTR is more effective than BRE_257-319 fragment alone. This may be due to the presence of additional sites in the *cad* 3'UTR that additively reduce translational repression. Alternatively, differences in the secondary structure present in full *cad* 3'UTR may be required for effective repression. The dnGFP levels of sensor 38F-Hp3' are reduced to $80.8\% \pm 2.4$ and of sensor 38F-H2 to $87\% \pm 2.9$ by BCD isoform G. These results suggest that the BRE_257-319 fragment may interact more effectively with BCD than the H2 fragment, leading to a stronger repression. Similarly, in EMSAs using the BCD homeodomain, I observed that complexes of the BCD homeodomain and the H2 fragment required much higher homeodomain concentrations as compared to complexes with the BRE_257-319 fragment, indicating a higher binding affinity of the homeodomain to BRE_257-319 than to H2. The dnGFP levels of the sensors containing the other *Hp'cad* 3'UTR fragments (H1 and H3) were not affected by BCD isoform G. Given that repression of a sensor with the full *Hp'cad* 3'UTR is stronger than with the H2 fragment alone, it is possible that in the context of the full *Hp'cad* 3'UTR the other regions flanking the H2 fragments can form a structure that allows stronger repression by BCD, either by providing additional BCD-binding elements or by stabilizing the BCD-binding element of the H2 fragment.

These results confirm the binding interactions revealed by EMSAs (see 3.1.2 and 3.1.3). The *Tc'cad* 3'UTR does not interact with BCD in the in vivo assay and RNAforester alignments with the *Tc'cad* 3'UTR did not detect any structure similarities with the BRE_257-319 fragment (APPENDIX 4). Thus, it cannot be excluded that the observed BCD-dependent translational repression of transgenic *Tc'cad* (Wolff et al., 1998) was mediated by an element situated in the 5' UTR or in the coding sequence. In fact, RNAforester alignment analysis of the predicted secondary structure of the *Tc'cad* 5'UTR+coding sequence and the BRE_257-319 fragment showed highest similarity to a region situated in coding sequence of *Tc'cad* (nt 451-485 with numbering starting with the first nt in the sequence of NCBI accession number AJ005421, APPENDIX 4). Similarly, the H2 fragment shows high structural similarity to the same fragment in the *Tc'cad* coding sequence. Judging from this predicted secondary structure analysis and from the BCD homeodomain binding results so far, I propose this fragment (spanning nt 451-485 of the *Tc'cad* cDNA) as a promising candidate for the *cis*-regulatory element in the *Tc'cad* mRNA that mediated previously observed BCD-dependent translational repression in *Drosophila* embryos.

3.3 Testing the role of different Bicoid isoforms during *Drosophila* early embryogenesis

The *bcd* gene exists in 5 different splice isoforms (see Fig. 2.5). Current expression data for the morphogen *bcd* do not distinguish between different splice isoforms, because the probes used in these studies were usually obtained from the *bcd* cDNA that encodes the largest of the BCD protein isoforms (Berleth et al., 1988; Spirov et al., 2009). In fact, the generation of probes that would recognize individual isoforms is impossible, since none of the isoform transcripts contain sequences that are entirely unique to it.

However there is substantial evidence that each splicing product of *bcd* is present as maternal mRNA in the embryo: first, all isoform transcripts have been cloned from embryonic cDNA libraries and second, recent RNAseq data show that all exonic sequences of *bcd* are present in embryos (APPENDIX 5, Fig. A5.2).

Because it is not possible to deplete individual BCD isoforms, functional analyses are restricted solely to gain-of-function approaches. The five isoforms of BCD show some interesting features. Most notable are the absence of most known functional domains in isoform A, and the lack of the 4EHP-binding domain in the putative proteins of isoforms E and F. The latter are of particular interest regarding the mechanism of translational repression of *cad* mRNA, which was proposed to be mediated by the interaction of BCD with 4EHP.

In this study, the UAS/GAL4 system was employed to express each isoform of BCD in the context of the translational reporter system described above (see 3.2.1.3). The ectopic expression of each isoform individually will allow me to investigate their roles in the context of translational control of *cad* mRNA.

3.3.1 *hb* transcriptional activation and CAD translational repression by different BCD isoforms

The ORFs of the five BCD isoforms were cloned from a *Drosophila* embryonic cDNA library into the pUASp2 construct and inserted into the genome through *P*-element mediated transgenesis. Maternal expression was induced ubiquitously in the embryo

using the nos-GAL4:VP16 driver and embryos deriving from females expressing each UAS-BCD isoform by nos-GAL4:VP16 induction were collected for further analysis.

First, I analysed the ability of each isoform to ectopically activate expression of *hb*, which is a natural transcriptional target of BCD. Two transgenic lines of each UAS-BCD isoform were tested for their ability to activate the BCD target gene *hb*. *In situ* hybridizations were performed using an *hb* ORF antisense probe and representative expression patterns are shown in Fig. 3.13.

In wt embryos (yw), *hb* mRNA are provided maternally and distributed homogenously in the early embryo (Fig. 3.13, A). *hb* becomes translationally regulated and forms an anterior domain (Fig. 3.13, B). All embryos with ectopically expressed BCD isoforms show normal maternal *hb* expression in early embryos similar to wt (Fig. 3.13, compare A with C, E, G, I, K). In pre-cellular embryos isoforms G and D have a strong activation effect leading to uniform *hb* expression (Fig. 3.13, D and F) or to an expanded expression domain towards the posterior (not shown). Isoforms E and F induce a shift of the anterior expression domain towards the posterior in syncytial embryos, with the posterior boundary at ~60 % EL (Fig. 3.13, H and J). Embryos with isoform A show wt expression of *hb* transcripts (Fig. 3.13, K, L). In summary, all isoforms except isoform A induce dramatic shifts of the early anterior *hb* expression domain towards the posterior albeit in slightly different fashions.

Next I investigated which isoforms can mediate translational repression of the endogenous *cad* mRNA, by using immunohistochemical stainings with an antibody against CAD. In blastoderm stage embryos (nuclear division cycle 10-14) that derived from females expressing isoform G, D, E and F, *cad* mRNA translation was downregulated, as seen by a reduction of α -CAD staining in comparison to stainings in wt embryos (Fig. 3.14). Embryos that derived from females expressing isoform A did not show any differences in α -CAD stainings as compared to wt (not shown). It has to be pointed out that isoform E and F do not possess the 4EHP-binding domain, which is thought to be necessary for d4EHP- and BCD-dependent translational repression of *cad* mRNA (Cho et al., 2005). To further substantiate these results, I analysed whether these isoforms can repress the translation of 38F-Dm3' sensor.

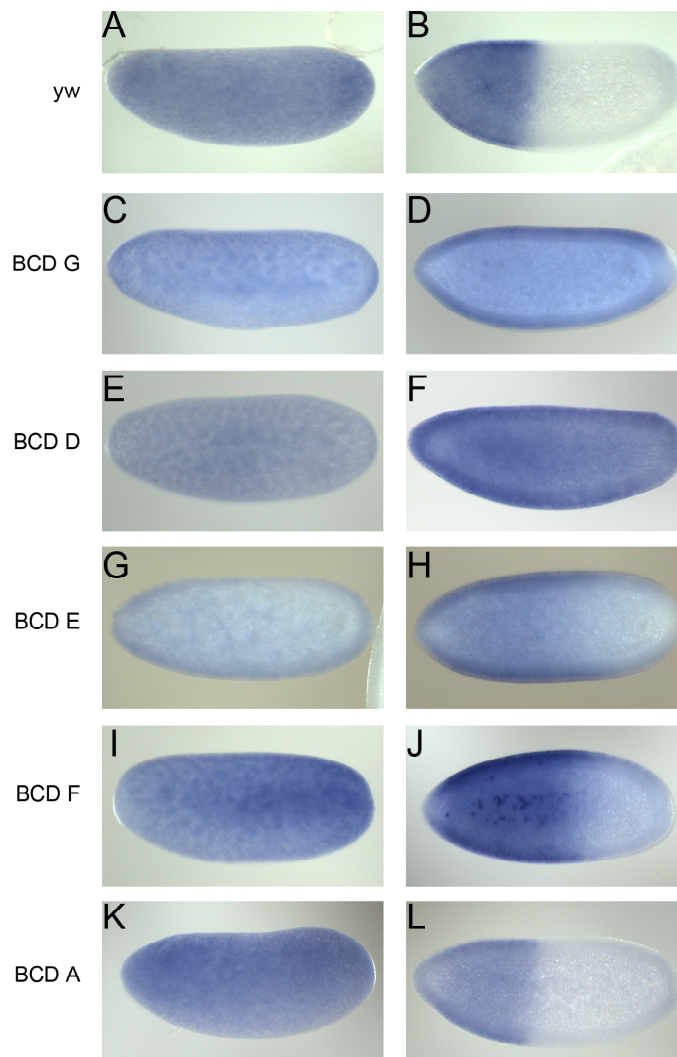


Fig. 3.13: *hb* expression in the presence of different BCD isoforms. *In situ* hybridization using an antisense probe of the *hb* ORF of wt embryos (A,B) and of embryos derived from females expressing isoform G (C,D), isoform D (E,F), isoform E (G,H), isoform F (I, J) and isoform A (K,L). Embryos in left column show pre-blastoderm embryos, embryos in the right column show pre-cellular blastoderm stages. Representative embryos are shown with anterior the left .

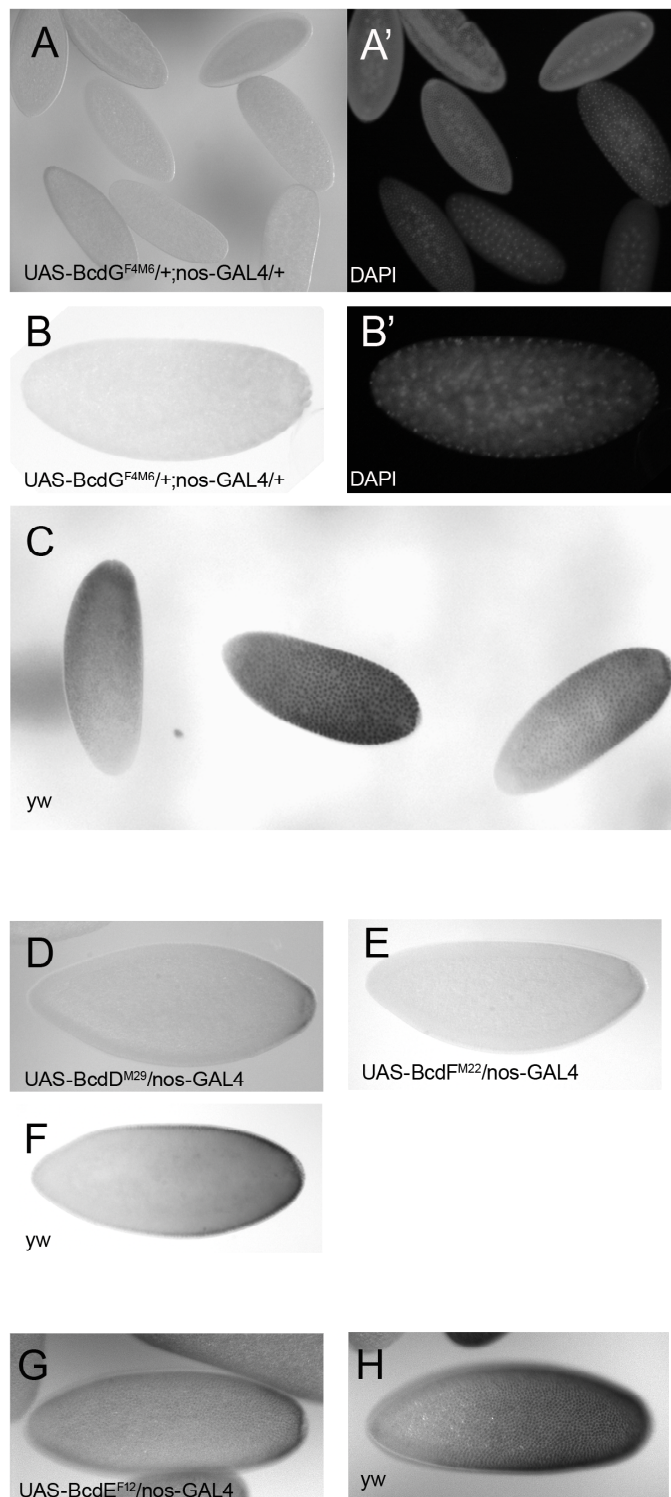


Fig. 3.14: *cad* translational repression in the presence of different BCD isoforms. CAD antibody stainings in blastoderm stage embryos derived from females expressing different BCD isoforms were performed on different days. yw embryos stained in parallel on the same day served as controls. Compare embryos derived from females expressing isoform G (A,B), isoforms D and F (D, E) and isoforms E (G), to their respective controls (C, F and H). (A') and (B') show DAPI staining of the nuclei.

3.3.2 Translational repression of sensor 38F-Dm3' by different BCD isoforms

Immunohistochemical-staining procedures can give variable results depending of the antibody and the strength of the staining and they may not be suitable to adequately quantify downregulation of CAD translation. Analysis of the dnGFP reporter can give more reproducible and quantitative results. The information output in form of fluorescence levels of the sensor representing the “wild-type” situation is much less variable.

I analysed the dnGFP levels of the sensor 38F-Dm3' in the presence of each BCD isoform in comparison to the sensor alone. Sensor line 38F-Dm3' was crossed to two transgenic UAS responder lines of every BCD isoform in the presence of nos-GAL4:VP16. The dnGFP intensities were measured in embryos deriving from females expressing the sensor and the respective BCD isoform (see Fig. 3.15 for maternal genotypes). Fig. 3.15 shows that the average dnGFP intensity of the sensor is reduced to about 40 % in the presence of BCD isoform G (40 % \pm 1.4 with UAS-BCDG^{F4M6} and 41.8 \pm 1.7 with UAS-BCDG^{F8M1}), isoform E (41.5 % \pm 1.6 with UAS-BCDE^{F12} and 38.3 % \pm 1.4 with UAS-BCDE^{F79}) and isoform F (41.7 % \pm 0.8 with UAS-BCDF^{F9M3} and 45.5 % \pm 0.9 with UAS-BCDF^{M22}). BCD isoform D gives a reduction in fluorescence levels to about 30 % of the initial dnGFP levels (27.1 % \pm 1.3 with UAS-BCDD^{F15} and 31.5 % \pm 1.3 with UAS-BCDD^{M29}). Isoform A does not seem to have an effect on the fluorescence levels of the sensor.

Taken together, these results confirm the conclusions drawn from immunohistochemical stainings of CAD protein in embryos with ectopic expression the BCD isoforms. Isoforms G, D, E and F can repress translation of sensor transcript carrying the *cad* 3'UTR.

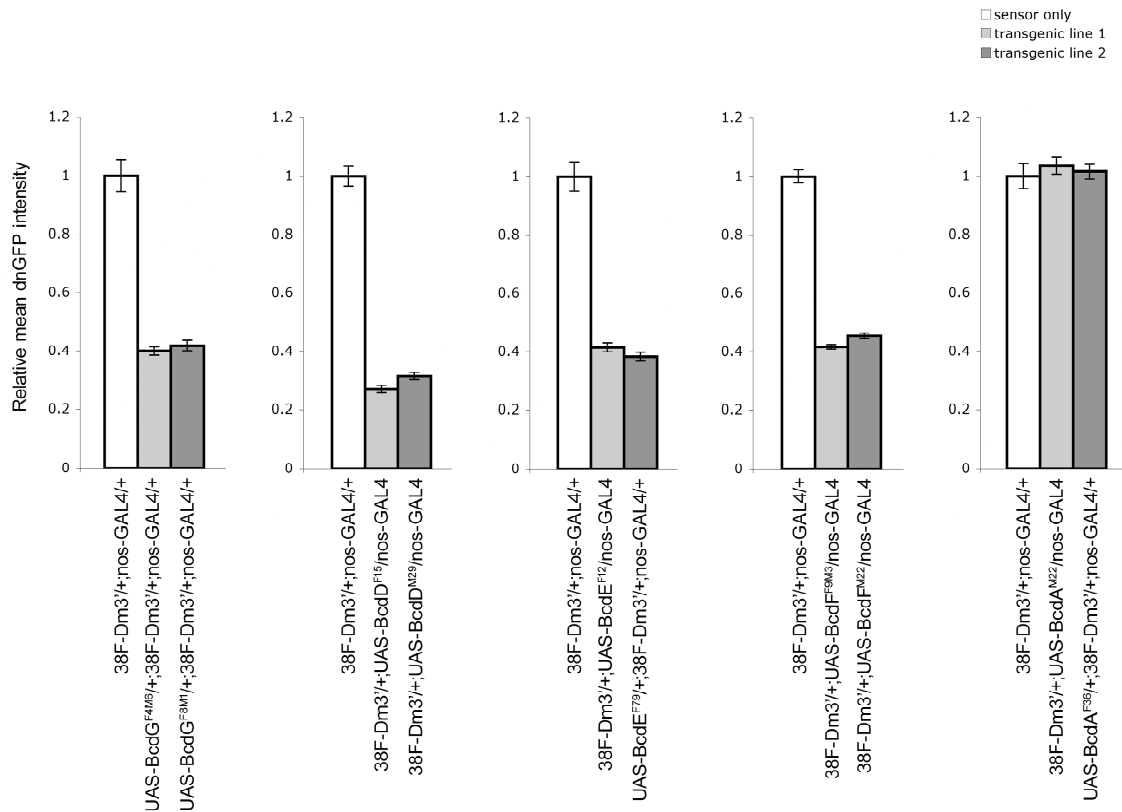


Fig. 3.15: Translational repression effect of different BCD isoforms on the 38F-Dm3' sensor. Average dnGFP intensities were measured in embryos deriving from females expressing the sensor 38F-Dm3' in the absence (white bars) or in the presence of the BCD isoforms (grey shaded bars, two lines analysed). Isoforms G, D, E and F give significant reduction of dnGFP levels of the sensor; isoform A does not seem to have an effect on dnGFP fluorescence levels.

3.3.3 Conclusions

As previously described, the binding of d4EHP to both BCD and the cap-structure is critical for translational repression of *cad* mRNA (Cho et al., 2005). In hypomorphic mutants of d4EHP (*d4EHP^{CP53}*), *cad* mRNA becomes ectopically expressed in the anterior, however only about 50% of the progeny deriving from homozygous *d4EHP^{CP53}* females did hatch, the other 50% died due to severe patterning defects mostly affecting anterior segmentation (Cho et al., 2005). This hypomorph was produced through *P*-element excision of the first exon and part of the first intron of the d4EHP gene, creating transcripts with an alternative ATG start codon. These transcripts give rise to truncated d4EHP protein detectable by western blots. The presence of a partial CAD gradient and hatching rate of 50% of these hypomorphic mutants was explained

stipulating a residual activity of d4EHP in these embryos (Cho et al., 2005). However it is not clear whether this hypomorphic d4EHP protein is active.

My results from the gain-of-function study of the BCD isoforms, suggests an alternative explanation. I show that even in the absence of a d4EHP-binding domain, isoform E or F can still the translationally repress transcripts bearing the *cad* 3'UTR. The ectopic activation of *hb* transcription illustrates that these two protein isoforms are not impaired in their function as transcriptional activators and that thus the homeodomain, which is the DNA/RNA-binding domain, is functional. It is therefore possible that the CAD translational repression observed in *d4EHP^{CP53}* embryos was not a result of residual d4EHP activity, but mediated through an alternative mechanism, which functions independently of d4EHP.

CAD translational repression could be result of cooperative action of endogenous BCD protein (bearing the d4EHP-binding domain) with the ectopically expressed BCD isoforms. However this is not the case in the analysis with the translational reporter assay. As previously noted, the sensor reveals dnGFP protein produced during oogenesis, and its regulation by BCD isoforms expressed during that stage using the nos-GAL4:VP16 driver.

So far, it is not known whether the individual BCD isoforms actually exist as proteins in the embryo and it would be interesting to further address this question in the future. The existence of different BCD isoforms or BCD-modifications could have important implications for the formation of the BCD activity gradient in the early embryo, an issue that has not been taken into account in most models of BCD action (Grimm et al., 2010). For instance, the BCD isoform pairs G/D and E/F differ from each other in a short peptide sequence (DVFPS), which is present only in isoform G and E, while isoforms E and F are missing a large part of the N-terminus, which is present in isoforms G and D. These peptide sequences could be post-translationally modified or mediate protein-protein interactions, which influence the activity of the protein. Different isoforms might also interact and exert different functions cooperatively.

3.4 Hints for alternative mechanisms of BCD-mediated translational repression

The *cad* 3'UTR contains predicted target sites for the miRNAs miR-308 (target sequence nt 299-316) and miR-305 (target sequence nt 534-545) (Brennecke et al., 2005; Stark et al., 2005). The miR-308 binding target lies within the sequence that is highly conserved among different *Drosophila* species of the BRE_257-319 fragment (Fig. 3.16). The predicted secondary structure of the BRE_257-319 fragment contains a putative helical region of seven base pairs (termed stem-A), a short stem of three Watson-Crick base pairs and one G•U wobble pair (termed stem-B) and a hairpin-loop (Fig. 3.16). This structure is consistently predicted within the sensor transcripts, either within the full Dm3' (in 38F-Dm3') or when BRE_257-319 is followed directly by the SV40 3'UTR (in 38F-BRE_257-319) (not shown). The miR-308 target site, which is not overlapping with stem-A, constitutes most of stem-B and the hairpin loop (indicated in yellow, Fig. 3.16). Similarly, the H2 fragment of the Hp3' forms a stem-loop structure (termed H2-stem-A), which shows some structural similarity to stem-A of BRE_257-319 in alignments of the predicted secondary structures using the RNAforester program (see Fig. 3.7). The H2 fragment, however, does not contain any predicted *Drosophila* miRNA target sites. Thus, when tested in *Drosophila*, the H2 fragment is an RNA fragment that is regulated most likely independently of miRNA function.

So far there are two indications that point towards independent mechanisms for translational control of *cad*. First, the putative miRNA mediated repression of sensors carrying *Drosophila cad* 3'UTR (38F-Dm3', see 3.2.1.3) or BRE_257-319 (38F-BRE_257-319, see 3.2.2.1) and second, d4EHP-independent translational repression of sensor 38F-Dm3' by BCD isoform E or F (see 3.3.2). In this part, I am asking whether miR-308 is likely to be involved in translational control of *cad* and whether it might interact with BCD to mediate translational control. Can we learn something about the d4EHP-independent mechanism of translational repression by studying the effects of miR-308? Can the H2 fragment, which lacks putative *Drosophila* miRNA binding sites be repressed by BCD isoform F (which lacks 4EHP-binding domain)?

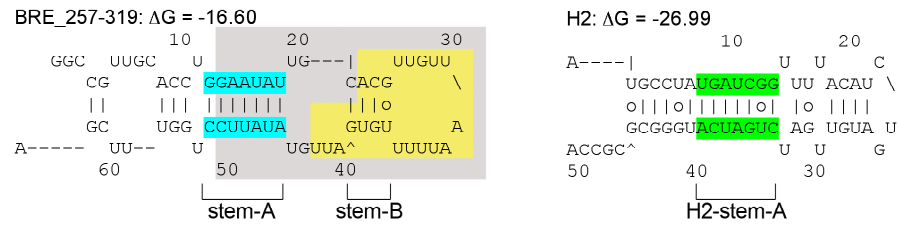


Fig. 3.16: Predicted secondary structures of BRE_257-319 and H2. In the predicted secondary structure of BRE_257-319 (left), the area in grey indicates the sequence that is conserved among different *Drosophila* species; the area in yellow shows the miR-308 binding target. The predicted secondary structure of H2 (right) contains a putative stem structure (marked in green, H2-stem-A), which shows structural similarity to the stem structure in BRE_257-319 (marked in blue, stem-A). Secondary structure predictions were performed using the mfold program (version 2.3).

3.4.1 Mutations in the miR-308 target site abolish BCD-mediated translational repression

To investigate the role of miR-308 in *cad* mRNA translational regulation, I introduced 4 point mutations in the Dm3' that lead to the disruption of miR-308 binding. Two base pairs in stem-B, nt 281C, 282G and nt 294G, 295U, were changed into 281G,282U and 294A,295C, so that the overall structure may be retained (Fig. 3.17, A). The resulting sensor, 38F-Dm3'mut, should be incapable of interacting with miR-308 through that site. I analysed the expression levels of the sensor 38F-Dm3'mut in embryos and in comparison to sensor 38F-Dm3' (Fig. 3.17, B). Embryos deriving from females with the sensor 38F-Dm3'mut show about 50 % increase in dnGFP fluorescence intensities as compared to sensor 38F-Dm3', which carries the wt *cad* 3'UTR (Fig. 3.17, C, $100\% \pm 3.6$ in embryos deriving from 38F-Dm3'mut/+;nos-GAL4:VP:16 females; $53.1\% \pm 2.2$ in embryos deriving from 38F-Dm3'/+;nos-GAL4:VP:16 females; $p = 3.10 \times 10^{-13}$). These results indicate a de-repression, which is most likely due to loss of miR-308 binding.

38F-Dm3'mut sensor transcripts lost their susceptibility to BCD, because dnGFP fluorescence of 38F-Dm3'mut is unaffected by BCD isoform G (Fig. 3.17, C; maternal genotype: UAS-BCDG^{F4M6}/+;38F-Dm3'mut/+;nos-GAL4VP:16/+; $p = 0.46$). Next I asked, whether the other homeodomain-bearing BCD isoforms are capable of mediating the repression of 38F-Dm3'mut, perhaps through binding to other sites in the mutated *cad* 3'UTR. The analysis, including BCD isoform D, E or F, revealed that none of these isoforms are able to downregulate dnGFP in the 38F-Dm3'mut sensor (Fig. 3.17, D). It seems therefore that the nucleotides that have been mutated in 38F-Dm3'mut are crucial for translational repression by any homeodomain-bearing isoform of BCD.

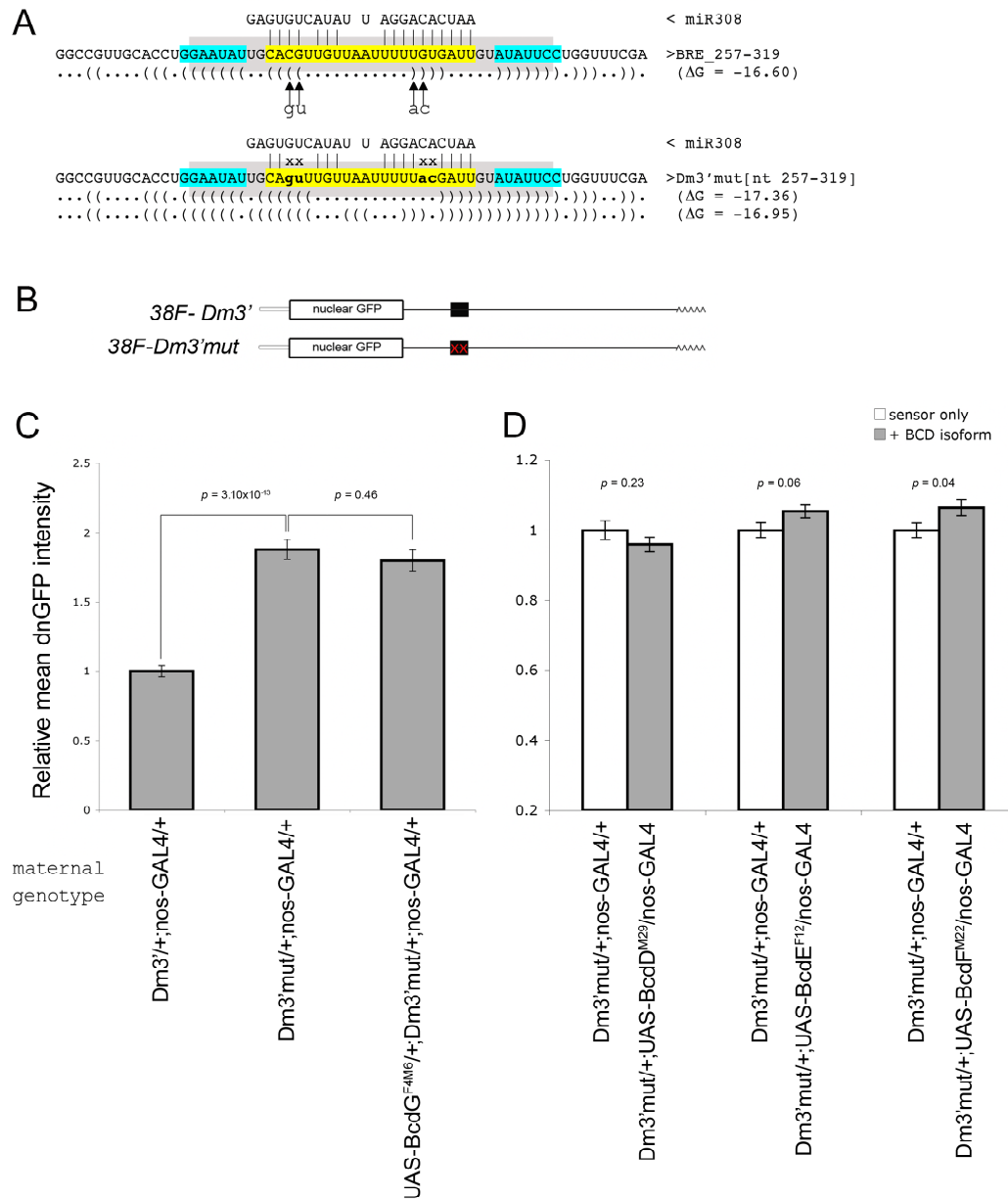


Fig. 3.17: Translational reporter assay for repression of the mutated *cad* 3'UTR in sensor 38F-Dm3'mut by different BCD isoforms. (A) miR-308 binding to wt target in BRE_257-319 of Dm3' (indicated in yellow) and mutated target Dm3'mut (mutated nt in small, bold letters). The predicted secondary structures (Vienna format) are indicated below the sequence of the wt and mutated BRE_257-319. The area in grey indicates the sequence, which is conserved among different *Drosophila* species. Blue regions form the putative stem structure stem-A. Nucleotides that were changed in 38F-Dm3'mut are indicated by arrows. (B) Schematic overview of the transgenic reporter transcripts. (C) Average dnGFP intensities of 38F-Dm3'mut are roughly 50% higher as compared to 38F-Dm3' ($p = 3.10 \times 10^{-10}$) and unaffected by the presence of UAS-BcdGF^{F4M6} ($p = 0.46$). (D) Average dnGFP intensities of 38F-Dm3'mut in the presence of BCD isoform D ($p = 0.23$), E ($p = 0.06$) and F ($p = 0.04$). The p value obtained for isoform F is marginally above the 5% threshold of statistical significance. This difference could not be reproduced in independent measurements and the dnGFP levels of the 38F-Dm3'mut sensor in the presence of isoform F are therefore regarded as not different. Bars represent relative mean dnGFP values \pm SE, statistical significance was analysed using Students t-test. dnGFP intensity values were measured from region of interests of identical size from the surface of blastoderm embryos at nuclear division cycle 11.

3.4.2 Translational repression of 38F-BRE₂₅₇₋₃₁₉ and 38F-H2 by BCD isoform F

Mutations that disrupt the miR-308 target site in 38F-Dm3'mut not only abolish miRNA-induced repression, but also result in loss of BCD-dependent repression by all isoforms. This could suggest that miR-308 activity may be necessary for BCD to function as a translational repressor. However, the mutations in sensor 38F-Dm3'mut may have changed the structure of the BRE₂₅₇₋₃₁₉ fragment or affected BCD binding directly (further discussed in 4.1.3). The H2 fragment contains a BCD-binding element (see 3.2.2.2), which is most likely independent of miRNA function, because H2 lacks predicted miR-308 binding target sites. Using this fragment I wanted to investigate whether there might be a difference in the translational output by a BCD isoform with and without d4EHP-binding domain (BCD isoform G and F, respectively) in the absence of miRNA activity.

Sensor 38F-BRE₂₅₇₋₃₁₉ or sensor 38F-H2 were co-expressed with isoform F (yw;38F-H2/+;UAS-BCDF^{M22}/nos-GAL4:VP16) or with isoform G (UAS-BCDG^{F4M6}/+;38F-BRE₂₅₇₋₃₁₉/+;nos-GAL4:VP16/+) and the dnGFP levels analysed in embryos deriving from those females. Fluorescence levels of sensor 38F-BRE₂₅₇₋₃₁₉ show a reduction of about 20% induced by BCD isoforms G (80.6 % ± 1.4 of initial dnGFP levels, $p = 4.8 \times 10^{-15}$) and isoform F (75.3 % ± 1.2 of initial dnGFP levels, $p = 2.8 \times 10^{-20}$) (Fig. 3.18, A and B). In contrast, fluorescence levels of sensor 38F-H2 were reduced to only 87 % ± 2.9 of the initial sensor levels by BCD isoform G ($p = 0.001$) and 93.9 % ± 1.8 by BCD isoform F ($p = 0.03$) (Fig. 3.18, D and E). These results show that BCD isoforms G and F are both able to repress dnGFP levels of sensor 38F-BRE₂₅₇₋₃₁₉, but repression of sensor 38F-H2 is significantly lower, with repression by BCD isoform F being marginally significant.

In comparison to the BRE₂₅₇₋₃₁₉ fragment, interaction of BCD with H2 is less efficient in mediating the translational repression. This is consistent with the weaker binding affinity of the BCD homeodomain to the H2 fragment seen in EMSAs. Furthermore, BCD isoform F seems to be less effective than isoform G but is still capable of repressing sensor 38F-H2. This result suggest the existence of mechanism for BCD-mediated translational repression, which is independent of miR-308 and d4EHP.

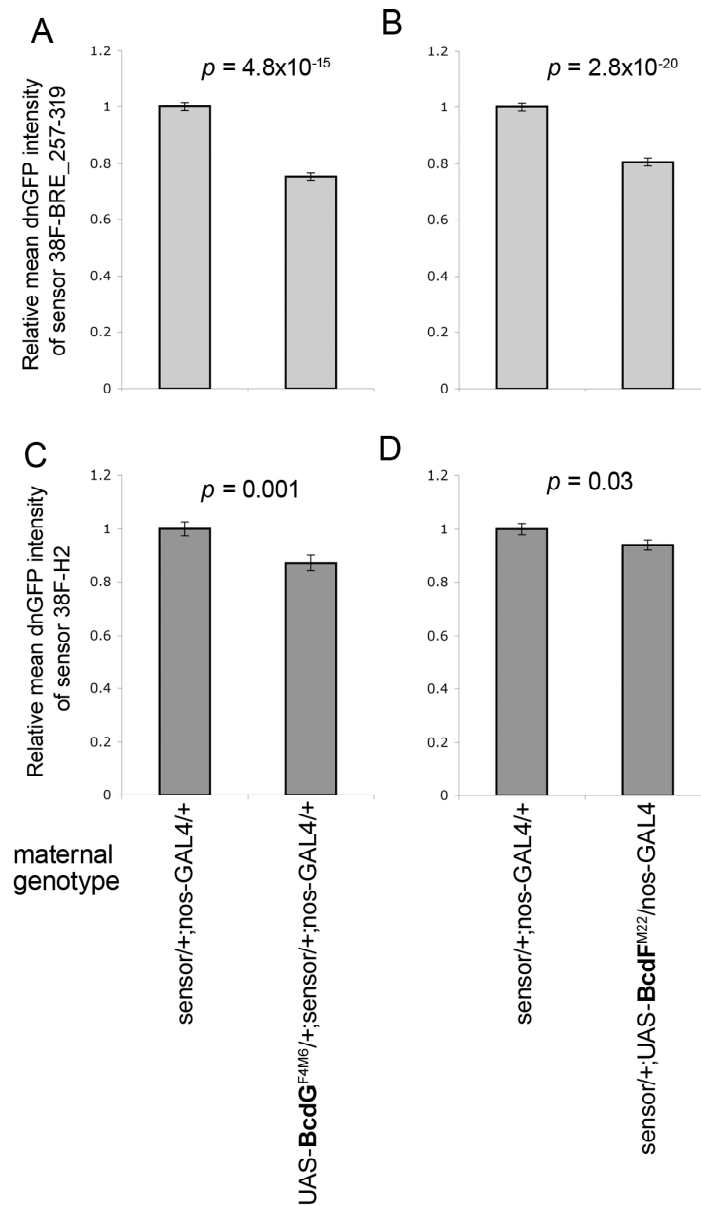


Fig. 3.18: Translational reporter assay for repression of BRE₂₅₇₋₃₁₉ and H2 by BCD isoforms G and F. (A) Mean dnGFP intensities of sensor 38F-BRE₂₅₇₋₃₁₉ in the presence of BCD isoform G ($p = 4.8 \times 10^{-15}$) and BCD isoform F (B, $p = 2.8 \times 10^{-20}$) are reduced by about 20 % compared to dnGFP levels of the sensor alone. Mean dnGFP intensities of sensor 38F-H2 are reduced by about 10 % in the presence of BCD isoform G (C, $p = 0.001$) and BCD isoforms F (D, $p = 0.03$) compared to the dnGFP levels of the sensor alone.

3.4.3 Conclusions

The *cad* 3'UTR contains a predicted target site for miR-308 (Brennecke et al., 2005; Stark et al., 2005). miR-308 has previously been cloned from embryonic total RNA extracts, showing low expression levels, which were undetectable by Northern blotting

(Aravin et al., 2003; Leaman et al., 2005). Here I show that a mutation in the miR-308 binding target of the *cad* 3'UTR elevates the expression levels of a sensor as compared to the wt 3'UTR. These observations suggest that miR-308 represses expression of a sensor that carries the *cad* 3'UTR. Because the miR-308 target site is located in the BCD binding fragment BRE_257-319, miR-308 may be involved in BCD-mediated control of *cad* translational repression. To address this question, I analysed whether the 38F-Dm3'mut sensor, which carries four point mutations in the miR-308 binding site, is susceptible to BCD repression. None of the BCD isoforms showed an effect on the dnGFP levels of the 38F-Dm3'mut sensor.

This finding would be consistent with a mechanism for BCD-mediated translational repression that also involves miR-308. However, mutations present in Dm3'mut may have disrupted the RNA structure due to the initial mutagenesis design. Secondary structure predictions of the mutated *cad* 3'UTR fragment revealed that the introduced sequence modifications could also influence the secondary structure of stem-A (Fig. A4.3). Hence, it cannot be excluded that along with the destruction of the miR-308 target site, structural changes in the RNA occurred that altered the putative BCD-binding motif. Therefore, the mutations in 38F-Dm3'mut might change the secondary structure, which might be essential for BCD action, or the mutations may directly affect BCD binding.

The translational repression of sensor 38F-Dm3' by BCD isoforms that lack the d4EHP-binding domain (BCD isoforms E and F) could indicate the existence of a d4EHP-independent mechanism. I wanted to ask, whether the effects of miRNA action are important for translational repression by such BCD isoforms. Sensor 38F-H2, which is free of putative miRNA target sites in *Drosophila*, is translationally repressed by BCD isoform F. The level of repression, however, is very low compared to repression by BCD isoform G and only marginally significant. This shows that the repression of 38F-H2 mediated by BCD isoform F is less effective than the repression mediated by isoform G. Therefore, the absence of d4EHP function reduces BCD activity with sensor transcripts that lack miRNA target sites. It is possible that the presence of miRNA activity may aid BCD activity, however is dispensable for BCD-mediated translational repression.

4 General Discussion

4.1 Insights into translational control of *cad* in *Drosophila*

Rivera-Pomar et al. (1996) reported binding of the BCD homeodomain to a fragment corresponding to nt 66-185 (here termed BRE_66-185) of the *cad* 3'UTR. The authors presented *in vivo* data from a CAT reporter assay with *cad* 3'UTR fragments showing reduction of translational efficiency in the presence of BCD. Only BCD derivatives containing the homeodomain could interact with the full *cad* 3'UTR (Rivera-Pomar et al., 1996). Sequence-specificity of BCD binding to the BRE_66-185 fragment using competition experiments were not performed. Subsequently, this RNA fragment was used to analyse different BCD protein regions that are involved in *cad* translational repression and the DNA/RNA-binding properties of the BCD homeodomain (Niessing et al., 1999; Niessing et al., 2000).

Dubnau and Struhl (1996) showed that a 342-nucleotide fragment (here termed BRE_210-553) of the *cad* 3'UTR is necessary and sufficient for BCD-dependent translational repression of a reporter transcript. They provided evidence for at least two binding sites in the BRE_210-553 fragment shown by direct binding of the BCD homeodomain to nt 210-318 and to nt 319-433 of the *cad* 3'UTR in cross-linking experiments. In the same assay, binding to a fragment containing *cad* 3'UTR nt 434-533 did not occur. Reporter constructs containing nt 1-318 and 553-940, or nt 1-443 did not mediate anterior repression of the reporter (see Dubnau and Struhl, 1996, Fig. 2c). Hence, the authors suggested that the full region of the BRE_210-553 element is necessary for translational repression *in vivo*.

The binding specificity of the BCD homeodomain to a fragment within BRE_210-553, spanning only the 43 nt (here termed BRE_210-253), was further characterized *in vitro* using electrophoretic mobility shift assays. The authors reported sequence-specific binding of the BCD homeodomain to this fragment (Chan and Struhl, 1997).

In my translational reporter assay, sensors carrying the BRE_257-319 fragment can interact with BCD and mediate translational repression of the reporter, while four point mutations, in this fragment within region nt 281-295 (sensor 38F-Dm3'mut) result in loss of BCD-mediated repression. Therefore, the region 281-295 of the *cad* 3'UTR

contributes to BCD-binding in the BRE₂₅₇₋₃₁₉ fragment, which is sufficient to mediate translational repression of reporter transcripts by BCD.

This finding is in conflict with the results obtained with the reporter assay of Dubnau and Struhl (1996). Reporter constructs carrying nt 1-318 and 553-940 and nt 1-443 of the *cad* 3'UTR (including BRE₂₅₇₋₃₁₉) did not mediate anterior repression of the reporter in the embryo. One possible explanation is that their reporter assay was not sensitive enough to detect subtle differences in translational repression levels mediated by different BCD-binding elements and required the presence of multiple BCD-binding sites to show anterior repression by BCD. This would imply the presence of several BCD-binding sites, with additive effects on translational repression of this reporter. Alternatively, proper folding of the BCD-binding element might have been disrupted in these reporter derivatives. The reporter was capable to detect translational repression only when the complete BRE₂₁₀₋₅₅₃ fragment was present.

The use of a fluorescent protein in my reporter assay, combined with the ectopic expression of BCD, allows the quantitative analysis of small but significant differences in expression. Thus it was possible to detect loss of BCD repression in a fragment with only four nucleotide changes. It is possible that previously undetected BCD-binding sites in the *cad* 3'UTR, which function *in vivo* but are of lower efficiency in mediating repression, may be identified by using my translational reporter assay.

Most *cis*-regulatory elements that regulate the translational output of an RNA lie within untranslated regions of mRNAs. These regions are usually under lower selective pressure to maintain their primary sequence than the coding sequences. One of the reasons might be that *cis*-regulatory elements can be encoded by structural features of the RNA molecule, which can be formed by different primary sequence (reviewed in Schroeder et al., 2004). The BCD-binding signal might be encoded by secondary structures of RNA fragments. The BRE₂₅₇₋₃₁₉ and H2 fragments do not share sequence similarities, however, these fragments share a similar stem in their predicted secondary structures, stem-A in BRE₂₅₇₋₃₁₉ and H2-stem-A in H2. Both fragments are bound *in vitro* by the BCD homeodomain and mediate BCD-dependent repression of sensor transcripts in embryos.

Could this stem structure “mimic” the structure of the BCD double stranded (ds) DNA target and therefore co-opt the homeodomain’s DNA-binding properties for RNA binding? DNA recognition of the BCD homeodomain occurs through direct contacts in the major groove of the DNA targets, which are mediated by the residues K50 and R54

(Baird-Titus et al., 2006; Niessing et al., 2000). Interestingly the side-chains of K50 and R54 seem to show some flexibility in their precise positioning during the contact making of the DNA target (Baird-Titus et al., 2006). dsRNA normally adopts A-form helices, displaying a major groove which is narrower and deeper than the B-form helices of dsDNA and cannot be accessed by an α -helix as occurs in dsDNA binding. However, a sequence of purines can cause dsRNA to adopt a different helical conformation (so-called A' conformation), with an expanded major groove, similar to that of B-form dsDNA (Bullock et al., 2010).

The fact that the BCD homeodomain binds to RNA fragments like BRE_257-319 and the H2 fragment, but not to unstructured RNA fragments (CU58mer) could be an indication for the preference of the homeodomain to bind to RNA molecules that contain helical structures. It is conceivable that within the physical constraints of the BCD homeodomain the binding occurs to an RNA molecule that is mimicking the DNA target and allowing the homeodomain to access the major groove of the RNA helix, e.g. A'-form helix. Perhaps binding to the RNA depends primarily on a specific structure rather than a specific sequence, which would explain how the BCD homeodomain binds to different RNA sequences. At the same time, it is possible that the BCD homeodomain requires specific base contacts with a few bases of the RNA, especially if the binding to RNA occur in a similar way as the DNA binding.

Whether the stem structures in the BRE_257-319 or H2 fragments adopt an A'-form or B-form-like conformations can only be revealed by crystallizing the RNA:HD complex and inferring the structure of the complex. As a first approach, it would be interesting to further investigate the role of the stem structure of the BRE_257-319 or the H2 fragment in BCD RNA binding by testing point mutations that interfere with binding by using the *in vivo* translational reporter assay.

A more indirect indication can be drawn from the analysis of the *Tc'cad* 3'UTR, which does not interact with BCD in the translational reporter assay and cannot interact *in vitro* with the BCD homeodomain. I could not find any structural similarities in the *Tc'cad* 3'UTR to the BRE_257-319 fragment using the RNAforester program (data not shown). Thus, the remaining sequences in the *Tc'cad* mRNA have to be further analysed for putative BCD binding element(s). In fact, a region situated in the ORF spanning nt 451-485 of the *Tc'cad* cDNA (numbering begins from the first nt in the cDNA) shows structural similarities to the BRE_257-319, but can at this point only be suggested as a promising candidate that observed BCD-dependent translational repression.

Another discrepancy between my results and previously published data concerns the binding specificity of the BCD homeodomain to the *cad* 3'UTR. Chan and Struhl (1997) reported specific binding of the BCD homeodomain to an RNA fragment containing nt 210-253 of the *cad* 3'UTR (here termed BRE_210-253). The BRE_210-253:BCD homeodomain-complex was undisturbed in the presence of a 100-fold excess of Tub α -1 RNA. From Figure 1a of Chan and Struhl (1997), we deduce that this fragment was approximately 300 nucleotides long, similar in size to the fragment of Tub α -1 RNA. In my competition experiments, binding of the BCD homeodomain to a similar sized fragment, the BRE_164-339 (a 214 nt fragment, which includes nt 210-253), occurred with dramatically lower specificity. The interaction of the BCD homeodomain with the BRE_257-319 fragment was also weak and showing relatively low specificity in competition experiments. This interaction was confirmed using my *in vivo* translational reporter assay, which strongly supports a functional interaction of BCD with this fragment. *In vitro* the binding of the BRE_257-319 fragment to the BCD homeodomain seems to be easily competed by unrelated RNAs such as shSV40. However, BCD is unable to bind to SV40 3'UTR with high affinity in the EMSA experiments and the *in vivo* results show that expression of the sensor carrying the SV40 3'UTR is unaffected by BCD. This might also suggest that *in vivo* RNA-binding specificity of the full-length BCD protein is higher than homeodomain binding *in vitro*.

My results suggest that recruitment of additional factor(s) may increase the RNA-binding specificity of the protein *in vivo*. This means that perhaps the presence of other sites of the BCD protein or factors acting in *trans* help in conferring this specificity.

4.2 Alternative mechanisms of translational control of *cad* mRNA

4.2.1 Evidence for d4EHP-independent *cad* translational repression

The role of d4EHP in *cad* translational repression by BCD has been previously identified through genetic and biochemical analysis (Cho et al., 2005). The authors showed that BCD derivatives carrying mutations in the d4EHP-binding domain were unable to exert translational regulation on *cad* mRNA. These mutants included *bcd*^{Y66A} and *bcd*^{L73R} that carried changes in the amino acid residues Y66 and L73. In contrast, in my experiments, BCD isoforms E and F, which lack the 4EHP-interaction domain, were capable to mediate translational repression of sensors like 38F-Dm3' (Tab. 4.1).

Perhaps, BCD isoforms E and F are able to exert different protein functions and are thus to mediate the translational repression of sensor 38F-Dm3. This could be due to different properties imparted by the N-terminal domain, which is present in BCD isoforms G and D, but absent in E and F. Alternatively, translational repression of *cad* with *bcd*^{Y66A} and *bcd*^{L73R} without d4EHP was not detectable due to visualisation with α -CAD antibodies. My translational reporter assay is a more sensitive assay for translational repression. BCD isoforms E and F are ectopically expressed during oogenesis and might therefore be able to show an effect on translation of the sensor.

Niessing et al. (1999) used a dicistronic reporter assay to investigate the role of BCD protein domains other than the homeodomain in *cad* translational repression. The first cistron encoded the chloramphenicol acetyltransferase (CAT), the second cistron encoded luciferase (Luc). Both cistrons were separated by an internal ribosome entry site (IRES), making it possible to distinguish between cap-dependent (CAT activity) and cap-independent (Luc-activity) translational repression. The 3'UTR of this reporter contained the BBR of the *cad* 3'UTR, which was previously characterized by Rivera-Pomar et al. (1996). This reporter was then co-transfected with effector plasmids containing different truncated BCD proteins. The deletion analysis with the truncated BCD proteins showed that C-terminal deletions up to the PEST domain and N-terminal deletions up to close to the homeodomain are able to exert translational repression of the reporter. Of these N-terminal deletions, Bcd⁷⁷⁻²⁰² (deletion of aa 1-76 and 202-489; the full length BCD protein must refer to BCD isoform D, which contains 489 aa) gave a weaker repression of translation of the reporter than Bcd⁴¹⁻²⁰². The protein domains that

lie between amino acid 41 and 77 are the SID (aa 52-61) and the d4EHP-binding domain (65-77), therefore the truncated protein BCD⁷⁷⁻²⁰² lacks these domains.

These findings agree with my results, suggesting that BCD can mediate translational repression of the reporter in the absence of the d4EHP-binding domain: this is seen both with truncated Bcd⁷⁷⁻²⁰² with the CAT/Luc reporter in S2 cells and by BCD isoforms E and F in my translational reporter assay in embryos. In both approaches translational repression of sensors with the *cad* 3'UTR was assayed out of the natural context of early embryogenesis. It is therefore possible that additional mechanisms available in S2 cells and during oogenesis were employed to mediate repression.

4.2.2 The putative role of miR-308 in BCD-dependent *cad* translational repression

The de-repression of sensor 38F-Dm3'mut, which contains four point mutations in the miR-308 binding target site, provides the first evidence for a role of miR-308 in control of *cad* mRNA expression in *Drosophila*. Interestingly, the miR-308 target site is located within a characterized BCD-binding fragment. It seems though that miRNA activity may be a redundant mechanism for BCD translational repression, as demonstrated with sensor 38F-H2, which lacks predicted miRNA binding targets, but mediates low repression (discussed further below). For the putative involvement of miR-308 in translational repression, these findings can be interpreted in three ways:

(1) BCD and miR-308 act independently from each other. While miR-308 reduces overall mRNA levels, BCD mediates translational repression to prevent CAD protein from being expressed at the anterior part of the embryo. Both share an overlapping interaction site in the *cad* 3'UTR. The mutations introduced in 38F-Dm3'mut therefore destroyed both the BCD-mediated and the miR-308-mediated translational regulation.

(2) miR-308 binding is involved in BCD-mediated translational repression, but dispensable. BCD can follow other mechanisms to mediate translational repression, however the absence of miR-308 activity results in a reduced BCD-dependent repression as it was observed with sensor 38F-H2. The loss of BCD-dependent repression of sensor 38F-Dm3'mut could be explained by changes in the RNA secondary structure that affect BCD binding.

(3) miR-308 binding is necessary for the BCD-mediated translational repression. In this case, it should be possible to regain BCD-dependent translational repression of the 38F-Dm3'mut sensor by providing a miRNA that carries nucleotide changes that are complementary to those in Dm3'mut mutations.

In a variation of interpretation (3), I speculated that translational repression by BCD isoform F may entirely depend on the miRNA interaction, while BCD isoform G can mediate the repression through the d4EHP-mediated mechanism. To test this hypothesis, I analysed sensor 38F-H2 in the presence of BCD isoform F. BCD isoform F shows a less translational repression of sensor 38F-H2 in comparison to 38F-BRE_257-319. However, the translational repression of 38F-H2 by BCD isoform F is at the border of statistical significance. At this point these results are not conclusive and a more detailed investigation of fragment H2 with BCD isoform F will be required. If it will be shown that BCD isoform F is indeed incapable to mediate translational repression of sensor 38F-H2, then this would be the first indication for a miRNA dependence of translational repression by a 4EHP-independent mechanism.

Tab. 4.1: Presence of d4EHP-binding domain in different BCD isoforms and their ability to mediate translational repression of different sensors. Only isoform G and D contain a d4EHP-binding domain (indicated by +). *The translational repression of sensor 38F-H2 remains to be confirmed as current measurements were found to be only marginally significant. (+) indicates repression; (-) indicates no repression; n.a. = not analysed.

		BCD isoform				
		G	D	E	F	A
d4EHP-binding domain		+	+	-	-	-
repression of reporter	Dm3'	+	+	+	+	-
	BRE_257-319	+	+	+	+	n.a.
	Dm3'mut	-	-	-	-	n.a.
	H2	+	n.a.	n.a.	+*	n.a.

4.3 Implications for the evolution of *cad* translational regulation

Drosophila cad promotes posterior identity and it is crucial to prevent its expression in the anterior of the early embryo (Macdonald et al., 1986; Rivera-Pomar et al., 1995; Schulz and Tautz, 1995). The anterior determinant BCD has acquired the function to repress *cad* mRNA translationally (Rivera-Pomar et al., 1996; Dubnau and Struhl, 1996). BCD is an evolutionary novelty of higher dipteran flies, thus, different factors or mechanisms must mediate this process in other insect species. For example the parasitic wasp *Nasonia*, which is thought to have evolved long-germ embryogenesis independently from flies, localizes *cad* mRNA at the posterior pole of the embryo, which then creates a posterior to anterior concentration gradient of the *cad* mRNA and most likely also of the CAD protein (Olesnicky et al., 2006) (Fig. 4.1).

In the beetle *Tribolium*, *Tc'cad* is maternally expressed and distributed uniformly in the early embryo. Unlike in *Drosophila*, the Tc'CAD protein is detected uniformly at early blastoderm stages and shortly after the protein becomes restricted to the posterior part, resembling a posterior to anterior gradient (Schulz et al., 1998). The onset of zygotic *Tc'cad* expression is not clearly distinguishable from the maternal expression at the time of the protein gradient formation. The earliest zygotic *Tc'cad* transcripts, however, occur at a rather early blastoderm stage (person. comm., A. Peel). The repression of anterior *Tc'cad* expression is thought to be mediated by two zygotic genes, *Tc'zen-2* and *Tc'mex-3*, and is suggested to represent the ancestral state of *cad* translational repression in insects (Schoppmeier et al., 2009) (see below and Fig.4.1).

In order to gain further insight into when and how *cad* translational control evolved from a still undefined ancestral state to the BCD-dependent mechanism observed in *Drosophila* we can gather clues from comparisons with other related insect species. Presumably there are two aspects in the process of *cad* translational repression that have evolved or may be conserved among different species: (1) the RNA target sequence in the *cad* 3'UTR and (2) the mode of *cad* regulation, e.g. the ability of an anterior factor to bind to this sequence and mediate translational repression.

To address the former, I analysed the regulation of *cad* 3'UTRs of the dipteran *Haematopota* and the beetle *Tribolium* in the presence of BCD using the translational reporter assay. The *Haematopota cad* 3'UTR is translationally regulated by BCD in *Drosophila* and the BCD homeodomain directly binds to the H2 fragment of the *Hp'cad* 3'UTR *in vitro*. In contrast, sensors with the *Tribolium cad* 3'UTR are not regulated by BCD, therefore the previously reported BCD-dependent translational repression of

Tc'cad in transgenic *Drosophila* embryos (Wolff et al., 1998) most likely depends on unidentified sequences in the 5' UTR or the coding sequence of the *Tc'cad* mRNA.

The discovery that the *Hp'cad* 3'UTR can mediate BCD-dependent translational repression in *Drosophila* suggests the existence of an RNA signal that is conserved among these insect species. Although there are no extensive sequence similarities, there are hints, provided by comparisons of the 3'UTR fragments BRE_257-319 and H2, that the secondary structure may contribute to this conserved BCD-recognition signal. This hypothesis may be tested through the identification of putative conserved secondary structures in the *cad* 3'UTRs of other related insect species and the investigation of the ability of these *cad* 3'UTR fragments to confer translational repression by BCD.

The second aspect in the process of *cad* translational repression concerns the ability of an anterior factor to bind to the 3'UTR. Conserved 3'UTR elements indicate the existence of similar or related factors, repressing the mRNA bearing these elements. Which factor(s) might be involved in the translational repression of the *cad* homologues in different insect species and do they recognize the same RNA-elements? BCD arose through a gene duplication of a *Hox3/zen-like* gene progenitor in the lineage of the cyclorrhaphan flies (Falciani et al., 1996; Stauber et al., 1999). The 4EHP-binding domain of BCD is highly conserved among different Drosophilid species, and therefore *cad* translational repression most likely employs the 4EHP-mediated mechanism of translational repression in all Drosophilids. The sister gene of *bcd*, *zen* seems to be a good candidate for *cad* translational repression in other insect species. In dipterans like *Empis livida*, *Haematopota pluvialis* or *Clogmia albipunctata*, the *Hox3/zen-like* genes share more similarities with *zen* genes and lack a 4EHP-binding domain (Stauber et al., 2002). The homeodomain of *Haematopota zen* (*Hp'zen*) does not contain the amino acid residue (R54), which has been shown to define the RNA-binding specificity in BCD (Niessing et al., 2000; Stauber et al., 2002). *Hp'cad* and *Hp'zen* mRNAs are maternally expressed, however it is not clear, how the mRNAs are distributed in the embryo and whether Hp'ZEN may regulate *Hp'cad* translation.

One of the *zen* orthologues in *Tribolium*, *Tc'zen-2*, has been shown to repress *Tc'cad* mRNA, but so far there is no evidence for a direct interaction of Tc'ZEN-2 with the *Tc'cad* mRNA. Tc'ZEN-2 does not contain a 4EHP-binding domain and *Tribolium* 4EHP RNAi does not affect *Tc'cad* mRNA translation (Schoppmeier et al., 2009). Tc'ZEN-2 also lacks Arginine at position 54 of the homeodomain. It is therefore unclear if the *Tribolium zen* orthologue is able to mediate *cad* translational repression directly.

Taken together it seems unlikely that *zen* proteins in other insects would confer translational repression in a similar way as BCD does in *Drosophila*, although a more detailed analysis of *Tc'cad* and *Hp'cad* translational repression should be undertaken to address this question. Because *zen* proteins do not seem to fulfil the requirements that have been shown to be necessary for BCD RNA-binding, it is likely that ancestrally one or more unknown factors, perhaps in concert with ZEN, were employed for *cad* translational repression. The analysis of the BCD isoforms has revealed that a d4EHP-independent mechanism(s) exist for *cad* translational repression in *Drosophila*. I suggest that this mechanism might represent aspects of an ancestral state of *cad* translational repression. It will therefore be important to identify the factors involved, as they might have a role during translational repression of *cad* homologues in other insect species.

Which evolutionary event preceded the other: the amino acid changes in the BCD homeodomain that lead to the BCD RNA-binding properties or RNA nucleotide adaptations in the *cad* transcript, creating a binding signal for a DNA-binding protein? The adaptability of RNA molecules is thought to be very high; it is even possible to create RNA sequences that artificially adopt DNA-binding target signals of transcription factors that were not known to bind to RNA (Cassiday and Maher III, 2002). Conserved functional interactions of the *Drosophila* and *Haematopota* 3'UTR fragments with BCD suggest that there was selective pressure on these 3'UTR sequences to maintain a signal for translational repression. While, sequence similarities are largely lost, the predicted secondary structures of BRE_257-319 and H2 show overall similarities. However, it is not clear to what extent the secondary structures and/or perhaps specific nucleotides within these structures may contribute to BCD homeodomain binding. A detailed analysis of these two structures may help to reveal which nucleotide substitutions within the secondary structure can be tolerated and which reduce or abolish BCD RNA-binding. Such an analysis might give clues about the adaptations of RNA sequences and the switch to an anterior regulator that used to be a DNA-binding protein, like the *Hox3/zen*-like derived *bcd* gene, which was co-opted into a new function in translational regulation.

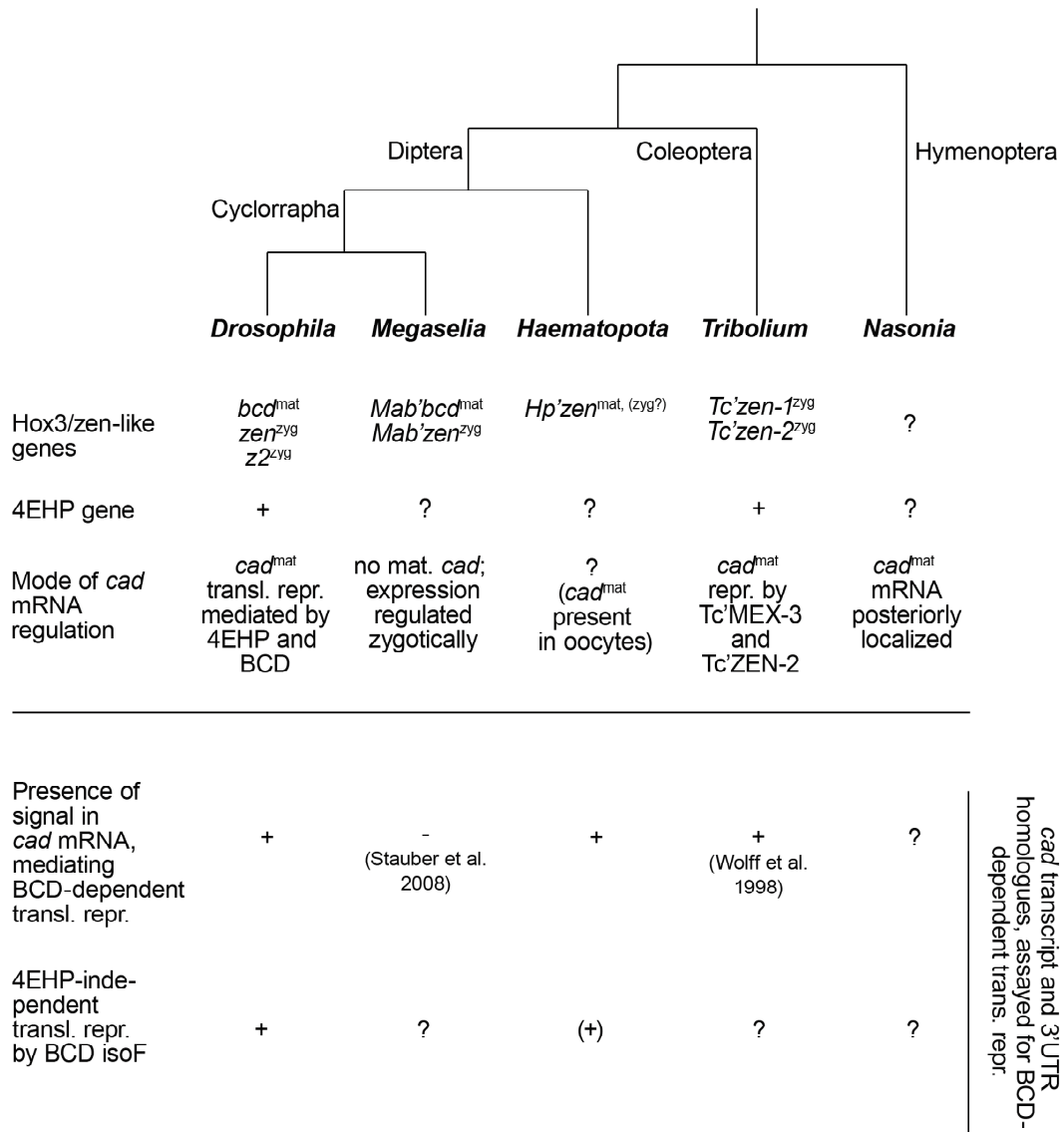


Fig. 4.1: Phylogeny of insect species (after Savard et al., 2006) discussed with features of *cad* translational repression mapped on. Uncertain characters states have been left clear (?) or are marked if further experiment are required to confirm the result (*). mat = maternal; zyg = zygotic; trans. repr. = translational repression.

4.4 Summary and future directions

In *Drosophila*, the simultaneous binding of the anterior determinant Bicoid (BCD) to the 5'-cap associated factor d4EHP and the mRNA of the posterior patterning gene *caudal* (*cad*) leads to translational repression of the transcript. Because BCD is an evolutionary novelty in the lineage that lead to *Drosophila*, other insect species most likely follow alternative strategies to restrict *cad* mRNA to the posterior of the embryo. The establishment of an *in vitro* assay using EMSA and an *in vivo* sensor assay for BCD-mediated translational repression allowed me to identify elements in the *cad* 3'UTR of *Drosophila* and *Haematopota pluvialis* that mediate BCD-dependent translational repression. These elements show similarities in their predicted secondary structures.

The BCD-binding region of the *Dm'cad* 3'UTR co-localizes with a miR-308 target site and mutations in this region that abolish miRNA-binding suggest a miRNA-dependent function in BCD-mediated translational repression. Furthermore, BCD isoforms that lack the d4EHP-binding domain are able to mediate translational repression of sensors carrying the BCD-binding region. Taken together, these findings suggest that alternative mechanism(s) for the translational repression of *cad* mRNA are likely to exist in *Drosophila* and may also be present in other insect species.

The model of *cad* translational repression by BCD has become a paradigm for translational regulation, in which translational repression is mediated through competition of translational initiation factors by 4EHP (Cho et al., 2005). I suggest that other mechanisms may exist by which BCD can mediate *cad* translational repression in the absence of 4EHP activity. Thus, the model of *cad* translational repression by BCD has to be re-evaluated for a more complete picture. The following questions are posed by this work: How does this 4EHP-independent mechanism(s) function and how relevant is it for the development of the *Drosophila* embryo? How does miR-308 and/or other miRNAs contribute to translational control of *cad*? How important is the secondary structure of the BCD-binding element?

Generating an *in vivo* reporter that quantitatively senses BCD-dependent translational repression will be a useful tool in answering some of these questions. For instance it will be possible to introduce specific point mutations into BCD-binding regions that disrupt the secondary structure of the RNA and measure to what extent these mutations influence BCD-mediated repression. The role of miR-308 in *cad* translational

repression may be approached by a rescue experiment. Providing a miRNA that contains complementary changes to the mutations introduced in the sensor 38F-Dm3'mut may result in a recovery of BCD-dependent translational repression of 38F-Dm3'mut, which can be tested using the *in vivo* reporter assay.

The findings of my PhD have also opened new directions for the investigation of the evolution of *cad* translational repression and early axis patterning in general. How conserved is 4EHP-independent regulation of *cad* among different insect species? Does this mechanism perhaps create a link between BCD-dependent anterior patterning in *Drosophila* and anterior patterning by Tc'MEX-3 and Tc'ZEN-2, the factors that regulate the *cad* homologue in *Tribolium*? Could it be a remnant of an ancestral mechanism that functioned before the co-option of BCD into translational control? It would be important to identify the factors that are involved in the 4EHP-independent mechanism of BCD isoform E and F and to see, whether they play a role in translational regulation of *cad* in other insect species. This questions could be addressed by using co-immunoprecipitation of protein complexes formed with BCD isoform F and compare these to co-immunoprecipitated proteins of complexes formed with BCD isoform G. Potential factor(s) that are present only in precipitates of BCD isoform F may then be identified using mass spectroscopy.

5 Materials and Methods

5.1 Oligonucleotides

5.1.1 Oligonucleotides for cloning procedures

Tab. 5.1: Oligonucleotides for cloning procedures; restriction sites are indicated in small letters.

Primer	Sequence (5' to 3')
SV40-R01	AGGGGGAGGTGTGGGAGG
006-R_AscI	ttggcgccGTGAACGTTAACCTTATTAACC
007-F_EcoRI	ttgaattcTTCCCTCACAACCTCATATGACCG
008-R_AscI	tgccgcccCAAATAAAATCATTTATTCTTCAC
009-F_BamHI	cgggatccATGTGACACGACCATTCC
011-F_EcoRI	cggaattcTGACCACATTAACGCAT
012-R_AscI	aggcgcccCTAAGTAATTTAAGTATAATTA
021-F_NdeI	ggaattccatagCCACGTGCGACCCGCACC
022-R_BamHI	cgggatccCTACTAGGACTGGTCCTTGTGCTGATC
038-F_KpnI	cgggtaccATGGCGCAACCGCCG
039-R_BamHI	gcggtaccATTGAAGCAGTAGGCCAACTGCG
043-F_KpnI	gcggtaccATGGTGAGCAAGGGCGAG
044-R_AscI	ggcgcccCTAGACGTCTCCACCTTG
046-F	TAACAACTGCAATATTCCAGGTGCAACGGCCGCAAGTCCT CCATTCCG
047-R	ATTTTACTGATTGTATATTCCTGGTTTCGACACGCGCCAGAGT CCTCACAGC
050-F_EagI	ggcgcccGAAAATGCCCAAGCCAGAGGAG
058-F_KpnI	cgggtaccATGCCCAAGCCAGATGTCTTCCCTCAG
059-F_AscI	ggcgcccGTAATACGACTCACTATAGGG
060-R_AscI	ggcgcccGGCATAACATGGTGACAT
061-F-AvrII	ccctaggaATGGTTTCGCACTACTACAAC
062-R-AscI	ccctaggaATGGTTTCGCACTACTACAAC
6M-NLS-FW-AvrII	gcctaggAGGATCCCATCGATTTAAAGCTATGG

5.1.2 Oligonucleotides for template generation of *in vitro* synthesized RNA probes

Tab. 5.2: Oligonucleotides for template generation of RNA probes PCR; restriction sites are indicated in small letters, T7 promoter region indicated by underlined letters

Primer name	Sequence (5' to 3')
015-R_XbaI	gctctagaGGCATAACATGGTGACAT
017-R_AscI	tggcgcgccCATGATCAGATCAACATCAG
027-F_T7	<u>GTAATACGACTCACTATAGGGCGA</u> ATTGGAGCTCGGCCGTTGCACCTGG
028-R	GCGAATTCGAAACCAGGAATATACAATCAC
033-F_T7	<u>GTAATACGACTCACTATAGGGCGA</u> ATGACCACATTAACGCATTTG
034-F_T7	<u>GTAATACGACTCACTATAGGGCGA</u> ATATGCCTATGATCGGTTTTAC
035-F_T7	<u>GTAATACGACTCACTATAGGGCGA</u> ATTTGAATTAATTTTAATTATAC
040-F_T7	<u>GTAATACGACTCACTATAGGGCGA</u> GGCACC GGATTATCTAG
041-R	AAGCAACAAGAAGGCACATAAACGTTTGTAC
055-F_T7	<u>GTAATACGACTCACTATAGGGCGA</u> ACTAGATCATAATCAGCC
056-F_T7	<u>GTAATACGACTCACTATAGGGCGA</u> CTCTCTCTTCTTCTCTCTC
057-R	AGAAGAGGAGAGAGAAGGAGAGGAGAAAGAGAGAGAGGAAGAAGAG

5.1.3 Oligonucleotides for generation of ds DNA probe

Tab. 5.3: Oligonucleotides for generation of ds DNA probe; restriction sites are indicated in small letters.

Primer name	Sequence (5'->3')
031-F_EcoRI	gaattcGCTCTAATCCCCGAA
032-R_EcoRI	gaattcCGGGGATTAGAGC

5.2 In vitro Methods

5.2.1 Cloning procedures

5.2.1.1 Cloning of protein expression construct

pET16b-HisMBP-HD The fragment encoding the Bicoid homeodomain (spanning amino acids 97-163) was amplified from an embryonic cDNA library (given by M. Kiparaki) by PCR using primers 021-F_NdeI and 022-R_BamHI and cloned into NdeI and BamHI in frame to the Maltose binding protein (MBP) of pET16b-HisMBPTev (courtesy of A. Economou). pET16b carries a N-terminal His-tag, followed by MBP, a cleavage site for the TEV protease and the NdeI and BamHI sites for directional cloning.

5.2.1.2 Cloning of 3'UTRs used for EMSAs

pSL-Dm3' The *Drosophila caudal* 3'UTR (spanning nt 1-862, numbering starts at first nucleotide after the stop codon, followed by 40 nt of genomic sequence) was amplified from *Drosophila* genomic DNA by PCR using primers 009-F_BamHI and 006-R_AscI and cloned as an BamHI/blunt fragment into BamHI/EcoRV sites of pBluescript II KS(+) (Stratagene), creating **pBS-Dm3'**. The *Drosophila caudal* 3'UTR was cloned from pBS-Dm3' as a SpeI/HindIII fragment into pSLfa1180fa (Horn and Wimmer, 2000).

pBS-BRE_Styl/PstI The BRE_Styl-PstI fragment (spanning nt 164-512, numbering starts at first nucleotide after the stop codon) from the *Drosophila caudal* 3'UTR was cloned into XbaI and PstI sites of pBluescript II KS(+).

pBS-BRE_164-339 A NotI/XhoI fragment from pBS-BRE_Styl/PstI was isolated, digested with AluI to create the BRE_164-339 fragment (spanning nt 164-339, numbering starts at first nucleotide after the stop codon) and cloned into NotI/EcoRV sites of pBluescript II KS(+).

pSL-Hp3'ΔEcoRI The *Haematopota caudal* 3'UTR was amplified by PCR from plasmid #436 (courtesy of U. Schmidt-Ott) using primers 011-F_EcoRI and 012-R_AscI and

cloned as a blunt/Ascl fragment into EcoRV/Ascl sites of pBS-HAE-3xP3-DsRed -attB-SV40. The 3'UTR was excised as a BglII/NruI fragment, inserted into BamHI/EcoRV sites of pBluescript II KS(+), creating **pBS-Hp3'**, and then subcloned into pSLfa1180fa as a SpeI/HindIII fragment. Next, an EcoRI fragment was excised and the plasmid religated.

pSL-Tc3' The *Tribolium caudal* 3'UTR of splice variant A (spanning nt 751-1177, numbering starts at first nucleotide after the stop codon, followed by 47 nt of genomic sequence) was amplified from *Tribolium* genomic DNA by PCR using primers 007-F_EcoRI and 008-R_AscI and cloned as an EcoRI/blunt fragment into EcoRI/EcoRV sites of pBluescript II KS(+). Then it was cloned into pSLfa1180fa as an EcoRI/HindIII fragment.

pSL-SV40 The SV40 3'UTR was excised from pJB26 (Brennecke et al., 2003) as a HindIII/XbaI fragment and cloned into HindIII/XbaI sites of pBluescript II KS(+), creating **pBS-SV40**, and then cloned as an EagI/HindIII fragment into pSLfa1180fa .

pBS-Adh3'ΔPacl/EcoRV The Adh 3'UTR was excised from ract-vector (Swevers et al. 1996) as a XbaI fragment and cloned into the XbaI site of pBluescript II KS(+), with the 5' end towards the T7 promoter region. Excision of a Pacl/EcoRV fragment and religation results in pBS-Adh3'ΔPacl/EcoRV.

5.2.2 RNA probes

5.2.2.1 Template generation

BRE_164-339 pBS-BRE_164-339 was linearized with HindIII and RNA transcribed with T7 RNA polymerase, resulting in a RNA fragment of 214 nt including T7 promoter sequence.

BRE_257-319 A DNA fragment containing nt 257-319 from the *Drosophila caudal* 3'UTR (numbering starts at first nucleotide after the stop codon) was amplified by PCR using pBS-Dm3' as template and primers 027-F_T7 and 028-R, RNA transcribed with T7 RNA polymerase, resulting in a RNA fragment of 84 nt including T7 promoter sequence.

H1 A DNA fragment containing nt 1-52 of the *Haematopota caudal* 3'UTR (numbering starts at first nucleotide after the stop codon) was amplified by PCR using pSL-Hp3'ΔEcoRI as template and primers 033-F_T7 and 015-R_XbaI, RNA transcribed with T7 RNA polymerase, resulting in a RNA fragment of 67 nt including T7 promoter sequence.

H2 A DNA fragment containing nt 52-89 of the *Haematopota caudal* 3'UTR (numbering starts at first nucleotide after the stop codon) was amplified by PCR using pSL-Hp3'ΔEcoRI as template and primers 034-F_T7 and 017-R_AscI, RNA transcribed with T7 RNA polymerase, resulting in a RNA fragment of 59 nt including T7 promoter sequence.

H3 A DNA fragment containing nt 88-126 of the *Haematopota caudal* 3'UTR (numbering starts at first nucleotide after the stop codon) was amplified by PCR using pSL-Hp3'ΔEcoRI as template and primers 035-F_T7 and 012-R_AscI, RNA transcribed with T7 RNA polymerase, resulting in a RNA fragment of 51 nt including T7 promoter sequence.

H2/H3 A DNA fragment containing nt 52-126 of the *Haematopota caudal* 3'UTR (numbering starts at first nucleotide after the stop codon) was amplified by PCR using pSL-Hp3'ΔEcoRI as template and primers 034-F_T7 and 012-R_AscI, RNA transcribed with T7 RNA polymerase, resulting in a RNA fragment of 96 nt including T7 promoter sequence.

Tc_245-307 A DNA fragment containing nt 245-307 of the *Tribolium caudal* 3'UTR (numbering starts at first nucleotide after the stop codon) was amplified by PCR using pSL-Tc3' as template and primers 040-F_T7 and 041-R, RNA transcribed with T7 RNA polymerase, resulting in a RNA fragment of 75 nt including T7 promoter sequence.

shSV40 A DNA fragment containing a 72 nt fragment of the SV40 3'UTR was amplified by PCR using pSL-SV40 as template and primers 055-F_T7 and SV40-R01, RNA transcribed with T7 RNA polymerase, resulting in a RNA fragment of 79 nt including T7 promoter sequence.

Adh3' The pBS-Adh3' Δ Pacl/EcoRV plasmid was linearized using HindIII and RNA transcribed with T7 RNA polymerase, resulting in a RNA fragment of 184 nt including T7 promoter sequence.

CU58 A DNA fragment containing a randomized C/T sequence was generated by PCR using primers 056-F_T7 and 057-R that are complementary at their 3'-ends. Primer 056-F_T7 includes the T7 promoter sequence. RNA was transcribed with T7 RNA polymerase, resulting in a RNA fragment of 58 nt.

5.2.2.2 *In vitro* transcription and radioisotope-labeling of RNA probes

For all probes RNA was *in vitro* transcribed using the MEGAscript T7 kit (Ambion) according to manufacturers instructions. After synthesis, the template DNA was treated with TurboDNase, the RNA Phenol/Chloroform extracted and precipitated in Ammoniumacetate and 2-propanol. 50 pmole of RNA were resuspended in nuclease-free H₂O and dephosphorylated using 10 units of Shrimp Alkaline Phosphate (Roche) by incubating for 1 h at 37°C and heat inactivating for 20 min at 65°C. Next the RNA was precipitated in Sodiumacetate and EtOH, resuspended in nuclease-free H₂O and concentration and purity were determined spectrophotometrically. The RNA was 5' end labeled using 20 units of T4 Polynucleotide Kinase (New England Biolabs) and 5 μ l ³²P- γ ATP (10 μ Ci/ μ l, >3000 Ci/mmol), by incubating for 1-2 h at 37°C and purifying over a Sephadex G-50 column (GE Healthcare).

5.2.3 Radioisotope-labeling of dsDNA oligonucleotides

Radioisotope-labeled dsDNA oligonucleotides containing the consensus Bcd target site (5'-TAATCC-3') (Baird-Titus et al., 2006) were generated as follows: Oligonucleotides 031-F and 032-R (5 pmole/ μ l each) were mixed for annealing in an equimolar ratio in TE with 50mM NaCl, incubated for 2 min at 95° using a heat block and let to cool down to RT in the heat block. 20 pmole of the dsDNA were radioisotope-labeled using 2.5 units of the Large Klenow fragment (NEB), 3 μ l of 32 P- γ ATP (10 μ Ci/ μ l, >3000 Ci/mmol) in a total volume of 100 μ l, incubated for 10 min at RT and purified over a Sephadex G-50 column.

5.2.4 Protein purification

5.2.4.1 Purification of HisMBP-HD fusion protein

For the purification of the homeodomain fused to MBP, *E.coli* strain BL21(DE3)pLysS was transformed with pET16b-HisMBP-HD and grown in LB medium containing 100 μ g/ml ampicillin and 35 μ g/ml chloramphenicol. 500 ml of LB medium containing 100 μ g/ml ampicillin were inoculated to an OD₆₀₀ = 0.1 using an overnight culture and grown at 37°C with vigorous shaking (225 rpm) to an OD₆₀₀ = 0.4. Expression of the recombinant protein was induced by addition of IPTG to a final concentration of 0.1 mM. The cells were harvested, resuspended in 15 ml LEW buffer (50 mM NaH₂PO₄, 300 mM NaCl, pH 8.0) disrupted by sonication. All subsequent procedures were carried out at 4°C. The crude lysate was centrifuged for 30 min at 13000 rpm at 4°C and the supernatant transferred to a clean tube, containing 1.5 g Protino Ni-TED Resin. The lysate-resin mixture was incubated for 15 min, transferred to an empty chromatography column that was blocked with some glass wool and left to settle by gravity-flow. The column was washed with 25 ml of LEW buffer and the HisMBP-HD fusion protein eluted in 5 fractions of 5 ml Elution buffer (50 mM NaH₂PO₄, 300 mM NaCl, 250 mM imidazole, pH 8.0). The purity of the recombinant protein was analyzed by SDS-PAGE and the first two fractions combined. The protein solution was concentrated by dialysis in 1L of dialysis buffer (20 mM Tris-Cl (pH 7.5), 50 mM KCl, 0.5 mM EDTA, 10 % glycerol) for 3 h at 4°C and a second dialysis in 500 ml of storage buffer (20 mM Tris-Cl (pH 7.5), 50 mM KCl, 0.5 mM EDTA, 50 % glycerol) overnight at 4°C. The final volume of the protein solution was 2.5 ml, it was supplemented with DTT to a final concentration of 1 mM, divided into 250 μ l aliquots and stored at -80°C.

5.2.4.2 Purification of GST-HD fusion protein

For the purification of the homeodomain fused to GST, *E. coli* strain BL21(DE3)pLysS was transformed with PTA67A (Baird-Titus et al., 2006). PTA67A is a pET41 expression vector carrying the Bicoid homeodomain (spanning amino acids 97-163) fused C-terminally to Glutathione-S-transferase (GST), followed by a Tev protease cleavage site. Cells were grown in LB medium containing 50 µg/ml kanamycin and 35 µg/ml chloramphenicol. 1 L of LB medium containing 50 µg/ml kanamycin were inoculated to an OD₆₀₀ = 0.1 using an overnight culture and grown at 37°C with vigorous shaking (225 rpm) to an OD₆₀₀ = 0.4. Expression of the recombinant protein was induced by addition of IPTG to a final concentration of 0.2 mM. The cells were harvested, resuspended in 50 ml ice-cold PBS and disrupted by sonication. The crude lysate was incubated for 30 min with gentle shaking at 4°C with 1% Triton-X 100, centrifuged for 20 min at 13000 rpm at 4°C and the supernatant transferred into a fresh tube. 70 mg of Glutathione agarose resin (soaked overnight at 4°C in 15 ml PBS) were added as a slurry to the supernatant and incubated with gentle shaking for 30 min at RT. All subsequent procedures were carried out at 4°C. The lysate-resin mixture was transferred to an empty chromatography column that was blocked with glass wool and left to settle by gravity-flow. The column was washed with 30 ml of ice cold PBS and the GST-HD recombinant protein eluted in 5 fractions of 1 ml GST Elution buffer (10 mM reduced Glutathione, 50 mM Tris-Cl pH8.0). The purity of the recombinant protein was analyzed by SDS-PAGE and the first 4 fractions combined. The protein solution was concentrated by dialysis in 1L of dialysis buffer (20 mM Tris-Cl (pH 7.5), 50 mM KCl, 0.5 mM EDTA, 10 % glycerol) for 4 h and a second dialysis in 500 ml of storage buffer (20 mM Tris-Cl (pH 7.5), 50 mM KCl, 0.5 mM EDTA, 50 % glycerol) overnight. The final volume of the protein solution was 1 ml, it was supplemented with DTT to a final concentration of 1 mM, divided into 250 µl aliquots and stored at -20°C or -80°C.

5.2.4.3 Tev-protease digest of HD

The homeodomain was liberated from its fusion protein MBP or GST as follows: 100 µg of HisMBP-HD or GST-HD fusion protein were incubated with 50 units of AcTEV-Protease (Invitrogen) for 6 h at RT or overnight at 4°C in a final volume of 150 µl. The digest was tested by electrophoresis on a polyacrylamide gel and coumassie staining.

The homeodomain was then directly used for *in vitro* binding to RNA and EMSA experiments.

5.2.5 Electrophoretic Mobility Shift Assays (EMSAs)

5.2.5.1 RNA EMSAs

In binding experiments, different concentrations of HisMBP-HD or GST-HD or liberated homeodomain were incubated with 20 - 300 fmole of radioisotope-labeled RNA probes (reaction volume 10 μ l) for 10 min on ice in binding buffer (final concentrations during binding reaction 10 mM HEPES pH 7.5, 100 mM KCl, 1 mM MgCl₂, 0.5 mM EDTA, 1 mM DTT, 0.5 μ g/ μ l yeast tRNA, 10% glycerol). Prior to binding, the radioisotope-labeled probes were incubated in binding buffer (without tRNAs) at 70°C for 5 min and chilled on ice for 5 min. The binding reactions were loaded on 0.5x TBE polyacrylamide gels electrophorized for 5 - 6 h at 10V/cm at 4°C. The radioactivity was visualized using phosphoimager.

In competition experiments, constant amounts of radioisotope-labeled RNA probes were pre-incubated at 70°C for 5 min followed by 5 min on ice. HisMBP-HD, GST-HD or liberated homeodomain were then added and incubated (reaction volume 10 μ l) for 10 min on ice in binding buffer. 1 μ l of cold competitor, pre-incubated at 70°C for 5 min followed by 5 min on ice, diluted in binding buffer in different amounts were added to the binding reaction and incubated for 10 min on ice. The reactions were then loaded on 0.5x TBE polyacrylamide gels electrophorized for 5 - 6 h at 10V/cm at 4°C. The radioactivity was visualized using phosphoimager.

5.2.5.2 DNA EMSAs

Different concentrations of HisMBP-HD or GST-HD or liberated HD were incubated with 2 pmole of radioisotope-labeled dsOligo (reaction volume 10 μ l) for 10 min on ice in binding buffer (same as in 5.2.5.1) and electrophorized on a 0.5x TBE polyacrylamide gel for 5 - 6 h at 10V/cm at 4°C. The radioactivity was visualized using phosphoimager.

5.3 In vivo Methods

5.3.1 Cloning procedures of in vivo methods

5.3.1.1 Cloning of sensor constructs

pJBattP-tub α -1-nGFP-attP-SV40 The attP recombination site was cloned from pTA-attP (Groth et al., 2003) as a 326 nt XbaI and BamHI fragment into NheI and BamHI sites of pSLfa1180fa, resulting in pSL-attP>. The EGFP followed by six Myc-tag repeats and a NLS was cloned as a SpeI and XbaI fragment from GN1 (courtesy of G. Struhl) into the XbaI site of pSL-attP>, resulting in pSL-nGFP-attP>. The nGFP-attP> fragment was cloned as a KpnI and Sall fragment into KpnI and XhoI sites of pJB26 (Brennecke et al., 2003), which removes the EGFP and places the nGFP in frame with the ORF that initiates in the tub α -1 promoter fragment.

pHAE-3xP3-DsRed-attB-SV40 The MCS of pSLfa1180fa was excised as a AsclI fragment and inserted into BssHII sites of pBluescript II KS(+), placing the HindIII site next to the M13 -20 primer site and the EcoRI site next to the M13 reverse primer binding site. The plasmid was digested by NarI, filled-in and religated, creating in a new AsclI site (plasmid pHAE). The attB recombination site was amplified from pTA-attB (Groth et al., 2003) using primers pTA-attB-F2 and BamHI-pTA-attB-R and cloned as a blunt and BamHI fragment into SmaI and BamHI sites of pHAE resulting in pHAE-attB>. The SV40 3'UTR was cloned as XbaI and HindIII fragment from pJB26 into SpeI and HindIII sites of pHAE-attB>, resulting in pHAE-attB>-SV40. 3xP3-DsRed was cloned as a NotI-blunted/EcoRI fragment from pMi-3xP3-DsRed-SV40 (Pavlopoulos and Averof, 2005) into SmaI and EcoRI sites of pHAE-attB>-SV40.

pHAE-3xP3-DsRed-attB-Dm3'-SV40 The Dm3' was amplified by PCR using genomic DNA as template and primers 009-F_BamHI and 006-R_AscI, the PCR product digested with AsclI and cloned into EcoRV/AsclI sites.

pHAE-3xP3-DsRed-attB-Hp3'-SV40 The Hp3' was amplified by PCR using pSL-Hp3' as template and primers 011-F_EcoRI and 012-R_AscI, the PCR product digested with AscI and cloned into EcoRV/AscI sites.

pHAE-3xP3-DsRed-attB-Tc3'-SV40 The Tc3' was cloned as a FseI-blunted/AscI fragment from vector #538 (courtesy of Schmidt-Ott) into NruI/AscI sites.

pit-GFP The tub α -1-nGFP fragment was cloned as a HindIII/NotI-blunted fragment from pJBattP-tub α -1-nGFP-attP-SV40 into HindIII/XhoI-blunted sites of pHAE. Then it was removed as a HindIII and BglII fragment and inserted into HindIII and BamHI sites of piB-GFP (Bateman et al. 2006), replacing the hsp70 promoter and GFP sequences. The unique MluI and AscI sites following the ORF of the nGFP were used for cloning of 3'UTR fragments.

pit-GFP-Dm3' The Dm3' was inserted as a BssHI fragment from pBS-Dm3' into AscI.

pit-GFP-SV40 The SV40 was inserted as a BssHI fragment from pBS-SV40 into AscI.

piB-TdnGFP The tub α -1 promoter was cloned as a EcoRV and KpnI fragment from pJB26 into EcoRV and KpnI sites of pHAE, resulting in pHAE-tub α -1. A destabilized EGFP (BD Biosciences Clontech) fused C-terminally to 6 Myc-tags and a NLS (dnGFP) was amplified by PCR using primers 043-F_KpnI and 044-R_AscI from pd2EGFP6MNLS (given by P.Piwko) and cloned into KpnI and AscI sites of pHAE-tub α -1. The unique KpnI site in piB-GFP, which is lying outside of the attB recombination sites, was destroyed by KpnI digest, removal 3' overhangs by Klenow and religation, resulting in piB-GFP Δ KpnI. The tub α -1-dnGFP was then cloned as a BglII and XhoI fragment into BamHI and Sall sites of piB-GFP Δ KpnI, replacing the hsp70 promoter and GFP sequences, resulting in piB-TdnGFP. Due to inconsistencies in diagnostic digests, the tub α -1 promoter was replaced by excision of a HindIII and KpnI fragment and insertion of a HindIII and KpnI fragment from pit-GFP. Due to a point mutation, the NLS was replaced by a 6xMyc-NLS fragment, which was amplified

by PCR using primers 6M-NLS-FW-AvrII and 044-R_AscI and cloned into AvrII and AscI sites of piB-TdnGFP. The unique AscI and MluI sites following the ORF of dnGFP were used for cloning of 3'UTR fragments.

piB-TdnGFP-Dm3' The Dm3'UTR was inserted as a MluI/AscI fragment from pSL-Dm3' into AscI.

piB-TdnGFP-Hp3' The Hp3' UTR was inserted as an AscI fragment from pSL-Hp3'ΔEcoRI into AscI.

piB-TdnGFP-Tc3' The Tc3' UTR was inserted as an AscI fragment from pSL-Tc3' into AscI.

piB-TdnGFP-SV40 The SV40 UTR was inserted as an AscI fragment from pSL-SV40 into the MluI.

piB-TdnGFP-Dm3'mut The seed sequence of the predicted mir-308 target site was mutagenised by PCR using pBS-Dm3' as template and primers 046-F and 047-R, which are lying back-to-back, generating the full plasmid including 4 nt changes (mutated mir-308 target sequence TTGCAGtTTGTAAATTTTactTGATT, with changed nt indicated in small letters). The parental methylated non-mutated template DNA was digested with DpnI and the resulting linear mutagenised plasmid ligated into a circular form. The mutagenised Dm3'mut was then cloned as a NotI/HindIII fragment into EagI/HindIII sites of pSLfa1180fa, creating **pSL-Dm3'mut**. The mutated Dm3'UTR was inserted as a AscI fragment from pSL-Dm3'mut.

piB-TdnGFP-BRE_257 The BRE_257-319 fragment was amplified by PCR using primers 027-F_T7 and 028-R and cloned into blunted AscI site of piB-TdnGFP-SV40.

piB-TdnGFP-H1 The H1 fragment was amplified by PCR using primers 033-F_T7 and 015-R_XbaI and cloned into blunted AscI site of piB-TdnGFP-SV40.

piB-TdnGFP-H2 The H2 fragment was amplified by PCR using primers 034-F_T7 and 017-R_AscI and cloned into blunted AscI site of piB-TdnGFP-SV40.

piB-TdnGFP-H3 The H3 fragment was amplified by PCR using primers 035-F_T7 and 012-R_AscI and cloned into blunted AscI site of piB-TdnGFP-SV40.

piB-HdnGFP The maternal hbP1 promoter was cloned from pChbP1 Δ XbaI (Wimmer et al., 2000) as a XbaI and BamHI fragment into pSLfa1180fa. Next it was excised as an AvrII/XbaI fragment and inserted into NheI and XbaI sites of pSLfa1180fa. The hbP1 promoter was then excised as a SphI and KpnI fragment and inserted into SphI and KpnI sites of piB-TdnGFP, replacing the tub α -1 promoter. The unique Ascl and MluI sites following the ORF of dnGFP was used for cloning of 3'UTR fragments.

piB-HdnGFP-Dm3' The Dm3' was inserted as a MluI/Ascl fragment from pSL-Dm3' into Ascl.

piB-HdnGFP-SV40 The SV40 was inserted as an Ascl fragment from pSL-SV40 into Ascl.

piB-HR The HIST1H2BJ-mRFPruby was excised from pAc5.1-HIST1H2BJ-mRFPruby (Müller-Taubenberger et al., 2006) as a KpnI/MluI and inserted into piB-HdnGFP, replacing dnGFP. The unique MluI site which follows the ORF of HIST1H2BJ-mRFPruby can be used for cloning of 3'UTR fragments.

piB-HR-Dm3' The Dm3' UTR was inserted as a MluI/Ascl fragment from pSL-Dm3'.

piB-HR-SV40 The SV40 was inserted as an Ascl fragment from pSL-SV40 into Ascl.

piB-HGFPCAD The *cad* ORF was amplified from an embryonic cDNA library using primers 061-F_AvrII and 062-R_AscI and cloned into AvrII and Ascl sites of piB-HDN, replacing the 6xMyc-NLS and fusing the *cad* ORF C-terminally in frame to the d2EGFP. The unique Ascl site following the ORF of d2EGFP-CAD fusion was used for cloning of 3'UTR fragments. The Dm3' UTR was inserted as a MluI/Ascl fragment from pSL-Dm3'.

piB-HGFPCAD-Dm3' The Dm3' UTR was inserted as a MluI/Ascl fragment from pSL-Dm3'.

5.3.1.2 Cloning UAS constructs

pUASp2-6M A BamHI fragment from GN1 containing 6xMyc-tag was cloned into BamHI/BglII of pSLfa1180fa, destroying the C-terminal BamHI site. Next it was cloned as a BamHI/XbaI fragment into pUASp2 (Rørth, 1998).

pUASp2-BcdG-6M The ORF of Bcd isoform G (spanning 494 aa without stop codon) was amplified from an embryonic cDNA library by PCR using primers 038-F_KpnI and 039-R_BamHI and cloned into pGEM T easy. BcdG was then excised as a NotI/BamHI fragment and cloned N-terminally in frame to the 6xMyc-tag of pUASp2-6M.

pUASp2-BcdD-6M Bcd isoform D was ordered as a cDNA pOT2-LD36304 from the Drosophila Genomics Resource Center, Bloomington, IN. The ORF (spanning 489 aa without stop codon) was amplified by PCR using pOT2-LD36304 as template, primers 038-F_KpnI and 039-F_BamHI and cloned into pGEM T easy. BcdD was then excised as a KpnI/BamHI fragment and cloned N-terminally in frame to the 6xMyc-tag into pUASp2-BcdG-6M, replacing BcdG.

pUASp2-BcdE-6M Bcd isoform E (spanning 418 aa without stop codon) was amplified from an embryonic cDNA library by PCR using primers 058-F_KpnI and 039-R_BamHI and cloned into pGEM T easy. BcdE was cloned as a NotI/BamHI fragment N-terminally in frame to the 6xMyc-tag into pUASp2-BcdG-6M, replacing BcdG.

pUASp2-BcdF-6M Bcd isoform F (spanning 413 aa without stop codon) was amplified from a cDNA library by PCR using primers 050-F_EagI and 039-R_BamHI and cloned into pGEM T easy. BcdF was cloned as a NotI/BamHI fragment N-terminally in frame to the 6xMyc-tag into pUASp2-BcdG-6M, replacing BcdG.

pUASp2-BcdA-6M Bcd isoform A (spanning 149 aa without stop codon) was amplified from an embryonic cDNA library by PCR using primers 038-F_KpnI and 039-R_BamHI and cloned into pGEM T easy. BcdA was cloned as a NotI/BamHI fragment N-terminally in frame to the 6xMyc-tag into pUASp2-BcdG-6M, replacing BcdG.

5.3.2 *Drosophila melanogaster* handling and husbandry

Drosophila melanogaster cultures were kept at 25°C unless indicated otherwise and handled according to protocols described in Ashburner (1989). Food medium contained a mixture of yeast, sugar, agar, corn flour and Nipogen. Embryos were collected using cages and cherry juice plates (cherry juice, 3% agar, Nipogen), adding live yeast paste to enhance egg laying. General fly stocks used for transgenesis and genetic crosses are listed in Tab. 5.3.

Tab. 5.3: : General Fly stocks.

name	genotype
yw	Df(1)yw ^{67c23}
38F	yw; P{attP.w ⁺ .attP}JB38F
53F	yw; P{attP.w ⁺ .attP}JB53F
	nos-GAL4:VP16
yw;TM3Sb/TM6B	Df(1)yw ^{67c23} ; TM3, Sb,e/TM6B,Hu,e
yw;Sco/CyO	Df(1)yw ^{67c23} ; Sco /CyO
	FM7/w ^{lethal} ;CyO/Sp
	yw; CyO/if; MKRS/TM6B

5.3.3 Transgenesis

Microinjections of embryos were performed by Ioannis Livadaras using a NARISHIGE Microinjector IM - 300. Glass needles were pulled using SUTTER Flaming/ Brown Micropipette Puller P- 97. Injected embryos were covered with halocarbon oil and hatching larvae transferred to food vials.

5.3.3.1 ϕ C31 integrase mediated recombination system using a single *attP* landing site (strategy 1)

Capped mRNA of the ϕ C31 integrase was produced as follows: pET111[ϕ C31-integrase-pA] (Groth et al., 2003) was linearized by BamHI digest and used as template for *in vitro* transcription with the mMESSAGE mMACHINE T7 kit (Ambion). The template DNA was treated with TurboDNase, the RNA Phenol/Chloroform extracted, precipitated in 2-propanol and resuspended in nuclease-free H₂O. An injection mixture containing the attB donor plasmid at high purity (200-400 ng/ μ l), capped mRNA of ϕ C31-integrase (600-800ng/ μ l) and injection buffer (10 mM Tris-Cl pH 7.5, 0.1 mM EDTA, 10 mM NaCl) was injected into embryos of line pJBattP-M44 line. G0 adults were backcrossed to yw;Sco/CyO and the G1 progeny screened as larvae for 3xP3-DsRed expression. 3xP3-DsRed G1 individuals carrying the CyO balancer chromosome were backcrossed to yw;Sco/CyO and balanced over CyO.

5.3.3.2 Recombinase-mediated exchange cassette (RMCE) using ϕ C31 integrase (strategy 2)

The nos- ϕ C31-int;38F provides the ϕ C31 integrase maternally and was created by crossing line nos- ϕ C31-int (Bischof et al., 2007) to line 38F and making the progeny homozygous. An injection mixture containing the RMCE attB donor plasmid at high purity (200-400 ng/ μ l) and injection buffer (10 mM Tris-Cl pH 7.5, 0.1 mM EDTA, 10 mM NaCl) was injected into embryos of the line nos- ϕ C31-int;38F. G0 adults were backcrossed to yw;Sco/CyO and the G1 progeny screened as adults for loss of *mini-white* phenotype. G1 w^- males that originated from a G0 male were crossed to yw;Sco/CyO virgins and the G2 progeny kept as a balanced stock over CyO. G1 w^- males that originated from a G0 female, inherited the nos- ϕ C31-int chromosome and were crossed as single G1 w^- males to yw;Sco/CyO virgins, a single G2 w^- males to virgins of yw;Sco/CyO. The G3 progeny was kept as a balanced stock over CyO.

5.3.3.3 P-element based transgenesis

Injection mixtures containing P-element plasmids at high purity (300-400 ng/ μ l), Δ 2-3 helper plasmid (100-200 ng/ μ l) and injection buffer (10 mM Tris-Cl pH 7.5, 0.1 mM EDTA, 10 mM NaCl) were injected into yw embryos. G0 adults were backcrossed to yw and the G1 progeny screened for w^+ individuals. G1 w^+ individuals were backcrossed

to yw and the segregation of the w^+ analyzed in the G2 progeny to identify single insertions. Chromosome mapping of independent single insertions was done by segregation analysis as follows, G2 individuals were crossed to 2nd chromosome balancer stock yw; Sco/CyO and 3rd chromosome balancer stock yw; TM3Sb/TM6B. G3 individuals were backcrossed to the same respective balancer stock and the insertion mapped to the chromosome that does not give rise to flies with w phenotype in the following progeny. In the case of G1 w^+ males that originated from G0 females and that gave rise only to w^+ females and to w females, the insertion could be mapped directly to the 1st chromosome and the G2 w^+ females crossed to the FM7 balancer stock. Independent P-element mediated transgenic lines are listed in Table 5.4 and 5.5.

Tab. 5.4: *Drosophila* transgenic pJBattP lines generated by single P-element insertions.

pJBattP line	locus of insertion P[w^+ , tub α -1-nGFP-attP-SV40]	viability
pJBattPF17.F2	X chromosome	homozygous viable
pJBattPF17.F3	3 rd chromosome	homozygous viable
pJBattPM39	3 rd chromosome	homozygous lethal
pJBattPM40	3 rd chromosome	homozygous viable
pJBattPF15.F2	3 rd chromosome	homozygous viable
pJBattPM2	2 nd chromosome	homozygous viable
pJBattPM44	2 nd chromosome	homozygous viable
pJBattPM15.M1	2 nd chromosome	homozygous viable

Table 5.5: *Drosophila* transgenic UAS lines generated by single P-element insertions.

Injected construct	UAS line name	locus of insertion
pUASp2-BcdG-6M	UAS-BCDG ^{F4M6}	1 st chromosome
pUASp2-BcdG-6M	UAS-BCDG ^{F8M1}	1 st chromosome
pUASp2-BcdD-6M	UAS-BCDD ^{F15}	3 rd chromosome
pUASp2-BcdD-6M	UAS-BCDD ^{M29}	3 rd chromosome
pUASp2-BcdA-6M	UAS-BCDA ^{M22}	3 rd chromosome
pUASp2-BcdA-6M	UAS-BCDA ^{F36}	1 st chromosome
pUASp2-BcdE-6M	UAS-BCDE ^{F12}	3 rd chromosome
pUASp2-BcdE-6M	UAS-BCDE ^{F79}	1 st chromosome
pUASp2-BcdF-6M	UAS-BCDF ^{F9M3}	3 rd chromosome
pUASp2-BcdF-6M	UAS-BCDF ^{M22}	3 rd chromosome

5.3.4 *Drosophila* husbandry for expression of UAS-BCD isoforms during early embryogenesis

Males of UAS-BCD lines (Tab. 5.5) were crossed to virgins of nos-GAL4:VP16 and the progeny collected as embryos, fixed and the cellular localization of the ectopically expressed BCD isoforms identified by α -Myc antibody staining.

5.3.5 *Drosophila* husbandry for expression of UAS-BCD and sensor constructs during early embryogenesis

UAS-BCD lines with insertions on the 1st chromosome were crossed into FM7/w^{lethal};CyO/Sp background and made homozygous, UAS-BCD lines with insertions on 3rd chromosome were crossed into yw; CyO/if; MKRS/TM6B background and made homozygous. Subsequently the UAS-BCD lines were crossed to sensor lines and made homozygous. These flies were then crossed as males to nos-GAL4:VP16 virgins and the progeny collected as embryos and the GFP expression live imaged. For the two lines of isoform E (UAS-BCDE^{F12} and UAS-BCDE^{F79}) male flies were crossed to virgins of 38F-Dm3'; nos-GAL4:VP16, the female virgin progeny of this cross collected and crossed to yw/Y males for the collection of embryos. As a control, sensor lines were crossed to virgins of nos-GAL4:VP16. The crosses are summarized in Tab. 5.6.

General crossing scheme for 1st chromosome UAS-BCD lines, nos-GAL4:VP16 and sensor lines

♀ w, UAS-BCD isoform; CyO/Sp x ♂ yw/Y; sensor
 ↓ (made homozygous)
 ♀ w; nos-GAL4:VP16 x ♂ yw, UAS-BCD isoform/Y; sensor
 ↓
 ♀ yw, UAS-BCD isoform/w; sensor/+; nos-GAL4:VP16/+ x ♂ yw/Y
 ↓
 Collection of embryos and live imaging

General crossing scheme for 3rd chromosome UAS-BCD lines, nos-GAL4:VP16 and sensor lines

♀ yw; CyO/lf; UAS-BCD isoform x ♂ yw/Y; sensor
 ↓ (made homozygous)
 ♀ w; nos-GAL4:VP16 x ♂ yw/Y; sensor; UAS-BCD isoform
 ↓
 ♀ yw; sensor/+; UAS-BCD isoform/nos-GAL4:VP16 x ♂ yw/Y
 ↓
 Collection of embryos and live imaging

General crossing scheme for control cross of sensor line and nos-GAL4:VP16

♀ w; nos-GAL4:VP16 x ♂ yw/Y; sensor
 ↓
 ♀ yw; sensor/+; nos-GAL4:VP16/+ x ♂ yw/Y
 ↓
 Collection of embryos and live imaging

Table 5.6: Crosses for the expression analysis of UAS-BCD and sensor construct during early embryogenesis.

♀		♂
w; nos-GAL4:VP16	x	yw/Y; 38F-Dm3'
w; nos-GAL4:VP16	x	yw, UAS-BCDG ^{F4M6} /Y; 38F-Dm3'
w; nos-GAL4:VP16	x	yw, UAS-BCDG ^{F8M1} /Y; 38F-Dm3'
w; nos-GAL4:VP16	x	yw/Y; 38F-Dm3'; UAS-BCDD ^{F15}
w; nos-GAL4:VP16	x	yw/Y; 38F-Dm3'; UAS-BCDD ^{M29}
w; nos-GAL4:VP16	x	yw/Y; 38F-Dm3'; UAS-BCDA ^{M22}
w; nos-GAL4:VP16	x	yw, UAS-BCDA ^{F36} /Y; 38F-Dm3'
w; nos-GAL4:VP16	x	yw/Y; 38F-Dm3'; UAS-BCDF ^{F9M3}
w; nos-GAL4:VP16	x	yw/Y; 38F-Dm3'; UAS-BCDF ^{M22}
w; 38F-Dm3'; nos-GAL4:VP16	x	yw/Y
w; 38F-Dm3'; nos-GAL4:VP16	x	yw/Y; UAS-BCDE ^{F12}
w; 38F-Dm3'; nos-GAL4:VP16	x	yw, UAS-BCDE ^{F79} /Y
w; nos-GAL4:VP16	x	yw/Y; 38F-Dm3'mut
w; nos-GAL4:VP16	x	yw, UAS-BCDG ^{F4M6} /Y; 38F-Dm3'mut
w; nos-GAL4:VP16	x	yw/Y; 38F-Dm3'mut; UAS-BCDD ^{M29}
w; nos-GAL4:VP16	x	yw/Y; 38F-Hp3'
w; nos-GAL4:VP16	x	yw, UAS-BCDG ^{F4M6} /Y; 38F-Hp3'
w; nos-GAL4:VP16	x	yw/Y; 38F-Tc3'
w; nos-GAL4:VP16	x	yw, UAS-BCDG ^{F4M6} /Y; 38F-Tc3'
w; nos-GAL4:VP16	x	yw/Y; 38F-SV40
w; nos-GAL4:VP16	x	yw, UAS-BCDG ^{F4M6} /Y; 38F-SV40
w; nos-GAL4:VP16	x	yw/Y; 38F-BRE_257
w; nos-GAL4:VP16	x	yw, UAS-BCDG ^{F4M6} /Y; 38F-BRE_257
w; nos-GAL4:VP16	x	yw/Y; 38F-H1
w; nos-GAL4:VP16	x	yw, UAS-BCDG ^{F4M6} /Y; 38F-H1
w; nos-GAL4:VP16	x	yw/Y; 38F-H2
w; nos-GAL4:VP16	x	yw, UAS-BCDG ^{F4M6} /Y; 38F-H2

Table 5.6 (continued): Crosses for the expression analysis of UAS-BCD and sensor construct during early embryogenesis.

♀		♂
w; nos-GAL4:VP16	x	yw/Y; 38F-H3
w; nos-GAL4:VP16	x	yw, UAS-BCDG ^{F4M6} /Y; 38F-H3
w; nos-GAL4:VP16	x	yw/Y; 38F-Tc_245
w; nos-GAL4:VP16	x	yw, UAS-BCDG ^{F4M6} /Y; 38F-Tc_245

5.3.6 Immunohistochemistry

5.3.6.1 Antibody stainings

Embryos were dechorionated in 50% bleach for 1-2 min, washed several times with dH₂O and PBT. The dechorionated embryos were transferred into glass vials containing equal volumes of fixation solution (1xPEM, 4% FA) and heptane and fixed by shaking vigorously for 20 min. The fixation solution was removed, 100 % MeOH added to an equal volume of the heptane and shaken vigorously for 1 min. Devitellinized embryos fell to the bottom of the vial, while the non-devitellinized embryos and embryonic membranes remained in the interphase. The heptane and interphase debris were removed, the embryos washed several times in 100 % MeOH and immediately rehydrated by washing 1 x in PBT:MeOH [1:1] for 10 min and 4 x 10 min washes in PBT. Blocking was performed 1 h in PBT + 5x Western blocking (Roche).

Antibody stainings using Rabbit α -Myc as primary antibody were performed at 4°C (unless mentioned otherwise) as follows: Rabbit α -Myc [dilution 1:100, pre-absorbed] incubated overnight, 3 x 3 min washes in PBT, 1 h blocking in PBT + 0.1 % BSA, incubation of secondary antibody Donkey α -Rabbit-AP conjugated antibody [dilution 1:200, pre-absorbed] for 2 h, 3 x 3min washes in PBT. All subsequent procedures at RT: 2 x 3 min washes in staining buffer, 15 - 20 min incubation in staining solution (1 ml staining buffer + 20 μ l NBT/BCIP Stock Solution, Roche), 3 rinses in PBT, 10 min wash in PBT, 10 min wash in PBT:EtOH [1:1], 6 x 10 min washes in 100 % EtOH, 10 min

wash in PBT:EtOH [1:1], 3 x 10 min washes in PBT, last wash supplemented with DAPI, mounting in 70 % glycerol and storage at 4°C.

Antibody stainings using Guinea-pig α -CAD as primary antibody were performed as follows: Guinea-pig α -CAD [dilution 1:100, not pre-absorbed] were incubated overnight at 4°C, 3 x 10 min washes in PBT, 1 h blocking in PBT + 5x western blocking, incubation of secondary antibody Donkey α -Guinea-pig HRP conjugated [dilution 1:500] for 2 h at RT, 2 rinses in PBT, 3 x 10 min washes in PBT, 20 min soaking in 500 μ l DAB (0.3 mg/ml) solution + 0.2 % NiSO₄, addition of 10 - 30 μ l of 0.3 % H₂O₂ solution and 20 min color development, 2 rinses in PBT, 3 x 10 min washes in PBT, last wash supplemented with DAPI, mounting in 70 % glycerol and storage at 4°C.

5.3.6.2 *In situ* hybridization

The ORF of *hunchback* was liberated from a plasmid (# 143, M. Averof) and cloned into EcoRI and XbaI sites of pBluescript II KS(+) (pBS-hbORF). The plasmid was linearized with HindIII and 1 μ g used as template for *in vitro* transcription with the DIG-RNA Labeling Mix and T7 RNA Polymerase (Roche) in a reaction volume of 15 μ l. The reaction was incubated for 3 - 4 h at 37°C, 11 μ l nuclease-free H₂O added, 1 μ l checked on an 1 % TAE/EtBr agarose gel for integrity and approximately correct size. Next the reaction was incubated with 25 μ l of 2x Carbonate buffer (120mM Na₂CO₃, 80mM NaHCO₃, pH 10.2) for 20 min at 65°C and the following solutions added: 50 μ l of Stop Solution (0.2M sodium acetate), 10 μ l 4 M LiCl, 25 μ l of tRNAs (4 μ g/ μ l) and 300 μ l 100 % EtOH. The DIG-labeled RNA was precipitated at -20°C for 30 min or overnight, centrifuged for 30 min at 4°C, the pellet was washed with 70 % EtOH, centrifuged for 2 min at RT, air-dried, resuspended on ice in 200 μ l Hyb buffer and stored at -20°C.

Embryos were dechorionated in 50% bleach for 1-2 min, washed several times with dH₂O and PBT. The dechorionated embryos were transferred into glass vials containing equal volumes of fixation solution (1xPEM, 4% FA) and heptane and fixed by shaking vigorously for 25 min. The fixation solution was removed, 100 % MeOH added to an equal volume of the heptane and shaken vigorously for 1 min. Devitellinized embryos fell to the bottom of the vial, while the non-devitellinized embryos and embryonic membranes remained in the interphase. The heptane and interphase debris were removed and the embryos washed several times in 100 %

MeOH. The *in situ* hybridization with the *hb* probe was performed as follows: 5 min wash in EtOH:MeOH [1:1], 3 rinses in 100 % EtOH, 1 h wash in Xylene:EtOH [9:1], 3 rinses in 100 % EtOH, 5 min wash in 100 % EtOH, 3 rinses in 100 % MeOH, 5 min wash in 100 % MeOH, 5 min wash in MeOH:PBT [1:1] + 5 % FA, rinse in PBT + 5 % FA, 25 min post-fixation in PBT + 5 % FA, 4 x 10 min wash in PBT, 10 min wash in PBT:Hyb buffer [1:1], 2 min wash in Hyb buffer, 2 -3 h wash in Hyb buffer at 55°C with several changes of solution. The *hb* probe was diluted 1:100 in Hyb buffer, denatured for 5 min at 80°C, chilled on ice for 5 min and pre-heated for 10 min at 55°C. The Hyb buffer was aspirated from the embryos, the diluted probe added and incubated for 18 h at 55°C. Subsequent steps were: 2 x 10 min washes in Hyb buffer at 55°C, 6 x 30 min washes in Hyb buffer at 55°C, 10 min wash in PBT:Hyb buffer [1:1] at RT, 5 x 10 min washes in PBT at RT, incubation of pre-absorbed α -DIG-AP conjugated antibody (Roche) [dilution 1:2000] overnight at 4°C. All subsequent procedures at RT: 4 x 15 min washes in PBT, 2 x 3 min washes in staining buffer, 15 - 20 min incubation in staining solution (1 ml staining buffer + 20 μ l NBT/BCIP Stock Solution, Roche), 3 rinses in PBT, 10 min wash in PBT, 10 min wash in PBT:EtOH [1:1], 6 x 10 min washes in 100 % EtOH, 10 min wash in PBT:EtOH [1:1], 3 x 10 min washes in PBT, last wash supplemented with DAPI, mounting in 70 % glycerol and storage at 4°C.

5.3.7 Microscopy and Imaging

Immunohistochemically stained embryos were analyzed and photographed using Axioskop 2 Plus Zeiss-Biorad Confocal microscope unit.

The analysis of GFP expression in embryos was performed as follows: embryos were collected for 30 min and aged for 1h 30 min at 25°C, dechorionated in 50% bleach for 1-2 min, washed extensively with tap water, transferred on a microscope slide with a drop of halocarbon oil and covered with a cover glass. Once the halocarbon oil had spread underneath the cover glass the embryos were ready for immediate imaging. The quantitative analysis of fluorescence intensities was performed as follows: Live embryos of similar stage (nuclear division cycle 11) were analyzed and photographed using Leica MZ 16F Stereoscope, Leica DFC 300 FX camera and Leica EL6000 UV lamp source with the green fluorescence filter.

To avoid possible fluctuations in intensity of the UV lamp, the microscope settings and exposure time were kept identical for all experiments within the day. Because

photobleaching lowered the overall GFP intensity, care was taken to keep exposure to UV light as short as possible during photographing. This was also achieved by dividing the embryos on multiple microscope slides, so that few embryos are being exposed to the UV light at a time. The photographs from each experiment, e.g. embryos of UAS-BCDG^{F4M6}/+;38F-Dm3'/+;nos-GAL4:VP16, were always taken against the control embryos (sensor alone: 38F-Dm3'/+;nos-GAL4:VP16/+) and analyzed relative to the control.

For the quantification of fluorescence intensities the same rectangular region of interest (ROI) lying in the center of each embryo was measured using the "Measure" command in ImageJ. Mean values given by the ImageJ program were analyzed using Excel (Microsoft). The average values and relative average values of the fluorescence measurements can be seen in the APPENDIX 6.

6 Literature

Ameres, S., Martinez, J., and Schroeder, R. (2007). Molecular Basis for Target RNA Recognition and Cleavage by Human RISC. *Cell* 130, 101-112.

Aravin, A.A., Lagos-Quintana, M., Yalcin, A., Zavolan, M., Marks, D., Snyder, B., Gaasterland, T., Meyer, J., and Tuschl, T. (2003). The small RNA profile during *Drosophila melanogaster* development. *Dev Cell* 5, 337-350.

Baird-Titus, J.M., Clark-Baldwin, K., Dave, V., Caperelli, C.A., Ma, J., and Rance, M. (2006). The solution structure of the native K50 Bicoid homeodomain bound to the consensus TAATCC DNA-binding site. *J Mol Biol* 356, 1137-1151.

Bartel, D.P. (2004). MicroRNAs: genomics, biogenesis, mechanism, and function. *Cell* 116, 281-297.

Bate, M., and Martínez Arias, A. (1993). *The Development of Drosophila melanogaster*, Volume 1: 1558.

Bateman, J.R. (2006). Site-Specific Transformation of *Drosophila* via C31 Integrase-Mediated Cassette Exchange. *Genetics* 173, 769-777.

Becalska, A.N., and Gavis, E.R. (2009). Lighting up mRNA localization in *Drosophila* oogenesis. *Development* 136, 2493-2503.

Berleth, T., Burri, M., Thoma, G., Bopp, D., Richstein, S., Friegerio, G., noll, M., and Nüsslein-Vollhard, C. (1988). The role of localization of bicoid RNA in organizing the anterior pattern of the *Drosophila* embryo. *EMBO J* 7, 1749-1756.

Betel, D., Wilson, M., Gabow, A., Marks, D.S., and Sander, C. (2008). The microRNA.org resource: targets and expression. *Nucleic Acids Research* 36, D149-153.

Brennecke, J., Hipfner, D.R., Stark, A., Russell, R.B., and Cohen, S.M. (2003). bantam encodes a developmentally regulated microRNA that controls cell proliferation and regulates the proapoptotic gene hid in *Drosophila*. *Cell* 113, 25-36.

Brennecke, J., Stark, A., Russell, R.B., and Cohen, S.M. (2005). Principles of microRNA-target recognition. *Plos Biol* 3, e85.

Brown, S.J., Fellers, J.P., Shippy, T.D., Richardson, E.A., Maxwell, M., Stuart, J.J., and Denell, R.E. (2002). Sequence of the *Tribolium castaneum* homeotic complex: the region corresponding to the *Drosophila melanogaster* antennapedia complex. *Genetics* 160, 1067-1074.

Bullock, S.L., Ringel, I., Ish-Horowicz, D., and Lukavsky, P.J. (2010). A'-form RNA helices are required for cytoplasmic mRNA transport in *Drosophila*. *Nat Struct Mol Biol* 17, 703-709.

Carrington, J.C., and Ambros, V. (2003). Role of microRNAs in plant and animal development. *Science* 301, 336-338.

- Cassiday, L.A., and Maher III, L.J. (2002). Having it both ways: transcription factors that bind to DNA and RNA. *Nucleic Acids Research* 30, 4118-4126.
- Chan, S.-K., and Struhl, G. (1997). Sequence-specific RNA binding by Bicoid. *Nature* 388, 634.
- Chawengsaksophak, K., de Graaff, W., Rossant, J., Deschamps, J., and Beck, F. (2004). Cdx2 is essential for axial elongation in mouse development. *Proc Natl Acad Sci USA* 101, 7641-7645.
- Chendrimada, T.P., Finn, K.J., Ji, X., Baillat, D., Gregory, R.I., Liebhaber, S.A., Pasquinelli, A.E., and Shiekhattar, R. (2007). MicroRNA silencing through RISC recruitment of eIF6. *Nature* 447, 823-828.
- Cho, P., Gamberi, C., Chopark, Y., Chopark, I., Lasko, P., and Sonenberg, N. (2006). Cap-Dependent Translational Inhibition Establishes Two Opposing Morphogen Gradients in *Drosophila* Embryos. *Current Biology* 16, 2035-2041.
- Cho, P., Poulin, F., Chopark, Y., Chopark, I., Chicoine, J., Lasko, P., and Sonenberg, N. (2005). A New Paradigm for Translational Control: Inhibition via 5' -3' mRNA Tethering by Bicoid and the eIF4E Cognate 4EHP. *Cell* 121, 411-423.
- Copf, T., Rabet, N., Celniker, S.E., and Averof, M. (2003). Posterior patterning genes and the identification of a unique body region in the brine shrimp *Artemia franciscana*. *Development* 130, 5915-5927.
- Copf, T., Schröder, R., and Averof, M. (2004). From the Cover: Ancestral role of caudal genes in axis elongation and segmentation. *Proceedings of the National Academy of Sciences* 101, 17711-17715.
- Derobertis, E. (2008). Evo-Devo: Variations on Ancestral Themes. *Cell* 132, 185-195.
- Draper, B.W., Mello, C.C., Bowerman, B., Hardin, J., and Priess, J.R. (1996). MEX-3 is a KH domain protein that regulates blastomere identity in early *C. elegans* embryos. *Cell* 87, 205-216.
- Driever, W., and Nüsslein-Volhard, C. (1989). The bicoid protein is a positive regulator of hunchback transcription in the early *Drosophila* embryo. *Nature* 337, 138-143.
- Dubnau, J., and Struhl, G. (1996). RNA recognition and translational regulation by a homeodomain protein. *Nature* 379, 694-699.
- Dubnau, J., and Struhl, G. (1997). Correction: RNA recognition and translational regulation by a homeodomain protein. *Nature* 388, 697-697.
- Edgar, L.G., Carr, S., Wang, H., and Wood, W.B. (2001). Zygotic expression of the caudal homolog pal-1 is required for posterior patterning in *Caenorhabditis elegans* embryogenesis. *Developmental Biology* 229, 71-88.
- F. Gilbert, S., and R. Singer, S. (2010). *Developmental Biology*. 685.

- Falciani, F., Hausdorf, B., Schröder, R., Akam, M., Tautz, D., Denell, R., and Brown, S. (1996). Class 3 Hox genes in insects and the origin of zen. *Proceedings of the National Academy of Sciences* *93*, 8479-8484.
- Ferrandon, D., Koch, I., Westhof, E., and Nüsslein-Volhard, C. (1997). RNA-RNA interaction is required for the formation of specific bicoid mRNA 3' UTR-STAUFIN ribonucleoprotein particles. *The EMBO Journal* *16*, 1751-1758.
- Furriols, M., and Casanova, J. (2003). In and out of Torso RTK signalling. *EMBO J* *22*, 1947-1952.
- Gamberi, C., Peterson, D.S., He, L., and Gottlieb, E. (2002). An anterior function for the *Drosophila* posterior determinant Pumilio. *Development* *129*, 2699-2710.
- Gregor, T., Tank, D., Wieschaus, E., and Bialek, W. (2007a). Probing the Limits to Positional Information. *Cell* *130*, 153-164.
- Gregor, T., Wieschaus, E., Mcgregor, A., Bialek, W., and Tank, D. (2007b). Stability and Nuclear Dynamics of the Bicoid Morphogen Gradient. *Cell* *130*, 141-152.
- Grimm, O., Coppey, M., and Wieschaus, E. (2010). Modelling the Bicoid gradient. *Development* *137*, 2253-2264.
- Groth, A.C., Fish, M., Nusse, R., and Carlos, M.P. (2003). Construction of Transgenic *Drosophila* by Using the Site-Specific Intergrase from Phage ϕ C31. *Genetics* *166*, 1775-1782.
- Hernández, G., Altmann, M., Sierra, J.M., Urlaub, H., Diez del Corral, R., Schwartz, P., and Rivera-Pomar, R. (2005). Functional analysis of seven genes encoding eight translation initiation factor 4E (eIF4E) isoforms in *Drosophila*. *Mechanisms of Development* *122*, 529-543.
- Höchsmann, M., Töller, T., Giegerich, R., and Kurtz, S. (2003). Local similarity in RNA secondary structures. *Proc IEEE Comput Soc Bioinform Conf* *2*, 159-168.
- Höchsmann, M., Voss, B., and Giegerich, R. (2004). Pure multiple RNA secondary structure alignments: a progressive profile approach. *IEEE/ACM Trans Comput Biol Bioinform* *1*, 53-62.
- Horn, C., and Wimmer, E.A. (2000). A versatile vector set for animal transgenesis. *Dev Genes Evol* *210*, 630-637.
- Humphreys, D.T., Westman, B.J., Martin, D.I.K., and Preiss, T. (2005). MicroRNAs control translation initiation by inhibiting eukaryotic initiation factor 4E/cap and poly(A) tail function. *Proc Natl Acad Sci USA* *102*, 16961-16966.
- Hunter, C.P., and Kenyon, C. (1996). Spatial and Temporal Controls Target pal-1 Blastomere-Specification Activity to a Single Blastomere Lineage in *C. elegans* Embryos. *Cell*, *87*, 217-226.
- Iwasaki, S., Kawamata, T., and Tomari, Y. (2009). *Drosophila* argonaute1 and argonaute2 employ distinct mechanisms for translational repression. *Molecular Cell* *34*, 58-67.

- Jackson, R.J., and Standart, N. (2007). How do microRNAs regulate gene expression? *Sci STKE* 2007, re1.
- Janody, F., Sturny, R., Schaeffer, V., Azou, Y., and Dostatni, N. (2001). Two distinct domains of Bicoid mediate its transcriptional downregulation by the Torso pathway. *Development* 128, 2281-2290.
- Kiriakidou, M., Tan, G.S., Lamprinaki, S., De Planell-Saguer, M., Nelson, P.T., and Mourelatos, Z. (2007). An mRNA m7G cap binding-like motif within human Ago2 represses translation. *Cell* 129, 1141-1151.
- Lai, E.C., Tomancak, P., Williams, R.W., and Rubin, G.M. (2003). Computational identification of *Drosophila* microRNA genes. *Genome Biol* 4, R42.
- Leaman, D., Chen, P., Fak, J., Yalcin, A., Pearce, M., Unnerstall, U., Marks, D., Sander, C., Tuschl, T., and Gaul, U. (2005). Antisense-Mediated Depletion Reveals Essential and Specific Functions of MicroRNAs in Development. *Cell* 121, 1097-1108.
- Lemke, S., Busch, S.E., Antonopoulos, D.A., Meyer, F., Domanus, M.H., and Schmidt-Ott, U. (2010). Maternal activation of gap genes in the hover fly *Episyrphus*. *Development* 137, 1709-1719.
- Lemke, S., Stauber, M., Shaw, P.J., Rafiqi, A.M., Prell, A., and Schmidt-Ott, U. (2008). Bicoid occurrence and Bicoid-dependent hunchback regulation in lower cyclorrhaphan flies. *Evol Dev* 10, 413-420.
- Li, W.X. (2005). Functions and mechanisms of receptor tyrosine kinase Torso signaling: lessons from *Drosophila* embryonic terminal development. *Dev Dyn* 232, 656-672.
- Lynch, J.A., Brent, A.E., Leaf, D.S., Pultz, M.A., and Desplan, C. (2006). Localized maternal orthodenticle patterns anterior and posterior in the long germ wasp *Nasonia*. *Nature* 439, 728-732.
- Lynch, J.A., Peel, A.D., Drechsler, A., Averof, M., and Roth, S. (2010). EGF signaling and the origin of axial polarity among the insects. *Curr Biol* 20, 1042-1047.
- Macdonald, P.M., and Struhl, G. (1986). A molecular gradient in early *Drosophila* embryos and its role in specifying the body pattern. *Nature* 324, 537-545.
- MacDougall, N., Clark, A., MacDougall, E., and Davis, I. (2003). *Drosophila* gurken (TGFalpha) mRNA localizes as particles that move within the oocyte in two dynein-dependent steps. *Dev Cell* 4, 307-319.
- Mathews, D.H., Sabina, J., Zuker, M., and Turner, D.H. (1999). Expanded sequence dependence of thermodynamic parameters improves prediction of RNA secondary structure. *J Mol Biol* 288, 911-940.
- Mathonnet, G., Fabian, M.R., Svitkin, Y.V., Parsyan, A., Huck, L., Murata, T., Biffo, S., Merrick, W.C., Darzynkiewicz, E., Pillai, R.S., *et al.* (2007). MicroRNA inhibition of translation initiation in vitro by targeting the cap-binding complex eIF4F. *Science* 317, 1764-1767.

- Mcgregor, A.P. (2005). How to get ahead: the origin, evolution and function of bicoid. *Bioessays* 27, 904-913.
- Mlodzik, M., Fjose, A., and Gehring, W.J. (1985). Isolation of caudal, a *Drosophila* homeo box-containing gene with maternal expression, whose transcripts form a concentration gradient at the pre-blastoderm stage. *EMBO J* 4, No. 11, 2961-2969.
- Mlodzik, M., Gibson, G., and Gehring, W.J. (1990). Effects of ectopic expression of caudal during *Drosophila* development. *Development* 109, 271-277.
- Moor, C., Meijer, H., and Lissenden, S. (2005). Mechanisms of translational control by the 3' UTR in development and differentiation. *Seminars in Cell & Developmental Biology* 16, 49-58.
- Moreno, E., and Morata, G. (1999). Caudal is the Hox gene that specifies the most posterior *Drosophila* segment. *Nature* 400, 873-877.
- Müller-Taubenberger, A., Vos, M.J., Böttger, A., Lasi, M., Lai, F.P.L., Fischer, M., and Rottner, K. (2006). Monomeric red fluorescent protein variants used for imaging studies in different species. *Eur J Cell Biol* 85, 1119-1129.
- Murata, Y., and Wharton, R.P. (1995) Binding of pumilio to maternal hunchback mRNA is required for posterior patterning in *Drosophila* embryos. *Cell* 80, 747-756.
- Niessing, D., Dostatni, N., Jäckle, H., and Rivera-Pomar, R. (1999). Sequence interval within the PEST motif of Bicoid is important for translational repression of caudal mRNA in the anterior region of the *Drosophila* embryo. *EMBO J* 18, No. 7, 1966-1973.
- Niessing, D., Sprenger, F., Taubert, H., Jäckle, H., and Rivera-Pomar, R. (2000). Homeodomain Position 54 Specifies Transcriptional versus Translational Control by Bicoid. *Molecular Cell* 5, 395-401.
- Olesnicky, E.C., Brent, A.E., Tonnes, L., Walker, M., Pultz, M.A., Leaf, D., and Desplan, C. (2006). A caudal mRNA gradient controls posterior development in the wasp *Nasonia*. *Development* 133, 3973-3982.
- Pavlopoulos, A., and Averof, M. (2005). Establishing genetic transformation for comparative developmental studies in the crustacean *Parhyale hawaiiensis*. *Proc Natl Acad Sci USA* 102, 7888-7893.
- Peel, A.D. (2008). The evolution of developmental gene networks: lessons from comparative studies on holometabolous insects. *Philos Trans R Soc Lond, B, Biol Sci* 363, 1539-1547.
- Peel, A.D., and Averof, M. (2010). Early asymmetries in maternal transcript distribution associated with a cortical microtubule network and a polar body in the beetle *Tribolium castaneum*. *Dev Dyn* 239, 2875-2887.
- Peel, A.D., Chipman, A.D., and Akam, M. (2005). Arthropod segmentation: beyond the *Drosophila* paradigm. *Nat Rev Genet* 6, 905-916.

- Pillai, R.S., Bhattacharyya, S.N., Artus, C.G., Zoller, T., Cougot, N., Basyuk, E., Bertrand, E., and Filipowicz, W. (2005). Inhibition of translational initiation by Let-7 MicroRNA in human cells. *Science* 309, 1573-1576.
- Pultz, M.A., Diederich, R.J., Cribbs, D.L., and Kaufman, T.C. (1988). The proboscipedia locus of the Antennapedia complex: a molecular and genetic analysis. *Genes & Development* 2, 901-920.
- Rivera-Pomar, R., Lu, X., Perrimon, N., Taubert, H., and Jäckle, H. (1995). Activation of posterior gap gene expression in the *Drosophila* blastoderm. *Nature* 374, 253-256.
- Rivera-Pomar, R., Niessing, D., Schmidt-Ott, U., Gehring, W.J., and Jäckle, H. (1996). RNA binding and translational suppression by bicoid. *Nature* 379, 746-749.
- Rørth, P. (1998). Gal4 in the *Drosophila* female germline. *Mechanisms of Development* 78, 113-118.
- Rosenberg, M.I., Lynch, J.A., and Desplan, C. (2009). Heads and tails: evolution of antero-posterior patterning in insects. *Biochim Biophys Acta* 1789, 333-342.
- Rushlow, C., Doyle, H., Hoey, T., and Levine, M. (1987a). Molecular characterization of the *zerknüllt* region of the Antennapedia gene complex in *Drosophila*. *Genes & Development* 1, 1268-1279.
- Rushlow, C., Frasch, M., Doyle, H., and Levine, M. (1987b). Maternal regulation of *zerknüllt*: a homeobox gene controlling differentiation of dorsal tissues in *Drosophila*. *Nature* 330, 583-586.
- Sander, K., and Schmidt-Ott, U. (2004). Evo-Devo aspects of classical and molecular data in a historical perspective. *J. Exp. Zool.* 302B, 69-91.
- Savard, J., Tautz, D., Richards, S., Weinstock, G. M., Gibbs, R. A., Werren, J. H., Tettelin, H. & Lercher, M. J. (2006) Phylogenomic analysis reveals bees and wasps (Hymenoptera) at the base of the radiation of holometabolous insects. *Genome Res.* 16, 1334–1338.
- Schaeffer, V., Janody, F., Loss, C., Desplan, C., and Wimmer, E.A. (1999). Bicoid functions without its TATA-binding protein-associated factor interaction domains. *Proc Natl Acad Sci USA* 96, 4461-4466.
- Schoppmeier, M., Fischer, S., Schmitt-Engel, C., Löhr, U., and Klingler, M. (2009). An Ancient Anterior Patterning System Promotes Caudal Repression and Head Formation in Ecdysozoa. *Curr Biol* 19, 1-5.
- Schröder, R. (2003). The genes *orthodenticle* and *hunchback* substitute for *bicoid* in the beetle *Tribolium*. *Nature* 422, 621-625.
- Schröder, R., Beermann, A., Wittkopp, N., and Lutz, R. (2008). From development to biodiversity--*Tribolium castaneum*, an insect model organism for short germband development. *Development Genes and Evolution* 218, 119-126.
- Schroeder, R., Barta, A., and Semrad, K. (2004). Strategies for RNA folding and assembly. *Nat Rev Mol Cell Biol* 5, 908-919.

- Schulz, C., and Tautz, D. (1995). Zygotic caudal regulation by hunchback and its role in abdominal segment formation of the *Drosophila* Embryo. *Development* *121*, 1023-1028.
- Snee, M.J., Arn, E.A., Bullock, S.L., and Macdonald, P.M. (2005). Recognition of the *bcd* mRNA localization signal in *Drosophila* embryos and ovaries. *Mol Cell Biol* *25*, 1501-1510.
- Sommer, R.J., and Tautz, D. (1991). Segmentation gene expression in the housefly *Musca domestica*. *Development* *113*, 419-430.
- Spirov, A., Fahmy, K., Schneider, M., Frei, E., noll, M., and Baumgartner, S. (2009). Formation of the bicoid morphogen gradient: an mRNA gradient dictates the protein gradient. *Development* *136*, 605-614.
- St Johnston, D., and Nüsslein-Volhard, C. (1992). The origin of pattern and polarity in the *Drosophila* embryo. *Cell* *68*, 201-219.
- Stark, A., Brennecke, J., Bushati, N., Russell, R., and Cohen, S. (2005). Animal MicroRNAs Confer Robustness to Gene Expression and Have a Significant Impact on 3' UTR Evolution. *Cell* *123*, 1133-1146.
- Stauber, M., Jäckle, H., and Schmidt-Ott, U. (1999). The anterior determinant bicoid of *Drosophila* is a derived Hox class 3 gene. *Proceedings of the National Academy of Sciences* *96*, 3786-3789.
- Stauber, M., Lemke, S., and Schmidt-Ott, U. (2008). Expression and regulation of caudal in the lower cyclorrhaphan fly *Megaselia*. *Dev Genes Evol* *218*, 81-87.
- Stauber, M., Prell, A., and Schmidt-Ott, U. (2002). A single Hox3 gene with composite bicoid and *zerknüllt* expression characteristics in non-Cyclorrhaphan flies. *PNAS* *99*, 274-279.
- Stauber, M., Taubert, H., and Schmidt-Ott, U. (2000). Function of bicoid and hunchback homologs in the basal cyclorrhaphan fly *Megaselia* (Phoridae). *PNAS* *97*, 10844-1849.
- Steinhauer, J., and Kalderon, D. (2006). Microtubule polarity and axis formation in the *Drosophila* oocyte. *Dev Dyn* *235*, 1455-1468.
- Struhl, G., Struhl, K., and Macdonald, P.M. (1989). The gradient morphogen bicoid is a concentration-dependent transcriptional activator. *Cell* *57*, 1259-1273.
- Swevers, L., Cherbas, L., Cherbas, P., and Iatrou, K. (1996). Bombyx EcR (BmEcR) and Bombyx USP (BmCF1) combine to form a functional ecdysone receptor. *nsect Biochem. Mol. Biol.* *26*, 217-221.
- Tadros, W., and Lipshitz, H.D. (2005). Setting the stage for development: mRNA translation and stability during oocyte maturation and egg activation in *Drosophila*. *Dev Dyn* *232*, 593-608.
- Thermann, R., and Hentze, M.W. (2007). *Drosophila* miR2 induces pseudo-polysomes and inhibits translation initiation. *Nature* *447*, 875-878.

- Thorpe, H.M. (1998). In vitro site-specific integration of bacteriophage DNA catalyzed by a recombinase of the resolvase/invertase family. *Proceedings of the National Academy of Sciences* **95**, 5505-5510.
- Treisman, J., Gönczy, P., Vashishtha, M., Harris, E., and Desplan, C. (1989). A single amino acid can determine the DNA binding specificity of homeodomain proteins. *Cell* **59**, 553-562.
- Tweedie, S., Ashburner, M., Falls, K., Leyland, P., McQuilton, P., Marygold, S., Millburn, G., Osumi-Sutherland, D., Schroeder, A., Seal, R., *et al.* (2009). FlyBase: enhancing *Drosophila* Gene Ontology annotations. *Nucleic Acids Research* **37**, D555-D559.
- van den Akker, E., Forlani, S., Chawengsaksophak, K., de Graaff, W., Beck, F., Meyer, B.I., and Deschamps, J. (2002). *Cdx1* and *Cdx2* have overlapping functions in anteroposterior patterning and posterior axis elongation. *Development* **129**, 2181-2193.
- van den Berg, A., Mols, J., and Han, J. (2008). RISC-target interaction: cleavage and translational suppression. *Biochim Biophys Acta* **1779**, 668-677.
- van Der Zee, M., Berns, N., and Roth, S. (2005). Distinct functions of the *Tribolium* *zerknüllt* genes in serosa specification and dorsal closure. *Curr Biol* **15**, 624-636.
- Wagner, C., Ehresmann, C., Ehresmann, B., and Brunel, C. (2004). Mechanism of dimerization of bicoid mRNA: initiation and stabilization. *J Biol Chem* **279**, 4560-4569.
- Wagner, C., Palacios, I., Jaeger, L., St Johnston, D., Ehresmann, B., Ehresmann, C., and Brunel, C. (2001). Dimerization of the 3'UTR of bicoid mRNA involves a two-step mechanism. *J Mol Biol* **313**, 511-524.
- Wimmer, E.A., Carleton, A., Harjes, P., Turner, T., and Desplan, C. (2000). Bicoid-independent formation of thoracic segments in *Drosophila*. *Science* **287**, 2476-2479.
- Wolff, C., Schröder, R., Schulz, C., Tautz, D., and Martin Klingler, M. (1998). Regulation of the *Tribolium* homologues of caudal and hunchback in *Drosophila*: evidence for maternal gradient systems in a short germ embryo. *Development* **125**, 2645-2654.
- Yeates, D.K., and Wiegmann, B.M. (1999). CONGRUENCE AND CONTROVERSY: Toward a Higher-Level Phylogeny of Diptera. *Ann. Rev. Entomol.*, **34**.
- Zhao, C., York, A., Yang, F., Forsthoefel, D.J., Dave, V., Fu, D., Zhang, D., Corado, M.S., Small, S., Seeger, M.A., and Ma, J. (2002). The activity of the *Drosophila* morphogenetic protein Bicoid is inhibited by a domain located outside its homeodomain. *Development* **129**, 1669-1680.
- Zuker, M. (2003). Mfold web server for nucleic acid folding and hybridization prediction. *Nucleic Acids Res* **31**, 3406-3415.

APPENDIX

A1 EMSAs

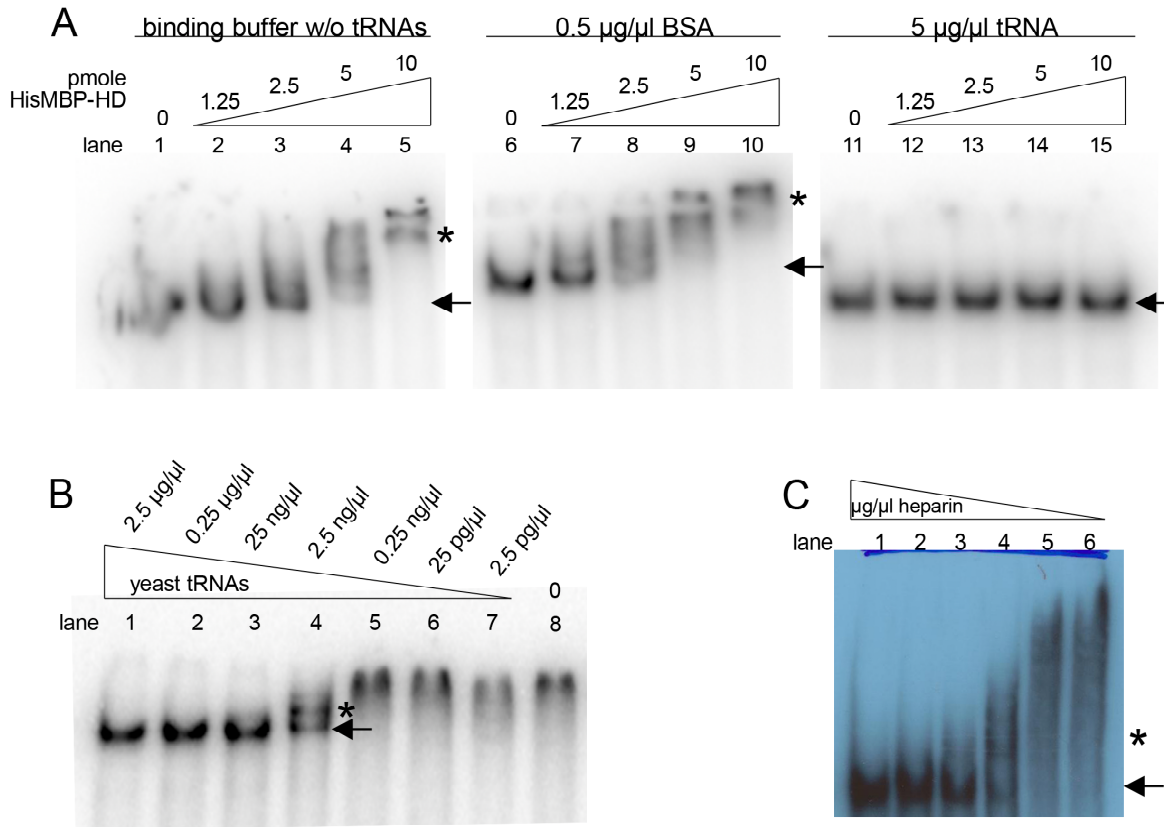


Fig. A1.1: Establishment of BCD homeodomain binding conditions for EMSAs. (A) Effect of 5 µg/µl yeast tRNA during RNA-binding of HisMBP-HD. 1.25-10 pmole of HisMBP-HD were incubated with 260 fmole of BRE_164-512 (see Fig. A1.3, B) in the presence of binding buffer without tRNAs (lanes 1-5), with 0.5 µg/µl BSA (lanes 6-10) or with 5 µg/µl yeast tRNAs (lanes 11-15). In the presences of the 5µg/µl tRNAs the RNA-binding of HisMBP-HD is inhibited (lanes 11-15). The presence of 0.5 µg/µl BSA seems to be beneficial to the RNA-binding as a shift occurs at slightly lower HisMBP-HD concentrations than in the absence of BSA (compare lane 3 and 8). **(B)** Binding of the BRE_164-512 fragment to HisMBP-HD with different yeast tRNA concentrations during RNA binding. Binding of the HisMBP-HD with high tRNA concentrations is inhibited (lanes 1-4), whereas with 2,5 ng/µl tRNA of yeast tRNA unspecific binding activity is blocked while binding to the BRE_164-512 can result in a shift (lane 4). tRNA concentrations below 2.5 ng/µl most likely fail to block unspecific binding of HisMBP-HD (lanes 5-8). **(C)** Effect of different concentrations of heparin (lanes 1-6: 2.25 µg/µl; 200 ng/µl; 18.5 ng/µl; 1.6 ng/µl; 0.15 ng/µl; 0) during RNA-binding of HisMBP-HD.

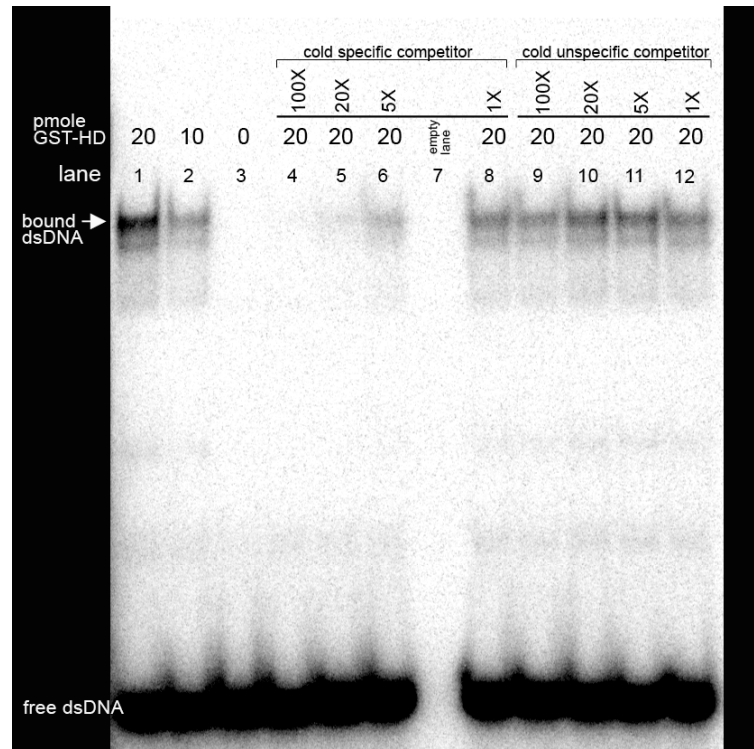


Fig. A1.2: Binding of bacterially expressed GST-HD protein to the BCD ds DNA target fragment (dsDNA) and competition with unlabeled (cold) dsDNA (specific) or cold unspecific DNA (023-F/024-R dsDNA oligo). Lanes 1 and 2 show binding of the dsDNA by the GST-HD (arrow). The dsDNA:GST-HD complex can be competed by an 5-fold to 100 fold excess of unlabeled dsDNA (lanes 4-6), however the unrelated cold unspecific competitor is not able to disrupt the complex (lanes 9-12).

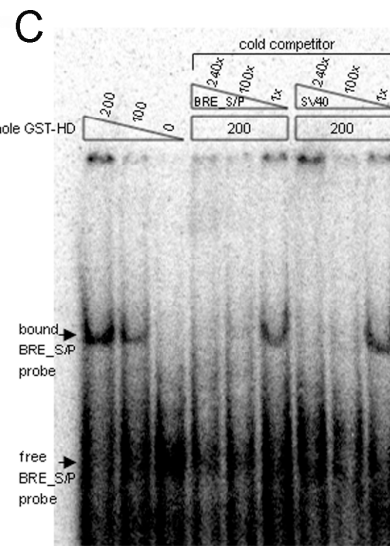
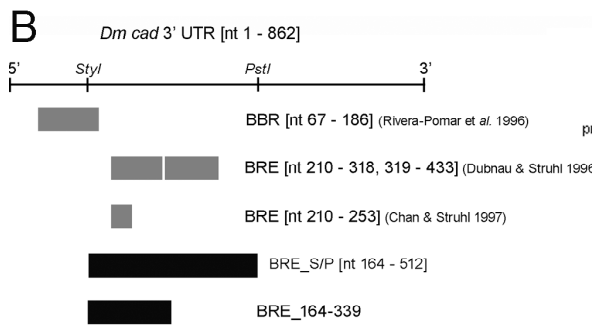
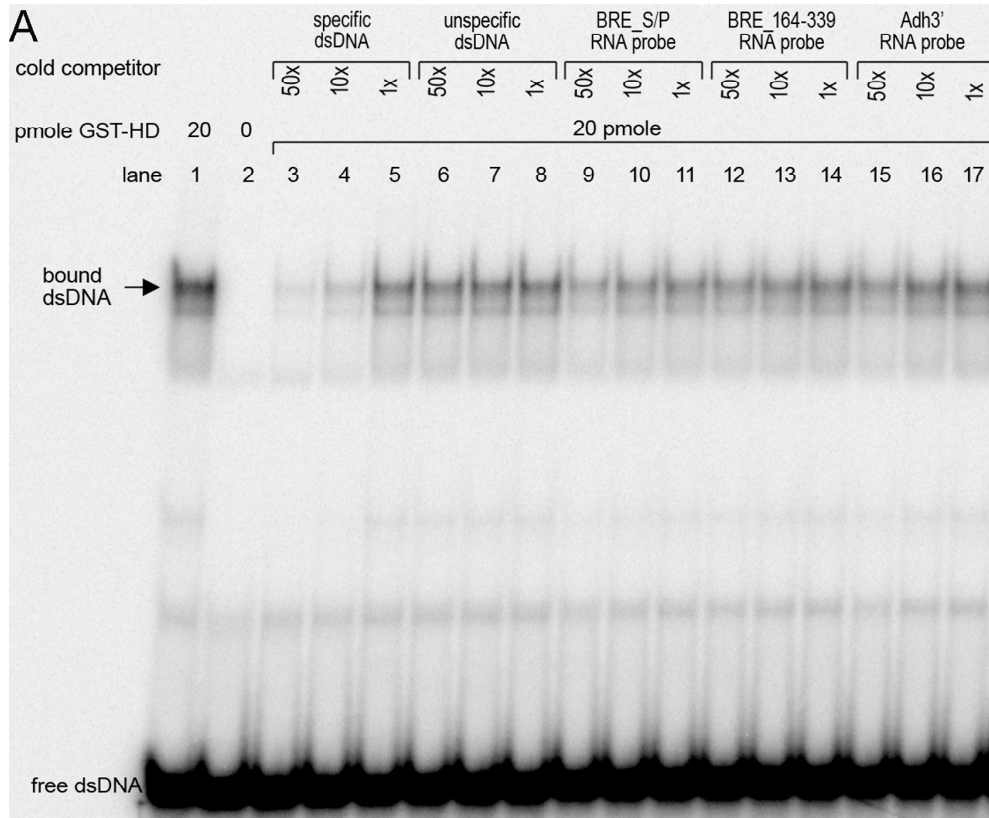


Fig. A1.3: (A) Binding of the GST-HD recombinant protein to the BCD dsDNA target and competition with unlabeled (cold) specific dsDNA (lanes 3-4), unspecific dsDNA (023-F/024-R dsDNA oligo, lanes 6-8), BRE_S/P RNA (lanes 9-11), BRE_164-339 (lanes 12-14) and Adh3' (lanes 15-17). Only a 50-fold and 10-fold excess of the cold specific dsDNA can efficiently compete the labeled dsDNA probe (lanes 3 and 4). In comparison, the RNA probes affect the GST-HD:dsDNA complex to a much lesser degree, with the BRE_S/P probe having the strongest impact, followed by the BRE_164-339 and the Adh3' (compare lanes 9, 12 and 15). (B) Schematic overview of the RNA probes BRE_S/P and BRE_164-339 (black) in comparison to BRE_ fragment of previous studies (grey). (C) Mobility shift assay of the GST-HD recombinant protein bound to the BRE_S/P fragment. Both cold specific (BRE_S/P) and unspecific (SV40) competitors can equally compete the labeled BRE_S/P probe.

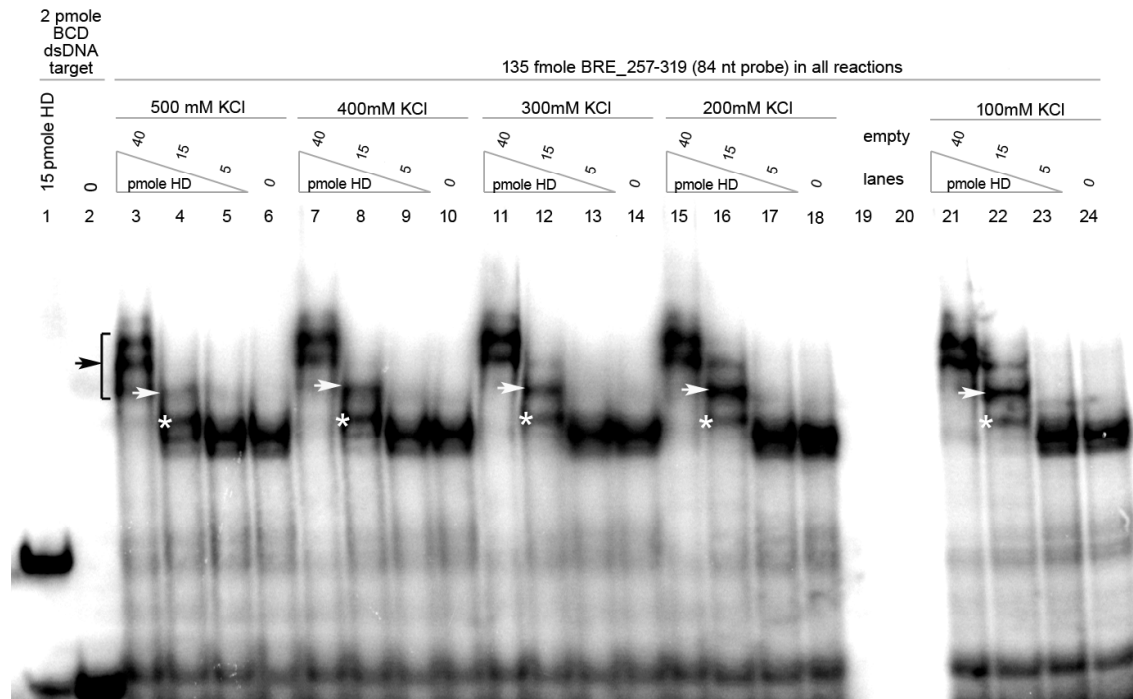


Fig. A.1.4: Binding of the BCD homeodomain to the BRE_257-319 fragment at different salt concentrations (lanes 3-6 500 mM KCl, lanes 7-10 400 mM KCl, lanes 11-14 300 mM KCl, lanes 15-18 200 mM KCl, lanes 21-24 100 mM KCl). Note that the mobility shift of the BRE_257-319 (asterisks) is best visible at 15 pmole homeodomain independently of the salt concentration, however the binding affinity does not increase with elevated salt concentrations. Rather the super-shifts (white arrows) that occur most likely due to unspecific binding of the homeodomain become inhibited at higher salt concentrations. Lanes 1 and 2 show DNA binding as a control for proper functionality of the homeodomain.

A2 Alignment of cad 3'UTR homologues

Multalin version 5.4.1
 Symbol comparison table: dna
 Gap weight: 5
 Gap length weight: 0
 Consensus levels: high=90% low=50%

```

MSF: 1188      Check: 0      ..
Name: Dmel      Len: 1188    Check: 129    Weight: 1.00
Name: Dpse      Len: 1188    Check: 1604   Weight: 1.00
Name: Dwil      Len: 1188    Check: 7120   Weight: 1.00
Name: Dvir      Len: 1188    Check: 5257   Weight: 1.00
Name: Dmoj      Len: 1188    Check: 4085   Weight: 1.00
Name: Consensus Len: 1188    Check: 9366   Weight: 0.00

//
      1                                     80
Dmel  UGACACGACC AUU-----C CUGUUAUGCG GCGAGCGGCG -----
Dpse  .....U..UU ..GAGGGGG. .AC.GC.... ..GC..CU. CCUCUGCUGC CGAUGGACAU CAUCCAAGAG CAGCGACGUC
Dwil  CC..CA..AU ..GGUAUCGA UCUAC.-----
Dvir  CAUG.UU.UG CAGGCGCCGU UGAGCC----
Dmoj  CCUG.UU.UG GGGCAGGGGA UGAGGU----
Consensus c.acaug.u. aug..g..g. u.....

      81                                     160
Dmel  -----AC AGUAACAACU ACAUGGAGCC CCAUCAUCCG CUGCGUGGUG
Dpse  GGGCUCGACA GCAAUGUGCU AUAGCAACAA UAUCAUCC.. .AC...GU. .U....U.A U....CGA. .A..AUCCGC
Dwil  -----CU AUAACAACAC CAACAACA.U ..C.G...A ..ACA.C.A .A.C..GAAC .AU.A.CA.A
Dvir  -----GA AUAGCUAUGA AAGCAGC--- .GGGG.GGC .GCG..G.AG G..G.GGGG. .G..A.CUAU
Dmoj  -----GC AUGGCUACCA GA--AUG--- -.G.G..G.. .UC.AAU.GA G..G..G.UA .A..AACAGU
Consensus ..... auagc.ac.a .a.ca.c.a. ag.agc.gcu ..auggagca .c...ag..g .ag.agc...

      161                                     240
Dmel  GUAGCGAGCG GGGUGGAGUA GGAGCGUAG GAGGCGUAGG AGGAGGAGGC GGACAACCGU GCGAUGUGUC CUUCAGUGCU
Dpse  UA.UG.G.GU .....U.GU ..U.UGAGC. .GC.G.G... ..AU....U ..UG----- .A.....
Dwil  A.G..A.CA. CA.CUAUA.G .A.CAA.GGC AGCAACA.UC .UCUUUG..U .-----UCA G.GUU.CU..
Dvir  .G----- CUA..C..CG U.UCCACGU. AUCUG.CC.- U...UUU... .-----UAA GCA.UU..UA
Dmoj  UGGAGACCA. CUA..C.ACG U.UUC.AGU. AGCUG.CUU- .CUUCUA.U .-----A.A GAAA...GG
Consensus .....g. c.gug.ag.g ggu...g.g agc.gg.ag. ag.uu..g.u .....u.a guacagugcu

      241                                     320
Dmel  CCGCUCUCG CCUUGGACU GGCUUAACCC UUA--GGUCGC GCAGUCAGAC UGUUUUCGACC GAACCGAAAA GUUAAUAGGC
Dpse  U.U....U. .AG...U. .... .C...U. A...U... ..GUGA. CCCAA..U. UGGGCG.AUG
Dwil  .A.ACA.GU ...A.UGA.. U.GCCGUGGA .UG.C.UAG AGUUGGGACA GUACC.AUU. CC.AAC.GUC AGACUGUCAG
Dvir  UUG.UCGG.C AGGG..GGG. U.UGGGUGAG .GUGU..G.G AG..GGGAUG GUGGG..GGG UC.AAC.GUU AGACUGUUUG
Dmoj  .GU.GCAAGC AG..A...G CUUC..CAG. .GAUAAA.A .A..GAGA.G G.G.GG..GG UGGAGU.GG-
Consensus c..g.c.u.. c.uugga.uu .g..ua...c .u..ggu.g. a.agg.gaa. gg.u.cg..c .caaa..g.. .g..g.g.g

      321                                     400
Dmel  AGCCGGACGA AUGGAGGACU UGGCGGCCGU UGCACCUGGA AUAUUGCACG UUGUUAA-UU UUGUGAUUG UUAUUCUUG
Dpse  U.AAU.GGAG .A..UA.UG. G.CGCAG.AA ...-U... ..----- .A.....
Dwil  G.A.U.U.AC CAUA..AUUA GA.GCAA.AG C.UCAU.U. .... .C.. .-----UAA
Dvir  U.-----AG CC...U.CG. AU..C.U... C.AC.U.U. .... .-.. .-----AC.
Dmoj  -----AG GC..C..CG- -----C.U.U. .... .-.. .-----GCA
Consensus .g...g.cag ..ggagg.gu ..g.c..cg. .g.ccu.u.. ..... .-----g

      401                                     480
Dmel  GUUUUCGACAC GCGCCAGAGU CCUCACAGCU AAACAAGU-- -----
Dpse  .G.UAUA.. ..UG.CCCAC G.....CGC .C...AAAC CCCUCCAAAA GCUCUCCAAU UUGAUGUAAA UUUGAUA AAC
Dwil  .CGCUA.A.- -----A UG.UG.CA.G .CC...AAUA AAAAAUGAGA GGAGUAGAAG AGGUUUUCUG UCUAAGCCAU
Dvir  .CG.UCGUGG CACG.CUCC. GGCU----- GGC..C.CCC ACAGCGGCAC A-----
Dmoj  .CG.UC.ACG CACG.CUCCA .GC.UUCAAC GGC..C.CCC ACAGCCAGGC AGCAGCAAGA GAAAUUUAAA UUAUUAAAA
Consensus .cguu.aaa. ...gcc.c.. .guc.c.... a.c..ag..c aca.c..... .-----a.. .u.u.u.. u.....a.

      481                                     560
Dmel  -----C UUAUAUU-- ----- -AUUCUUGUA UUAUGUUUGU UUUUUGUUCA
Dpse  AUACCUUUC CCCACAAUG. GC.CU.C-- -U.GUA... ..-----
Dwil  CUCCUAAGC CAGAAAACA. A.....UCC AGUAUGAUGU AUAACUGUAA A.AAA..U.. .CUAUA.AUA .A..A..AU
Dvir  -----AAU UCAUUGCAUA ACU.UG.GGC CCAAUUGUUA GUAAUAUGUU UU.AU..U.U .U.C..G.. .-----U
Dmoj  AUAACACAU GAAGAAAUA. ...G..CAA UUAUUUAUU AUCAUAUUA U.AAUG.A.. .GUA... .A.....AA.
Consensus .u...a... ..aa..c .uau.uu... ..au..u.u .u.a..... .auuu...a .uuu.u.ugu u..g.uca

      561                                     640
Dmel  ACGUGUGUAG UAGCUAAAAG UAAAAUGAAU AGCUCGU-- -----
Dpse  .AAGUAA.UU A.AG.A..U. .UU.UC.UC. .AU.UU.-- -----
Dwil  UAU.A.UAUU .UC.ACUIIU. ..UGUAC... UAU.GU.UUU UGUUU----- -A GAACCUUUA.
Dvir  .G---.UA.U GUUUAA..U. ..GCGC..G .UU.GA.UAG UUAGCAUCGA GACACACACA CACACACACA CACGC.CA..
Dmoj  CAA.U.U.GU AU.UA.U.U. .UUUG.UUU. UUU.UUGUUC UUAGUUAACA UUUAGCCUUA AAGAAAGACA GAGAC.CAA.
Consensus aa.u.uuu.u .u..a.aau. .au...aau a.u..uuu.. u..... .-----a .a..ca.a..

      641                                     720
Dmel  GUAGUAAGUA AAGUU-----GC CCGAGAAAAA CAAGAACA AUCAAACCAGC CGUCCAGCC GAUUAAACGU
Dpse  UCUA.G.A.C U....CUUAA GUUCUAAA.. .UG..... .----- .CUUU... ..CC.G UU...AAAG
Dwil  .A.U.G.A.G U....UAUA GUUGCCA.G ----- -A AAAA.A.AU C...UUUAGC

```

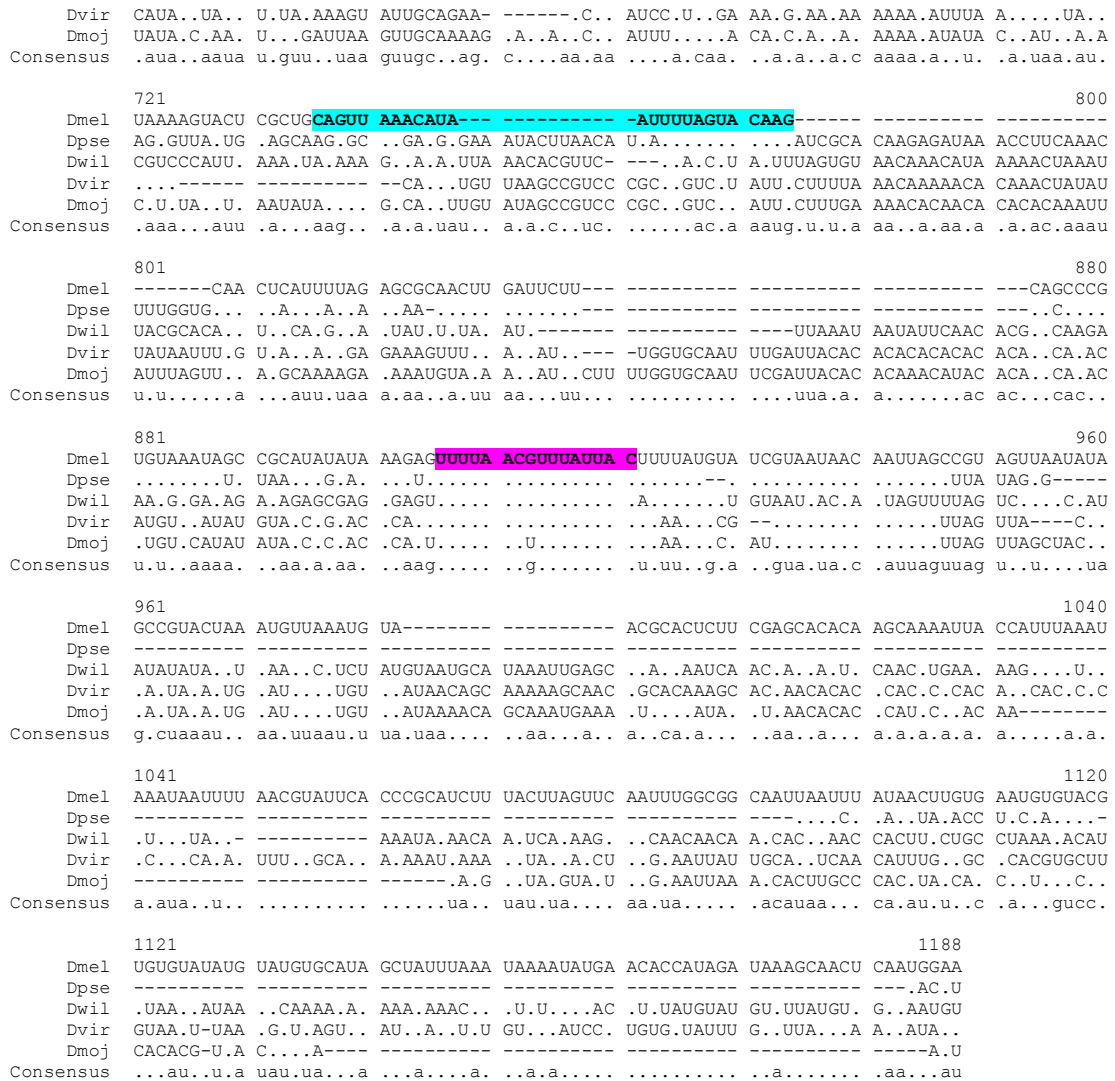



Fig. A2.1: Sequence alignment of cad 3'UTRs from different *Drosophila* species. The BBR_66-185 (indicated with bold, blue letters) and the BRE_210-253 (indicated with green, bold letter) of the *D. melanogaster* cad 3'UTR do not show extensive sequence similarities to the other *Drosophila* species. The BRE_257-319 fragment (indicated as yellow box) contains a 38 nt sequence region, which is present in all species (conserved nt are indicated with a point). Interestingly, this box overlaps with a target site of miR-308 (underlined) in *Drosophila*. The target site of miR-315 is situated further towards the 3' end (indicated with a blue shaded box) (Brennecke et al., 2005; Stark et al., 2005). Another conserved sequence region among these Drosophilid species contains 16 nt spanning nt 906-912 of the *D.mel* sequence (indicated with a pink shaded box). Alignments were performed with Multalin program version 5.4.1. (Multiple sequence alignment with hierarchical clustering, CORPET, 1988, Nucl. Acids Res., 16 (22), 10881-10890) Dmel = *D. melanogaster*, Dpse = *D. pseudoobscura*, Dwil = *D. willistoni*, Dvir = *D. virillis*, Dmoj = *D. mojavensis*.

A3 Myc-stainings

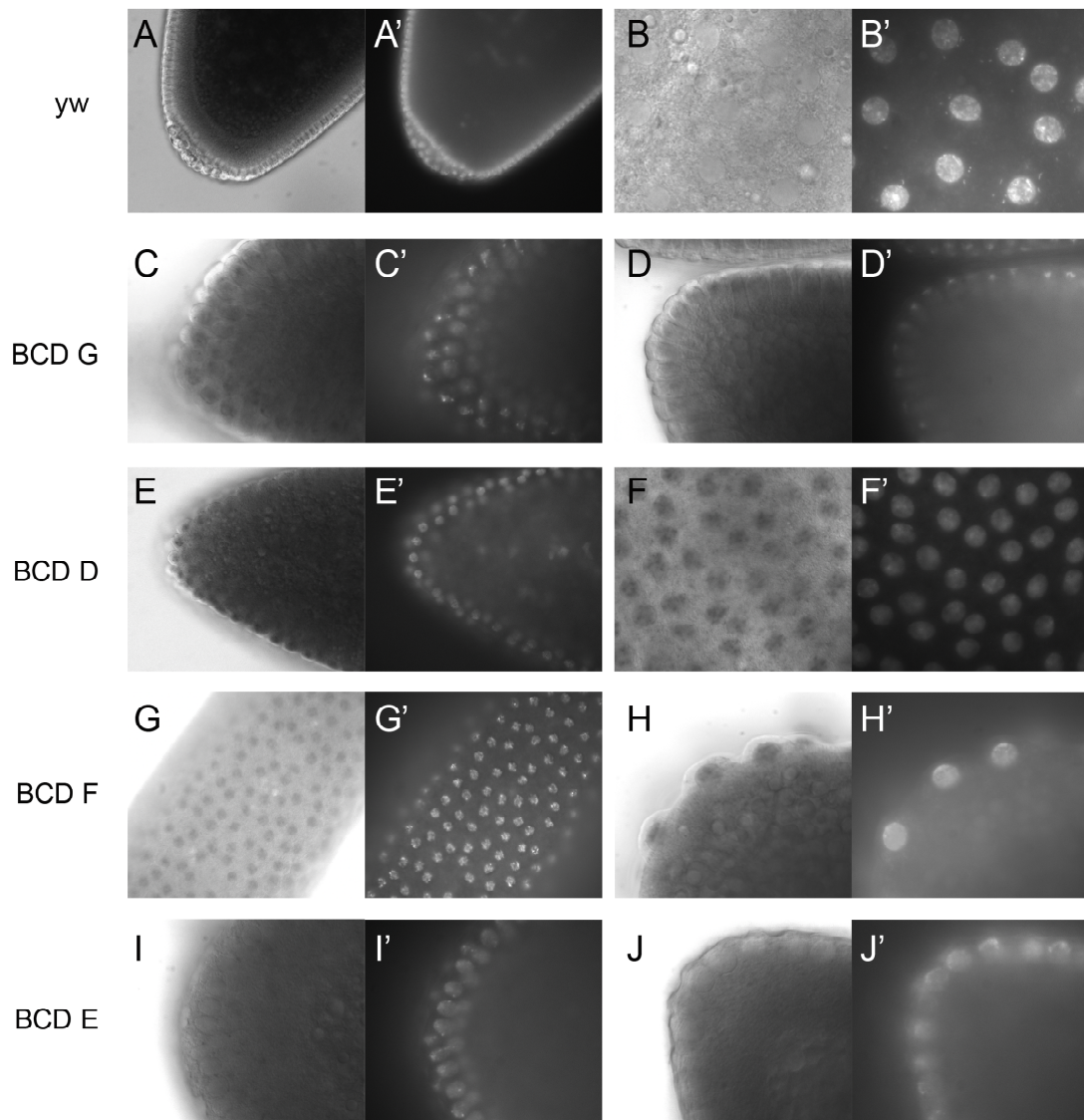


Fig. A3.1: Cellular localization of Myc-tagged BCD isoforms in embryos revealed by α -Myc staining. Control embryos (yw) do not show any staining (**A** and **B**). Embryos derived from females expressing BCD isoform G (**C** and **D**, maternal genotype UAS-BCDG^{F4M6}/+;nos-GAL4:VP16/+), isoform D (**E** and **F**, maternal genotype UAS-BCDD^{M29}/nos-GAL4:VP16) and isoform F (**G** and **H**, maternal genotype UAS-BCDF^{M22}/nos-GAL4:VP16) show staining in the cytoplasm and in the nuclei. Embryos derived from females expressing BCD isoform A show staining only in the cytoplasm (**I** and **J**, maternal genotype UAS-BCDA^{F36}/+;nos-GAL4:VP16). **A'**-**J'** show DAPI stainings of the nuclei. All isoforms are expressed ubiquitously, driven by the nos-GAL4:VP16 driver. Because isoform E was cloned during later stages of my PhD, α -Myc staining could not be performed for isoform E.

A4 Secondary structure predictions and RNAforester alignments

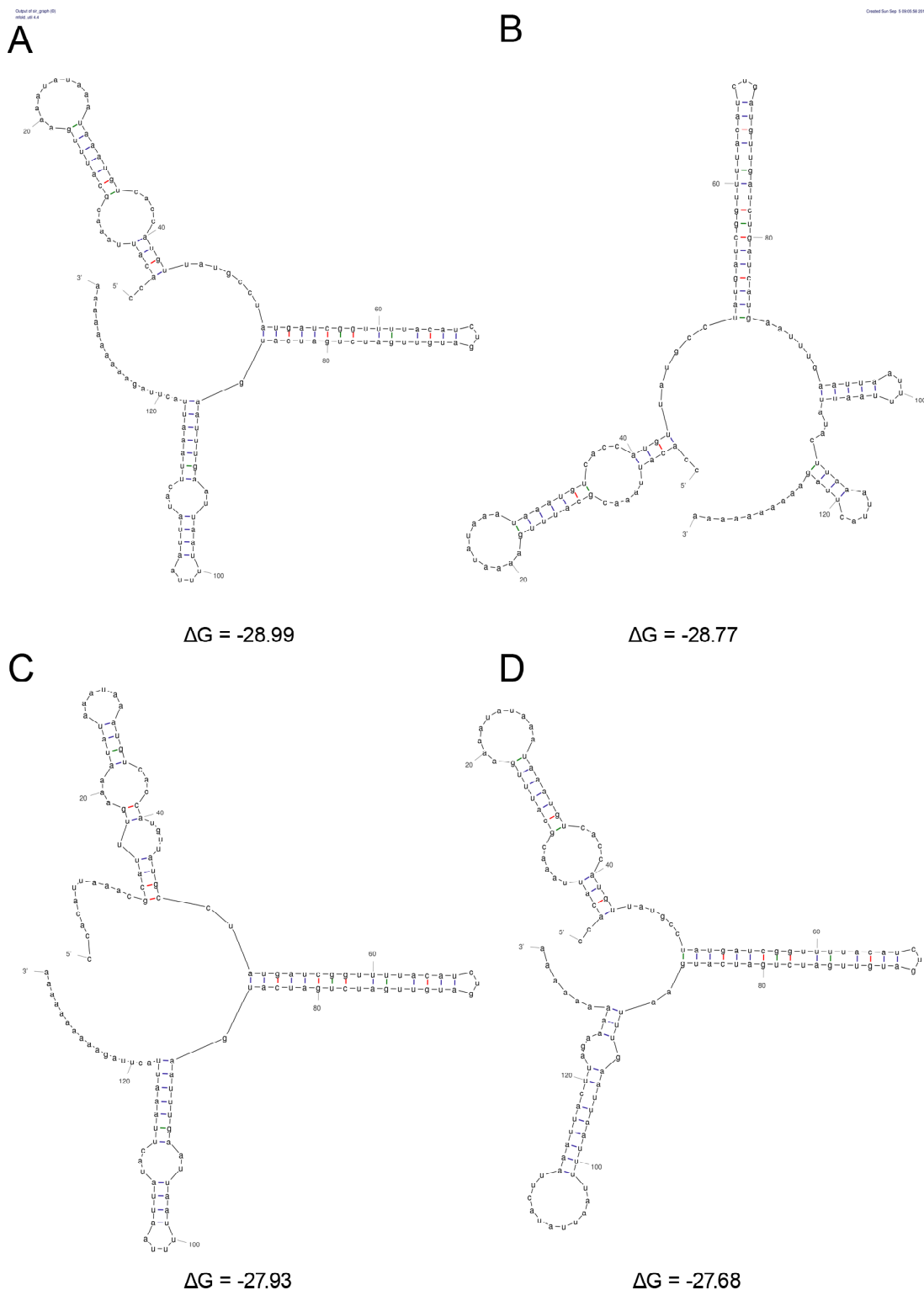


Fig. A4.1 Predicted secondary structures of the *Haematopota* 3'UTR using the mfold RNA folding program version 2.3. Four secondary structures are predicted, with different ΔG values (indicated below), which vary mostly in the first and third stem-loop structures.

BRE_257-319

GGCCGUUGCACCUGGAAUAUUGCACGUUGUAAUUUUUGUGAUUGUAUAUCCUGGUUUCGA
 ...(((.....(((.....(((.....(((.....(((.....)))))))).)))).)))).
 (-16.60)

H1

GACCACAUUAAACGCAUUUGAAAAUAUAAAUAUAAUGUCACCAUGUUAUGCCUCUAGAGC
((((.....(((.....(((.....)))))))).)))).((.....))
 (-6.86)
 GACCACAUUAAACGCAUUUGAAAAUAUAAAUAUAAUGUCACCAUGUUAUGCCUCUAGAGC
(((.....(((.....(((.....)))))))).)))).((.....))
 (-5.87)

H2

AUGCCUAUGAUCGGUUUUACAUCUGAUGUUGAUCUGAUAUGGGCGCGCCA
 .((((((((((((((.....)))))))).)))).
 (-26.99)

H3

AAUUUGAAUUAUUUUAAUUUAUACUAAAUAUACUUAGGGCGCGCCU
 (((((((.....(((.....)))))))).)))).((.....))
 (-9.29)
 AAUUUGAAUUAUUUUAAUUUAUACUAAAUAUACUUAGGGCGCGCCU
(((.....))))).((.....))
 (-8.97)

shSV40

CUAGAUCAUAAUCAGCCAUACCACAUUUGUAGAGGUUUUACUUGC UUAAAAAACCUCCACACCUC
 CU
 ...(((.....)).....(((.....)).((((((((.....)))))))).
 ..
 (-15.83)
 CUAGAUCAUAAUCAGCCAUACCACAUUUGUAGAGGUUUUACUUGC UUAAAAAACCUCCACACCUC
 CU
 ...(((.....)).....(((.....)).((((((((.....)))))))).
 ..
 (-15.02)

Dm3'mut [nt 257-319]

GGCCGUUGCACCUGGAAUAUUGCAGUUUGUAAUUUUUACGAUUGUAUAUCCUGGUUUCGA
 ...(((.....(((.....(((.....(((.....)))))))).)))).)))).
 (-17.36)
 GGCCGUUGCACCUGGAAUAUUGCAGUUUGUAAUUUUUACGAUUGUAUAUCCUGGUUUCGA
 ...(((.....(((.....(((.....(((.....)))))))).)))).)))).
 (-16.95)

Tc'cad 3'UTR only

UUCCUCACAACUCAUAGACCGUCCCUUACGUCGAAUGGAAAGAAGACAAUCUUCAGUGUUUGUGAUG
 AAUUGUGUUGUGAUUUUGCGUUUUUAUUUAUUUUUACGAGUCACAUCACCUCGGAGAUUACUGUGCAUA
 AUUCAUAUUAUUUAUCUUUUUGUUACGGCAUUGUGUAUAUAGUAUUGUAUAAAGGUUUUAUCUGUUGUGUA
 GUAGCAUUUUUAAACUGUUCUUCGAGUGUGGCACCGGAUUAUCUAGAAAUUCGCACUUUGUAAAUUUGU
 ACAACGUUUUAUGUGCCUUCUUGUUGCUUCUUCUACUAUACCUUGUAAAUAAGGUCGCUGUAUCCAC
 GUCUUGUUGUGUUGCAGAGUAGGGGCAGAUUGUAACUUAUUUUUUGGUAUCGAGUGAAGAAUAAAUGAUU
 UUAUUUGAAAAA
((((((((.....(((.....)))))))).)))).((((((((.....(((.....)))))))).)))).
(((.....))))).((.....))
 ..

RNAforester alignments (see below) were performed using the local similarity option. The predicted secondary structures of H1, H2, H3, shSV40, Tc'cad 3'UTR and Tc'cad5'UTR+CDS were aligned against BRE_257-319. The local optimal score indicates the degree of similarity between the two secondary structures as result of the scoring parameters. Highest local optimal scores were calculated for secondary structures of BRE_257-319 and H2 (score = 55) and BRE_257-319 and nt 451-485 of Tc'cad 5'UTR+CDS (numbering begins with the first nt of the cDNA, indicated in grey in Fig. A5.2) (score = 57), which indicates highest structural similarity. In the RNAforester alignment with Tc'cad 5'UTR+CDS and H2, the same region of the *Tribolium* RNA is detected to show structural similarity, whereas the similarity score between Tc'cad 5'UTR+CDS and H2 is even higher (score = 95).

RNAforester alignment of BRE_257-319 and H1

Scoring type: local similarity

Scoring parameters:

pm: 10
pd: -5
bm: 1
br: 0
bd: -10

calculate suboptimals within 80% of global optimum

local optimal score: 33
starting at positions: 22,16

```
1          CACGUUGUAAUUUUUGUG
2          UUUGAAAAUA-UAAAAAA
           *   ** *   *
```

```
1          (((((((.....))))))
2          (((((((.....-.....))))))
           ***** *****
```

mapping:

1: BRE_257-319
2: H1

executed command: RNAforester --xml -f=input_data.txt -2d -l -so=80 -bm=1 -bd=-10 -br=0 -pm=10 -pd=-5

RNAforester alignment of BRE_257-319 and H2

Scoring type: local similarity

Scoring parameters:

```
pm: 10
pd: -5
bm: 1
br: 0
bd: -10
```

calculate suboptimals within 80% of global optimum

local optimal score: 55

starting at positions: 9,2

```
1          ACCUGGAAUAUUGCACGUUGUAAUUUUUGUGAUUGUAUAUUCUGGU
2          GCCUAUGAUCGGUUUUACAUCUGAUG--UUGA-UC--UGAUC AUGGGC
           ***  **          * ** *  *  **  **

1          (((.(((((((..((((.....))))).)))))))))
2          ((((((((((..((((.....))))).)))))))))
           *** ***** ** *  ***  * ** *  ***** **
```

mapping:

```
1: BRE_257-319
2: H2
```

executed command: RNAforester --xml -f=input_data.txt -2d -l -so=80 -bm=1 -bd=-10 -br=0 -pm=10 -pd=-5

RNAforester alignment of BRE_257-319 and H3

Scoring type: local similarity

Scoring parameters:

```
pm: 10
pd: -5
bm: 1
br: 0
bd: -10
```

calculate suboptimals within 80% of global optimum

local optimal score: 25

starting at positions: 13,0

```
1          GGAAUAUUGCACGUUGUAAUUUUUGUGAUUGUAUAUUC
2          AAUUUGAAUAAUUU-U-A-----AUUA-UAC-UUAAAAU
           *      * ** * *      *  *  **

1          ((((((((((..((((.....))))).)))))))))
2          ((((((((((..((((.....))))).)))))))))
           ***** ** *  ***** **
```

mapping:

```
1: BRE_257-319
2: H3
```

executed command: RNAforester --xml -f=input_data.txt -2d -l -so=80 -bm=1 -bd=-10 -br=0 -pm=10 -pd=-5

RNAforester alignment of BRE_257-319 and shSV40

Scoring type: local similarity

Scoring parameters:

pm: 10
 pd: -5
 bm: 1
 br: 0
 bd: -10

calculate suboptimals within 80% of global optimum

local optimal score: 44
 starting at positions: 21,34

```

1          GCACGUUGUUAUUUUUUGUG
2          GUUUUACUUGCUUUAAAAAA
           *      *      **

1          .((((.....))))
2          .((((.....))))
           *****
  
```

mapping:

1: BRE_257-319
 2: shSV40

executed command: RNAforester --xml -f=input_data.txt -2d -l -so=80 -bm=1 -bd=-10 -br=0 -pm=10 -pd=-5

RNAforester alignment of BRE_257-319 and Tc'cad 3'UTR

Scoring type: local similarity

Scoring parameters:

pm: 10
 pd: -5
 bm: 1
 br: 0
 bd: -10

calculate suboptimals within 80% of global optimum

local optimal score: 34
 starting at positions: 15,20

```

1          UAUGACCGUCCCCUACGUCGA
2          UGCACGUUGUUAUUUUUGUGA
           *          **      **

1          ..((((((.....)))))).
2          ..((((((.....)))))).
           *****  *****  *****
  
```

mapping:

1: Tc'cad 3'UTR
 2: BRE_257-319

executed command: RNAforester --xml -f=input_data.txt -2d -l -so=80 -bm=1 -bd=-10 -br=0 -pm=10 -pd=-5

RNAforester alignment of BRE_257-319 and Tc'cad 5'UTR+CDS

Scoring type: local similarity

Scoring parameters:

```
pm: 10
pd: -5
bm: 1
br: 0
bd: -10
```

calculate suboptimals within 80% of global optimum

local optimal score: 57

starting at positions: 450,5

```
1          GUCAGCCUAAUCCCGAACCGGCCGAUU-UC--GCUGAC
2          GAAUAUUGCACGUUGUUAUUUUUGUGAUUGUAUAUUC
           *      *      *      *      *      *
1          ((((((..(((((((.....)))..)))))-...--))))))
2          ((((((..(((((((.....)))..)))))-...--))))))
           *****      ***      ***** **      *****
```

mapping:

```
1: Tc'cad 5'UTR+CDS
2: BRE_257-319
```

executed command: RNAforester --xml -f=input_data.txt -2d -l -so=80 -bm=1 -bd=-10 -br=0 -pm=10 -pd=-5

RNAforester alignment of H2 and Tc'cad 5'UTR+CDS

Scoring type: local similarity

Scoring parameters:

```
pm: 10
pd: -5
bm: 1
br: 0
bd: -10
```

calculate suboptimals within 80% of global optimum

local optimal score: 95

starting at positions: 449,6

```
1          AGUCAGCCUAAUCCCGAACCGGCCGAUUUCGCUGAC
2          AUGAUCGGUUUACAUCUGAUG--UUGAUCUGAUCA
           *      *      *      *      *      **
1          .(((((((..(((((((.....)))..))))).))))))
2          .(((((((..(((((((.....)))--).))))).))))))
           *****      ***      *****      *      *****
```

mapping:

```
1: Tc'cad 5'UTR+CDS
2: H2
```

executed command: RNAforester --xml -f=input_data.txt -2d -l -so=80 -bm=1 -bd=-10 -br=0 -pm=10 -pd=-5 -r

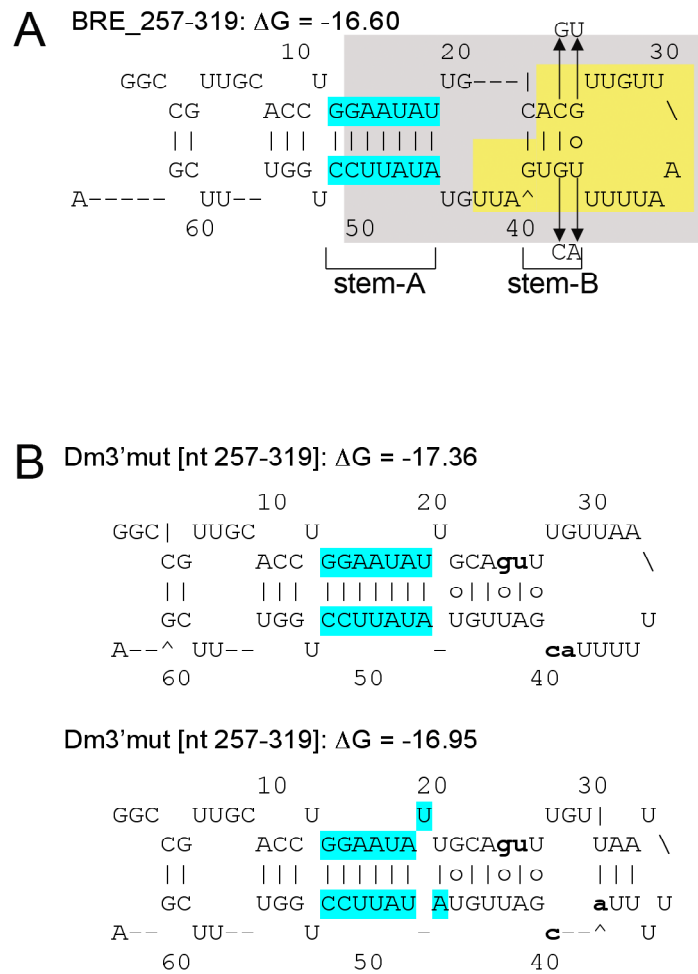


Fig. A4.3: Predicted secondary structures of BRE_367-319 and nt 257-319 of Dm3'mut. (A) In the predicted secondary structure of BRE_257-319, the area in grey indicates the sequence that is conserved among different *Drosophila* species; the area in yellow shows the miR-308 binding target. The changes introduced in 38F-Dm3'mut are indicated by arrows and shown as small bold letters in the predicted secondary structures of Dm3'mut (B). The predicted secondary structures of Dm3'mut (B) and BRE_257-319 (A) are different: stem-B is changed in both structures of Dm3'mut with additional base pairs, however, the mutated nucleotides do not base pair with each other. Stem-A changes in one of the predicted secondary structures, most likely due to the changes of stem-B. Secondary structure predictions were performed using the mfold program (version 2.3).

A5 Genomic region of *bcd*

ATCTCTTCGCTCATCCCTAAATAACGGCACTCTGCAGATGCGAAGCAGTGGATCGCAAAA exon
1

ACGCAAAATGTGGGCGAAATAAGTTCGCGAGCGTCTCGAAAGTAACCGGTTACTGAAAAT
ACAAGAAAGTTCCACACTCCTTTGCCATTTTTCCGCGCGGGCGCTTGAAATTCGTAAAG

M A Q P P P D Q N F Y

ATAACGCGGCGGAGTGTGGGAAATGCGCAACCGCCGCCAGATCAAACCTTTTACC

H H P L P H T H T H P H P H S H P H P H

ATCATCCGCTGCCACACGCACACACATCCGCATCCGCACTCCCATCCGCATCCGCACT

S H P H P H H Q H P Q L Q L P P Q F R N

CGCATCCGCACCCACATCACCAACATCCGCAGCTTCAGTTGCCGCCACAATTCCGAAATC

P F D L

CCTTCGATTTGgtgagttcccatcgagcagagaagggctcttgtcccaggaaagctaca
gtacagattccctatggtgaacaacaaccagtgcgatcactgatgaccataaacattta
ttgagccgcagaaatgtgtttctagaacatagggcgaaatcttctattatcttgtttgt
gacttttaaagtatcgtagcagaatctaaaaaccaattgatattattaatcgttacagtt
agtatagatataattgtatatgaattgtggggcatcatggtattagtgatttgccgaaa
tgttctaaaagggttttcattgaaatggacgaatgttaaacctggtgactcacaccgac
aatcagtaatgtctatTTTTTCAAAGCCACATCTATGGCCACTGGGTATACATTATTGAC
TTATACACTTCATACAACATTTTTCTAAAACAAGCATTGTTGTCTGCGATGATGATTA
GTGAAAGTAATATTGCAAGATTCGGTCCCCGAAGCGAATCGTCCTTTCACGTTTTTATAT

----- exon
2a

----- exon

2b

C T P stop L F D E R T G A I N

aaagacagTGTACCCCTTGAATTCTTTGAAGCTTTTCGATGAGCGAACGGGAGCGATAAAC

Y N Y I R P Y L P N Q M P K P

TACAACTACATACGTCCGTATCTGCCCAACCAGATGCCCAAGCCAGgtgagctcaaagcc

----- exon
3a

----- exon

3b

D V F P S E E L P D S L

aacaaagtcagccatcgtcttatcagATGTCTTTCCCTCAGAGGAGCTGCCCGACTCTCT

V M R R P R R T R T T F T S S Q I A E L

GGTGATGCGGCGACCACGTGCGACCCGCACTTTTTACCAGCTCTCAAATAGCAGAGCT

E Q H F L Q G R Y L T A P R L A D L S A

GGAGCAGCACTTCTGCGAGGACGATACCTCACAGCCCCCGACTTGCGGATCTGTCAGC

K L A L G T A Q V K I W F K N R R R R H

GAACTAGCCCTGGGCACAGCCCAGGTGAAGATATGGTTTAAGAACCCTCGGCGTCGTCA

K I Q S D Q H K D Q S Y E G M P L S P G

CAAGATCCAATCGGATCAGCACAAGGACCAGTCCTACGAGGGGATGCCTCTCTCGCCGG

M K Q S D G D P P S L Q T L S L G G G A

TATGAAACAGAGCGATGGCGATCCCCCAGCTTGCAGACTCTTAGCTTGGGTGGAGGAGC

T P N A L T P S P T P S T P T A H M T E
 CACGCCAACGCTTTGACTCCGTCACCCACGCCCTCAACGCCACTGCACACATGACGGA

H Y S E S F N A Y Y N Y N G G H N H A Q
 GCACTACAGCGAGTCATTCAACGCCTACTACAACACTACAATGGAGGCCACAATCACGCCCA

A N R H M H M Q Y P S G G G P G P G S T
 GGCCAATCGTCACATGCACATGCAGTATCCTTCCGGAGGGGGGCCAGGACCTGGGTGCAC

N V N G G Q F F Q Q Q Q V H N H Q Q Q L
 CAATGTCAATGGCGGCCAGTTCCTCCAGCAGCAGCAGGTCCATAATCACCAGCAGCAACT

H H Q G N H V P H Q M Q Q Q Q Q A Q Q
 GCACCACCAGGGCAACCACGTGCCGCACCAGATGCAGCAGCAGCAACAGCAGGCTCAGCA

Q Q Y H H F D F Q Q K Q A S A C R V L V
 QCAGCAATACCATCACTTTGACTTCCAGCAAAAGCAAGCCAGCGCCTGTGCGCTCCTGGT

K D E P E A D Y N F N S S Y Y M R S G M
 CAAGGACGAACCGGAGGCCACTACAACCTTCAACAGCTCGTACTACATGCGATCGGGAAT

S G A T A S A S A V A R G A A S P G S E
 GTCTGGCGCCACTGCATCGGCATCCGCTGTGGCCCAGGGCGCTGCCTCGCCGGGCTCCGA

V Y E P L T P K N D E S P S L C G I G I
 GGTCTACGAGCCATTAACACCCAAGAATGACGAAAGTCCGAGTCTGTGTGGCATCGGCAT

G G P C A I A V G E T E A A D D M D D G
 CGCGGACCTTGCGCCATCGCCGTTGGCGAGACGGAGGCGGCCGACGACATGGACGACGG

T S K K T T L Q
 AACGAGCAAGAAGACGACGCTACAGgtcaggcatgagtccacaacctttttgatctctt
 gattctgagtgtggcggtttataaattgaagctttaagctttgtaactttcaaactgtctg
 gtttgagatgttattctgaaagtacttctatttccgatcgatgagatttgggagttctcc
 aatatttaacatttaacttattaagttttgttttctaaattagacatggcattttctgaa
 aggaagtacaagtgttaaagatgtattttaatatagaatttgtatcaaaggttaagatt
 tcaaccgtttgaaagcccttagttttcagggtttttactttttattcatgtaatcact
 cttatacactgcaagttaaaatagcattttctttgaccagaaaaataagatctatgcatt
 ttaaagtgaaaacagactcatatgctgatgaacatttttagctataaattgtaacaata

atttagcaatttcaatcgaatttatttatggttctaaatgcggttcgctctctccctagATC
 4

I
 exon

L E P L K G L D K S C D D G S S D D M S
 TTGGAGCCTTTGAAGGCTTGGACAAGAGCTGCGACGATGGCAGTAGCGACGACATGAGC

T G I R A L A G T G N R G A A F A K F G
 ACCGGAATAAGAGCCTTAGCAGGAACCGGAAATCGTGGAGCGGCATTTGCCAAATTTGGC

K P S P P Q G P Q P P L G M G G V A M G
 AAGCCTTCGCCCCACAAGGCCCTCAGCCGCCCTCGGAATGGGGGGCGTGGCCATGGGC

E S N Q Y Q C T M D T I M Q A Y N P H R
 GAATCGAACCAATATCAATGCACGATGGATACGATAATGCAAGCGTATAATCCCCATCGG

N A A G N S Q F A Y C F N *
 AACGCCGCGGGCAACTCGCAGTTTGCCTACTGCTTCAATTAGCCTGGATGAGAGGGCGTGT
 TAGAGAGTTTCATTAGCTTTAGGTAACTACTGTTGTTCCCTGATTGTACAAATACCAAGT
 GATTGTAGATATCTACGCGTAGAAAGTTAGGTCTAGTCCTAAGATCCGTGTAAATGGTTC
 CCAGGGAAGTTTTATGTACTAGCCTAGTCAGCAGGCCGCACGGATTCCAGTGCATATCTT
 AGTGATACTCCAGTTAACTCTATACTTTCCCTGCAATACGCTATTTCGCTTAGATGTATC
 TGGGTGGCTGCCTCACTAAAGCCCGGGAATATGCAACCAGTTACATTTGAGGCCATTTGG

```

GCTTAAGCGTATTCCATGGAAAGTTATCGTCCCACATTTTCGGAAATTATATTCCGAGCCA
GCAAGAAAATCTTCTCTGTTACAATTTGACATAGCTAAAAACTGTACTAATCAAAAATGAA
AAATGTTTCTCTTGGGCGTAATCTCATAACAATGATTACCCTTAAAGATCGAACATTTAAA
CAATAATATTTGATATGATATTTTCAATTTCTATGCTATGCCAAAGTGTCTGACATAATC
AACATTTGGCGCATTCTTTGACCAAGAATAGTCAGCAAATTTGTATTTTCAATCAATGCAG
ACCATTTGTTTTAGATTCGGAGATTTTTTGTGCTGCCAAACGGAATAACTATCATAGCTCAC
ATTTCTATTTACATCACTAAGAAGAGCATTGCAATCTGTTAGGCCTCAAGTTTAATTTTAA
AATGCTGCACCTTTGATGTTGTCTCTTTAAGCTTTGTATTTTAAATTACGAAAATATATA
AGAACTACTTACTCGGGTAAATTGTGACTAACTAC

```

Fig. A5.1: Genomic region of *bcd* locus 3R:2581564,2585199 (FBgn0000166), from the *Drosophila melanogaster* genome (Release 5.31). Sequence was reversed and complemented for illustration in 5' to 3' orientation. Untranslated regions are indicated in black and capital letters. The coding sequence is indicated in blue letters, with the translated peptide sequence above in red letters. Intronic sequences are in black and small letters. Splice-donor sites are indicated in green, splice-acceptor sites are indicated in red, alternative splice acceptors are indicated in pink. The start codon of the open reading frame is indicated in light blue. Alternative splicing of exon 2a results in a premature stop codon (indicated in black and bold letters).

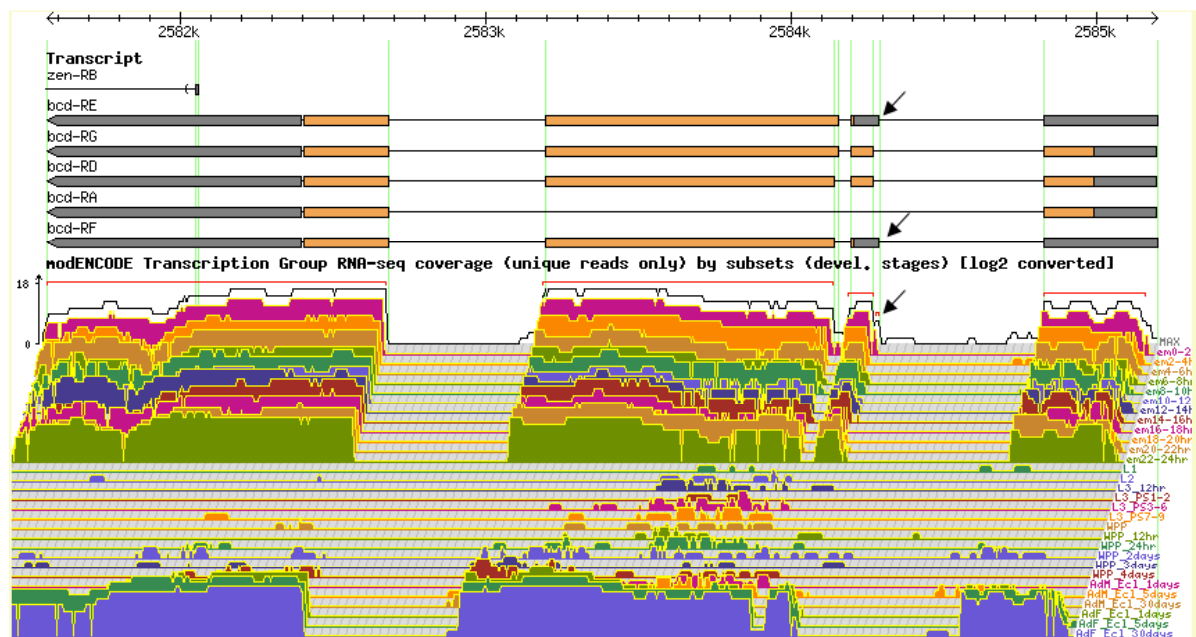


Fig. A5.2: Graphic presentation of RNA sequencing data from FlyBase (Release 5.31). The *bcd* transcripts are depicted in 3' to 5' orientation, coding sequences are indicated in orange, untranslated regions are indicated in grey. Below, the preview of the data from the Developmental Stage Timecourse Transcriptional profiling with RNA-seq (modENCODE Project). The presence of isoform E and F transcripts were recorded due to their different length (arrows). S. Tweedie, M. Ashburner, K. Falls, P. Leyland, P. McQuilton, S. Marygold, G. Millburn, D. Osumi-Sutherland, A. Schroeder, R. Seal, H. Zhang, and The FlyBase Consortium. FlyBase: enhancing *Drosophila* Gene Ontology annotations. *Nucleic Acids Research* (2009) **37**: D555-D559; doi:10.1093/nar/gkn788.

A6 Measurements of *in vivo* translational reporter assay

UAS- BCD isoform + 38F-Dm3': Measurements taken from photographs of embryos deriving from females expressing UAS responder line with a BCD isoform, sensor line 38F-Dm3' and nos-GAL4:VP16. Represented in each table are the values of each experiment and the respective control, which was used for normalization (relative average value set to 1).

maternal genotype	n	average	se	Relative average	Relative se	p (ttest)
38F-Dm3'/+;nos-GAL4:VP16/+	22	30.904	1.702250826	1	0.055083676	
UAS-BcdG^{F4M6}/+;38F-Dm3'/+;nos-GAL4:VP16/+	30	12.37496667	0.44618018	0.40044548	0.014438086	1.86115E-10
UAS-BcdG^{F8M1}/+;38F-Dm3'/+;nos-GAL4:VP16/+	23	12.9196087	0.54752263	0.418069724	0.017717459	2.50359E-10

maternal genotype	n	average	se	Relative average	Relative se	p (ttest)
38F-Dm3'/+;nos-GAL4:VP16/+	31	26.78764516	0.920271583	1	0.034354329	
38F-Dm3'/+;UAS-BcdD^{F15}/nos-GAL4:VP16	30	7.2609	0.356266729	0.27105406	0.013299666	7.29408E-22
38F-Dm3'/+;UAS-BcdD^{M29}/nos-GAL4:VP16	35	8.450771429	0.364582022	0.315472725	0.013610081	5.07777E-21

maternal genotype	n	average	se	Relative average	Relative se	p (ttest)
38F-Dm3'/+;nos-GAL4:VP16/+	27	41.53422222	2.077301275	1	0.050014209	1
38F-Dm3'/+;UAS-BcdE^{F12}/nos-GAL4:VP16	24	17.23804167	0.667302933	0.415032249	0.01606634	2.06896E-12
UAS-BcdE^{F79}/+;38F-Dm3'/+;nos-GAL4:VP16/+	26	15.94892308	0.60915882	0.383994745	0.014666431	6.67261E-13

maternal genotype	n	average	se	Relative average	Relative se	p (ttest)
38F-Dm3'/+;nos-GAL4:VP16/+	34	47.94791176	1.081367513	1	0.022552964	
38F-Dm3'/+;UAS-BcdE^{F9M3}/nos-GAL4:VP16	33	20.00727273	0.38965492	0.417270992	0.00812663	3.93876E-26
38F-Dm3'/+;UAS-BcdE^{M22}/nos-GAL4:VP16	30	21.839	0.456708889	0.455473434	0.009525105	1.21447E-25

maternal genotype	n	average	se	Relative average	Relative se	p (ttest)
38F-Dm3⁺;nos-GAL4:VP16/+	22	25.92740909	1.112531548	1	0.042909476	
38F-Dm3⁺;UAS-BcdA^{M22}/nos-GAL4:VP16	29	26.83668966	0.73565735	1.035070244	0.028373732	0.499543131
UAS-BcdA^{F36}/+;38F-Dm3⁺;nos-GAL4:VP16/+	32	26.3239375	0.662281522	1.015293792	0.025543683	0.761194307

UAS BCD isoforms + sensor: Measurements taken from photographs of embryos deriving from females expressing UAS responder line with a BCD isoform, a sensor line carrying a *cad* 3'UTR homologue and nos-GAL4:VP16. Represented in each table are the values of each experiment and the respective control, which was used for normalization (relative average value set to 1)

maternal genotype	n	average	se	Relative average	Relative se	p (ttest)
38F-BRE_257-319/+;nos-GAL4:VP16/+	20	25.62205	0.737960516	1	0.028801775	
UAS-BcdG^{F4M6}/+;38F-BRE_257-319/+;nos-GAL4:VP16/+	20	15.5258	0.63337806	0.605954637	0.024720038	1.56169E-12

maternal genotype	n	average	se	Relative average	Relative se	p (ttest)
38F-SV40/+;nos-GAL4:VP16/+	23	43.20817391	1.950060582	1	0.045131752	
UAS-BcdG^{F4M6}/+;38F-SV40/+;nos-GAL4:VP16/+	25	40.22504	1.6483047	0.930959038	0.038147983	0.248962738

maternal genotype	Relative average	Relative se	p (ttest)
38F-BRE_257-319/+;nos-GAL4:VP16/+	0.592990809	0.017079188	
38F-SV40/+;nos-GAL4:VP16/+	1	0.045131752	3.49225E-09

maternal genotype	n	average	se	Relative average	Relative se	p (ttest)
38F-H1/+;nos-GAL4:VP16/+	21	102.3991429	3.528145895	1	0.034454838	
UAS-BcdG^{F4M6}/+;38F-H1/+;nos-GAL4:VP16/+	22	105.3981364	3.779641716	1.029287291	0.036910873	0.565077385

maternal genotype	n	average	se	Relative average	Relative se	<i>p</i> (ttest)
38F-H2/+;nos-GAL4:VP16/+	54	19.33198148	0.513318512	1	0.026552814	
UAS-BcdG^{F4M6}/+;38F-H2/+;nos-GAL4:VP16/+	48	16.83685417	0.571623338	0.870932665	0.029568792	0.001537634

maternal genotype	n	average	se	Relative average	Relative se	<i>p</i> (ttest)
38F-H3/+;nos-GAL4:VP16/+	20	20.02185	0.922385335	1	0.046068936	
UAS-BcdG^{F4M6}/+;38F-H3/+;nos-GAL4:VP16/+	26	18.99507692	0.723879499	0.948717372	0.036154476	0.386622815

maternal genotype	n	average	se	Relative average	Relative se	<i>p</i> (ttest)
38F-Hp3'/+;nos-GAL4:VP16/+	19	81.37915789	2.02269139	1	0.024855153	
UAS-BcdG^{F4M6}/+;38F-Hp3'/+;nos-GAL4:VP16/+	23	65.83321739	1.99342019	0.808969017	0.024495463	2.97204E-06

maternal genotype	n	average	se	Relative average	Relative se	<i>p</i> (ttest)
38F-H2/+;nos-GAL4:VP16/+	34	74.20338235	1.573567109	1	0.021206137	
38F-H2/+;UAS-BcdF^{M22}/+;nos-GAL4:VP16	44	69.73513636	1.390376016	0.939783796	0.018737367	0.036802706

maternal genotype	n	average	se	Relative average	Relative se	<i>p</i> (ttest)
38F-Tc3'/+;nos-GAL4:VP16/+	20	35.2917	1.64440782	1	0.046594747	
UAS-BcdG^{F4M6}/+;38F-Tc3'/+;nos-GAL4:VP16/+	20	32.6276	1.729211975	0.924511996	0.048997696	0.271264825

UAS BCD isoforms + 38F-Dm3'mut: Measurements taken from photographs of embryos deriving from females expressing UAS responder line with a BCD isoform, sensor line 38F-Dm3'mut and nos-GAL4:VP16. Represented in each table are the values of each experiment and the respective control, which was used for normalization (relative average value set to 1).

maternal genotype	n	average	se	Relative average	Relative se	p (ttest)
38F-Dm3'+/+;nos-GAL4:VP16/+	27	23.09955556	0.965158605	1	0.041782562	
38F-Dm3'mut/+;nos-GAL4:VP16/+	24	43.42158333	1.604758527	1.879758388	0.069471403	3.1084E-13
UAS-BCDG^{F4M6}/+;38F-Dm3'mut/+;nos-GAL4:VP16/+	31	41.59634483	1.764890024	1.800742214	0.076403636	0.4560315

maternal genotype	n	average	se	Relative average	Relative se	p (ttest)
Dm3'mut/+;nos-GAL4:VP16/+	33	45.52769697	1.252315518	1	0.027506674	
Dm3'mut/+;UAS-BcdD^{M29}/nos-GAL4:VP16	31	43.64764516	0.946339261	0.958705317	0.020786012	0.235840665
Dm3'mut/+;UAS-BcdD^{F15}/nos-GAL4:VP16	32	46.87709375	1.002291348	1.02963903	0.02201498	0.403515702
Dm3'mut/+;UAS-BcdF^{M22}/nos-GAL4:VP16	8	46.4595	1.945114273	1.020466729	0.042723757	0.69341138

maternal genotype	n	average	se	Relative average	Relative se	p (ttest)
38F-Dm3'mut/+;nos-GAL4:VP16/+ (II)	34	47.95935294	1.038642895	1	0.021656733	
38F-Dm3'mut/+;UAS-BcdE^{F12}/nos-GAL4:VP16	37	50.5202973	0.853551302	1.053398226	0.01779739	0.061192215

maternal genotype	n	average	se	Relative average	Relative se	p (ttest)
38F-Dm3'mut/+;nos-GAL4:VP16/+	32	48.2561875	1.011951014	1	0.020970389	
38F-Dm3'mut/+;UAS-BcdF^{M22}/nos-GAL4:VP16	22	51.35718182	1.119409746	1.064261072	0.023197227	0.045374255

Curriculum vitae

Personal details

Name: Claudia Jasmin Rödel
Date of birth: 25.04.1981
Place of birth: Bremerhaven, Germany

Address of current working address

Institute for Molecular Biology and Biotechnology - FoRTH
Nikolaou Plastira 100
GR-70013, Heraklion, Crete
Greece
Telephone: +30 2810 391148
Email: roedel@imbb.forth.gr

University studies

University: Georg-August-University Göttingen, Germany
Country: Germany
Subjects: Developmental biology, zoology and biochemistry
From: October 2000
To: June 2006
Degree: Diploma
Thesis: "Isolation of developmental genes from the indian stick insect *Carausius morosus*" at the Dept. of Developmental Biology, GZMB, Georg-August-University Göttingen
Supervisor of thesis: Prof. Dr. Ernst A. Wimmer

University: University of Salamanca, Spain
Country: Spain
From: October 2004
To: March 2005
Purpose: Exchange semester supported by the ERASMUS/SOCRATES Exchange Program

PhD thesis

University: Georg-August-University Göttingen, Germany
Country: Greece
From: July 2006
Thesis: "Evolution of *caudal* translational repression in higher insects", at the Dept. of Developmental Biology, Institute of Molecular Biology and Biotechnology - FoRTH, GR-70013 Heraklion, Greece
External supervisor: Dr. Michalis Averof
Supervisor of thesis: Prof. Dr. Ernst A. Wimmer

Funding: July 2006 - June 2009, Scholarship awarded by the Marie Curie Early Stage Training Program "Functional analysis of microRNAs during early development",
October 2009 - June 2010, Scholarship of the Greek Government to foreign citizens awarded by the Hellenic Republic, Ministry of Education, Lifelong Learning and Religious Affairs.
October 2010 - June 2011, Scholarship of the Greek Government to foreign citizens awarded by the Hellenic Republic, Ministry of Education, Lifelong Learning and Religious Affairs.

Experiences

Student assistant: April 2003 – September 2003, April 2004 – September 2004, Zoological anatomical practical course for beginners.
April 2005 – September 2005, Animal identification.
October 2005 – March 2006, Practical course and tutorial of practical course of biology for medical students.

Johann-Friedrich-Blumenbach-Institute of Zoology and Anthropology, Georg-August-University Göttingen, Germany

Acknowledgements

I want to thank Dr. Michalis Averof for his scientific guidance and support during my PhD and for being available for discussions at all times. I am very grateful for his supervision, for allowing me to be part of his research group and for creating an inspiring scientific environment. Furthermore I would like to thank him for his support in all other matters outside the lab.

I want to thank my referees Prof. Ernst Wimmer and Prof. Gregor Bucher for their support and help and for the fruitful comments and constructive discussions. I want to thank Prof. Wimmer for having it made possible for me to conduct my research in Crete.

I would like to thank Prof. Andre Fiala, Prof. Reinhard Schuh, Prof. Andreas Stumpner and Prof. Andreas Wodarz, who agreed to be members of my commission board.

I would like to thank all members of the Averof Lab and the Delidakis Lab at the IMBB, Crete for their immediate hospitality, kindness, and friendliness. They created a pleasant and genial working environment during lab meetings, round tables, journal clubs and in our joint lab. In particular I want to thank Alexandros Kioupakis for his invaluable help during the early stages of my PhD, he has become a big hero of mine.

I want to thank Giannis Livadaras for performing the injections in *Drosophila* embryos for the transgenesis experiments.

I would like to thank Prof. Anastassios Economou for providing the pET16b-HisMBP plasmid and Prof. Urs Schmidt-Ott for providing the *cad* 3'UTR of *Haematopota pluvialis*.

I would like to thank my friends, who have become family in Crete, making this island what it is to me, a place that you never want to leave.

I want to thank my family in Germany for their short and long distance support, understanding and love during my PhD and all stages of my life.

Especially I want to thank my (to be) husband George, who is the only one who really understands me, for his love and support.